RHEOLOGICAL CHARACTERISTICS OF AQUEOUS WAX EMULSIONS USED FOR THE CONTROLLED RELEASE OF PHEROMONES AS AN ALTERNATIVE TO THE USE OF PESTICIDES FOR INSECT PEST MANAGEMENT

A thesis presented to the faculty of the Graduate School of
Western Carolina University in partial fulfillment of the
requirements for the degree of Master of Science in Chemistry.

By

Stephen Daniel Ballew

Director: Dr. Cynthia A. Atterholt
Associate Professor of Chemistry
Department of Chemistry and Physics

Committee Members: Dr. Brian D. Dinkelmeyer, Chemistry
Dr. David D. Evanoff, Jr., Chemistry

July 2011

ACKNOWLEDGEMENTS

I would like to thank my committee members and director for their assistance and encouragement. I would especially like to thank my director, Dr. Cynthia Atterholt, whose thoughtful, kind encouragements and experience really helped during this entire process.

I also extend sincere thanks to Isca Technologies, Inc. and the Western Carolina University Department of Chemistry and Physics for funding this project. Also, I would like to particularly thank Western Carolina University Department of Chemistry and Physics administrative support associate, Kathy Boland, without whom this thesis would not have been possible.

I thank God for the continuation of reality and my inclusion within it. Lastly, I offer my warmest regards and thanks to my parents for their continued support.

TABLE OF CONTENTS

LIST OF TABLES

LIST OF TABLES (Continued)

LIST OF FIGURES

LIST OF FIGURES (Continued)

LIST OF FIGURES (Continued)

LIST OF FIGURES (Continued)

Figures Page

LIST OF ABBREVIATIONS AND SYMBOLS

°C..... degree Celsius
cm..... centimeter
CR..... controlled release
CSD..... controlled shear deformation
CSR..... controlled shear rate
CSS..... controlled shear stress
g..... gram
G'..... storage modulus
G"..... loss modulus
HB..... Herschel/Bulkley
IPM..... integrated pest management
k..... consistency
kPa..... kilopascal
LVE..... linear viscoelastic
MCR..... modular compact rheometer
MD..... mating disruption
mm..... millimeter
mol..... mole
n..... flow index
N..... newton
Pa..... pascal
r^2..... coefficient of determination
rpm..... revolutions per minute
s..... second
Span 60®..... sorbitan monostearate
T..... temperature
TEA..... triethanolamine
γ..... shear strain
$\dot{\gamma}$..... shear strain rate
γ_A..... shear strain amplitude
γ_L..... limiting value of the linear viscoelastic range
η..... viscosity
η_∞..... infinite shear viscosity
µm..... micrometer
τ..... shear stress
τ_y..... yield point
ω..... angular frequency

ABSTRACT

RHEOLOGICAL CHARACTERISTICS OF AQUEOUS WAX EMULSIONS USED FOR THE CONTROLLED RELEASE OF PHEROMONES AS AN ALTERNATIVE TO THE USE OF PESTICIDES FOR INSECT PEST MANAGEMENT

Stephen Daniel Ballew, M.S.

Western Carolina University (July 2011)

Director: Dr. Cynthia A. Atterholt

Most pesticides produce some risk of harm to the environment because pesticides are designed to kill or adversely affect living organisms (US EPA, 2010). It is desirable that alternate, safer forms of pest control be developed. One alternative is the controlled release of pest insect sex pheromones to produce a mating disruption effect (Ahmed et al., 1993; Atterholt, 1996). Aqueous paraffin wax emulsions have shown much promise as formulations for this controlled release when applied to tree bark or foliage (Atterholt et al., 1996; Rice et al., 1997; Atterholt et al., 1998; Atterholt et al., 1999; Meissner et al., 2000; de Lame, 2003). Soy wax has recently become of interest in pheromone formulations because it is renewable, biodegradable, commercially available, and acceptable for organic farming (Behle, 2008).

Emulsions exhibit complex flow behavior which can be studied using rheometry (Macosko, 1994; Mezger, 2006). Rheometry refers to experimental techniques to determine the fundamental relationships between force and deformation in materials (Macosko, 1994). The rheological properties of emulsions are very important for production, storage, and application of these formulations (Mezger, 2006). In this project

the flow and viscoelastic properties of aqueous 30% paraffin wax and soy wax emulsions were investigated using three different emulsifiers: sorbitan monostearate (Span 60®), triethanolamine (TEA) stearate, and a 50%-50% mixture of both. Span 60® has already been used to make effective emulsions for the controlled release of pheromones, and it is food safe (Atterholt et al., 1996; Rice et al., 1997; Atterholt et al., 1998; Atterholt et al., 1999; Meissner et al., 2000; de Lame, 2003). TEA stearate is widely used to make non-toxic wax emulsions in the cosmetics industry (Wilkinson, 1940).

The investigations were carried out in both the rotational and oscillatory modes of a parallel-plate rheometer. The flow curves at three different temperatures (15 °C, 25 °C and 35 °C) of each emulsion were fitted with the Herschel-Bulkley model with the yield points determined using the one tangent method. The resulting equations can predict flow behavior at different conditions (Mezger, 2006). The emulsions were also tested using a temperature sweep at low shear from 15 °C to 50 °C to investigate temperature dependent changes. The viscoelastic properties were investigated using oscillatory shear tests and expressed in terms of elastic modulus and loss modulus. This gives information about time-dependant behavior like storage and the elastic character of the formulations which were found to be weak gels (Mezger, 2006). The Span 60® emulsions displayed faux shear-thickening behavior due to droplet subdivision while the other emulsions generally displayed shear-thinning behavior. Each emulsion approaches an infinite shear viscosity. The yield points and other flow parameters for the emulsions varied with temperature, depending on the formulation in question. All soy wax emulsions showed an increase in viscosity between 45 °C and 50 °C while the paraffin wax emulsions did not. Every emulsion showed long-term and short-term stability (Mezger, 2006).

INTRODUCTION

PESTICIDES

Pesticides are chemical substances used by humans for the control of agricultural or public health pests (Stenersen, 2004). Pesticide use goes back at least as far as our recorded history (Molnar et al., 2002; Sarpaki, 1995). The oldest record of pesticide use is the Egyptian medial compendium known as the *Ebers Papyrub* which dates from around 1600 BC (Bodenheimer, 1928; Sarpaki, 1995). Modern synthetic pesticides were first put on the market just after the Second World War. At that time, the impact of these chemicals on organisms including humans, and the environment was not well understood (Stenersen, 2004). In the 1960s and 1970s the effects of pesticides on the environment and human health became a general concern of the public and the government. This was due largely to the publication of *Silent Spring* (1962) by Rachel Carson (Stenersen, 2004).

The ramifications of pesticide use are now understood to a much greater degree. Most pesticide applications produce some risk of harm to the environment because pesticides are designed to kill or adversely affect living organisms (US EPA, 2010). Furthermore, the public perception of pesticide use is decidedly negative with an eager desire to reduce their use and impact (Molnar et al., 2002). Also, after prolonged use, many pests show resistance to pesticides, even to the point that some pesticides have been eliminated from the market all together (Stern et al., 1959). However, without pesticides modern farming would not be possible and food production would not be able to meet global demands (Molnar et al., 2002; Stenersen, 2004).

A viable alternative approach to pest management is necessary to minimize environmental impact and assuage public concern while still allowing for sustained agricultural production. One such approach is integrated pest management (IPM). First proposed in 1959, IPM integrates many methods of pest control, including biological, environmental and chemical (Stern et al., 1959). Chemical pesticides are only used when the level of intensity of a particular pest problem exceeds a threshold value. For example, this threshold could be a certain monetary value loss due to the crop sustaining injury from the pest.

MATING DISRUPTION

The biological component of IPM as proposed by Stern et al. (1959) involves the study and understanding of pests on a physiological and ecological level. This understanding is then applied to pest management in many forms. Present IPM programs use this information and available pest management methods to affect a sensitive approach to pest management. These programs are economical and present the least possible negative impact to people, property and the environment (US EPA, 2011).

New, less toxic methods of pest management are always being sought for IPM programs. One such method is the controlled release of pest insect sex pheromones to produce a mating disruption (MD) effect by producing specific behavior in individuals of the opposite sex in the same species (Ahmed et al., 1993; Atterholt, 1996). An effective method for MD is false trail following. In this method relatively high levels of female insect sex pheromones are introduced into an environment in order to disrupt the male insects' ability to locate female insects via pheromone sensors for the purpose of mating.

This method has been shown to produce a significant effect on breeding and is successful in reducing damage to crops (EPPO, 2008). MD integrates well into IPM as pheromones are specific to each species and produce very little impact on the environment. Pheromone MD is also more sustainable because there is no evidence that insects develop resistances to pheromones as with traditional insecticides (Rechcigl, 1999).

WAX EMULSIONS

Sprayable, paraffin wax emulsions that can carry pheromones when adhered to tree bark or foliage have shown promise as formulations for dispensing pheromones. They are inexpensive, biodegradable, non-toxic and easy to produce. They also produce a controlled release (CR) effect that releases pheromones slowly over a length of time necessary for practical application (Atterholt et al., 1996; Rice et al., 1997; Atterholt et al., 1998; Atterholt et al., 1999; Meissner et al., 2000; de Lame, 2003). Soy wax has also recently become of interest in pheromone formulations because it has all of the advantages of paraffin wax. It is also renewable and acceptable for organic farming (Behle, 2008).

In order to integrate these formulations into real-world IPM projects and have them available to the public, they need to be produced and distributed en masse. They will also have to be stored over time. The engineering necessary to accomplish this requires knowledge of the behavior of the emulsions under different conditions. This is accomplished, in part, through rheometry (Macosko, 1994).

Emulsions are mixtures of two immiscible liquids, with one of them dispersed in the other in the form of microscopic or nanoscopic droplets (Pal, 2000). In this case, the

emulsions are waxes dispersed in water. Emulsions exhibit complex flow behavior which can be studied using rheometry (Macosko, 1994).

RHEOLOGY

Rheology is a branch of physics and physical chemistry that studies deformation and flow (Macosko, 1994). The name of this discipline was coined around 80 years ago and was derived from the Greek word *rheos*, meaning "the river" or "flowing" (Mezger, 2006). Rheological experiments produce information about the flow behavior of liquids and the deformation behavior of solids (Mezger, 2006). All forms of shear behavior are within the purview of rheology (Macosko, 1994).

All rheological behavior is between two extremes: ideal viscous liquid flow and ideal elastic solid deformation (Macosko, 1994; Mezger, 2006). An example of a nearly ideal viscous liquid flow would be the spreading out of mineral oil poured onto a surface. Nearly ideal elastic solid deformation can be illustrated by the temporary deformation of a steal ball as it hits the same surface (Mezger, 2006). One is permanent and the other is temporary. A substance that displays a combination of both types of behavior is called viscoelastic (Macosko, 1994; Mezger, 2006). All materials are viscoelastic to some degree and wax emulsions exhibit complex flow behavior which can be studied using rheometry (Macosko, 1994; Mezger, 2006).

Rheometry refers to experimental techniques used to determine the fundamental relations between force and deformation (Macosko, 1994). Rheometry is the use of measuring technology that determines rheological data (Mezger, 2006).

A rheometer measures the mechanical responses of materials to precisely applied deformations (Kamerkar, 2010). Research-grade rheometers perform tests in two modes: rotational and oscillatory (Macosko, 1994; Mezger, 2006; Kamerkar, 2010). Rotational tests are used to generate flow curves characterizing the flow behavior of wax emulsions in order to better understand their flow properties under different conditions and temperatures (Pal, 2000). These are produced by either controlling the shear strain rate ($\dot{\gamma}$) in reciprocal seconds (s^{-1}) and measuring the shear stress (τ) in pascals (Pa) produced, or controlling the shear stress (τ) and measuring the shear strain rate ($\dot{\gamma}$) produced (Macosko, 1994; Mezger, 2006; Kamerkar, 2010). The data are then presented in terms of τ vs. $\dot{\gamma}$, or viscosity (η), in pascal-second (Pa·s) vs. one of these parameters (Macosko, 1994; Mezger, 2006; Kamerkar, 2010). The definition of viscosity (η) is shown in the following equation (Mezger, 2006):

$$\eta = \frac{\tau}{\dot{\gamma}} \tag{1}$$

Flow curves can be fitted by regression analyses using mathematical models specifically designed for this purpose (Mezger, 2006). One that is very common for emulsions is the Herschel/Bulkley (HB) model (Yaron, 1972; Ma, 1995). The parameters of this model are consistency (k), flow index (n) and yield point (τ_y). The equation for the Herschel/Bulkley (HB) model is shown below.

$$\tau = \tau_y + k \cdot \dot{\gamma}^n \tag{2}$$

Yield point (τ_y) is a parameter that can be assigned to some viscoelastic materials, and may be defined as the minimum shear stress necessary to induce flow (Mezger, 2006). It is a very important parameter which strongly influences engineering process calculations. In low-stress situations, stability is imparted to formulations possessing a yield point. Two such situations are storage and transportation, where the stresses involved are lower than the yield point (Ma et al., 1995). Yield points are due to hydrogen bonding and intermolecular forces (Van-der-Waals forces) producing three-dimensional network structures (Mezger, 2006).

The consistency (k) is a simple constant of proportionality, while the flow index (n) measures the degree to which the fluid is shear-thinning or shear-thickening. The flow index is less than one for shear-thinning, more than one for shear-thickening. If it is exactly one the sample shows "Bingham" plastic behavior (Ma et al., 1995; Mezger, 2006). With all these parameters, an equation for the curve is generated that can predict the behavior of the sample at different conditions (Nguyen et al., 1992; Pal, 2000).

Another type of rotational test is called a temperature sweep. This is performed by keeping a constant low $\dot{\gamma}$ and changing the temperature (Kamerkar, 2010). A temperature sweep produces a curve that shows viscosity (η) vs. temperature (Mezger, 2006).

The oscillatory test known as an amplitude sweep is mainly used to determine the limiting value of the linear viscoelastic (LVE) range (γ_L). The linear viscoelastic range is the range of shear strain (γ) amplitudes (γ_A) where the structure of the sample shows stability. At strains higher than γ_L, the limit of the LVE range is exceeded and the structure breaks down (begins to flow). This test allows for an amplitude to be chosen

for a frequency sweep test within the LVE range. In terms of shear stress, amplitude sweeps can also be used to calculate the yield point (τ_y) (Macosko, 1994; Mezger, 2006; Kamerkar, 2010).

Oscillatory tests are usually presented in terms of storage modulus (G') and loss modulus (G"). The storage modulus (G') is a measure of the deformation energy stored in the sample which corresponds to solid-like behavior. The loss modulus (G") is a measure of the deformation energy used in the shear process and lost to the sample which corresponds to liquid-like behavior (Mezger, 2006).

A frequency sweep is an oscillatory test that is performed at variable angular frequencies (ω), keeping the amplitude (γ_A) at a constant value. Frequency sweeps are used to investigate time-dependant behavior because frequency is the inverse value of time. Low frequencies simulate long-term behavior, like storage, and high frequencies simulate short-term behavior, like being dropped on the ground (Mezger, 2006; Kamerkar, 2010).

OBJECTIVE

The objective of this research was to better understand the rheological properties of paraffin wax and soy wax emulsion formulations used in controlled release of pest insect sex pheromones to produce a mating disruption effect as an alternative to pesticides (Atterholt et al., 1996; Rice et al., 1997; Atterholt et al., 1998; Atterholt et al., 1999; Meissner et al., 2000; de Lame, 2003). The rheological data gives future researchers insight into the production and handling of these emulsions as well as better elucidates the emulsions' behavior and stability. The rheology of paraffin wax and soy wax emulsions was compared in order to look at the physical differences between the two types of wax emulsions. This also allowed for a comparison of the two emulsifiers: sorbitan monostearate (Span 60®), triethanolamine (TEA) stearate.

There were three parts to this research. The first was to see how emulsifier concentration affects the rheology of emulsions. The second was to produce flow curves and temperature sweeps for all of the emulsions to better understand their flow properties under different conditions and temperatures (Pal, 2000). The third was to elucidate the viscoelastic properties of the emulsions via amplitude and frequency sweeps, which gives an understanding of their stability (Fischbach, 1987; Ma et al. 1995).

MATERIALS AND METHODS

PARAFFIN WAX AND SOY WAX

Paraffin wax is a byproduct of the petroleum industry composed of unbranched alkanes ranging from 18 to 24 carbons (Mansoori et al., 2003). The paraffin wax used in this research was Royal Oak Paraffin Wax #972 Household Gulf Wax®.

At room temperature, this material is a hard waxy solid with a melting point range between about 47 °C and 64 °C and a density of approximately 0.9 g/cm^3 (Kaye, 2011). Conversely, soy wax is partially hydrogenated soybean oil, which is made up of fatty acids ranging from 16 to 20 carbons (Chemicalland21.com, 2011). The soy wax used in this research is Golden Brands, LLC 415 Soy Wax. At room temperature, this material is a hard and waxy solid with a melting point range between about 48 °C and 52 °C and a density of approximately 0.9 g/cm^3 (*Shortening*, 2011). This soy wax was chosen because its properties were similar to paraffin wax.

EMULSIFIERS

Two emulsifiers were chosen for this research because they both work well in aqueous wax emulsions. The first was Span 60® which has a molecular weight of 430.62 g/mol and a molecular formula of $C_{24}H_{46}O_6$. The Span 60® used in this research was reagent grade from Alfa Aesar®. The chemical structure of Span 60® is shown below in Figure 1.

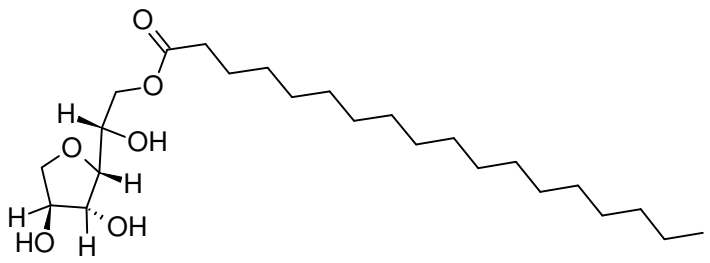

Figure 1. Span 60® Structure. IUPAC name: [(2R)-2-[(3R,4S)-3,4-dihydroxyoxolan-2-yl]-2-hydroxyethyl] octadecanoate. (NCIB, 2011)

The second emulsifier was TEA stearate which has a molecular weight of 433.67 g/mol and a molecular formula of $C_{24}H_{51}NO_5$. The TEA stearate used in this research was synthesized in-house. The chemical structure of TEA stearate is shown below in Figure 2.

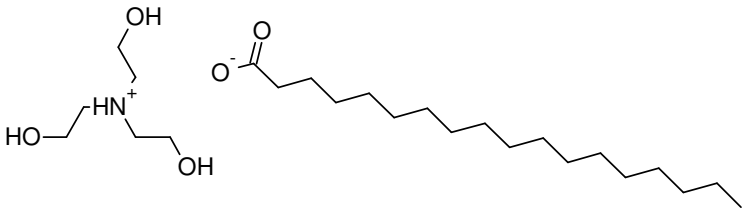

Figure 2. TEA Stearate Structure. IUPAC name: octadecanoate; tris(2-hydroxyethyl) azanium. (NCIB, 2011)

TEA stearate was synthesized from TEA and stearic acid according to the following equation:

$$\underset{\text{TEA}}{N(CH_2CH_2OH)_3} + \underset{\text{stearic acid}}{CH_3(CH_2)_{16}COOH} \rightarrow \underset{\text{TEA stearate}}{NH(CH_2CH_2OH)_3CH_3(CH_2)_{16}COO} \quad (3)$$

A stoichiometric amount of stearic acid (Laboratory Grade from Fischer Scientific) was weighted out and placed into a beaker. The beaker was placed into an 80 °C water bath and the stearic acid was allowed to melt. Sufficient TEA was added dropwise with stirring to the molten stearic acid. After all of the TEA was added, the temperature of the water bath was increased to 95 °C in order to obtain an isotropic solution. The TEA stearate produced was poured into an aluminum foil boat and allowed to cool to room temperature and harden. It was then ground to a powder with a mortar and pestle and stored in a glass bottle. This preparation has been used previously to produce TEA stearate (Kung, 1969 et al.; Zhu et al., 2005).

EMULSION PREPARATION

All emulsions were prepared with 66% (w/w) water, 30% (w/w) wax, and 4% (w/w) emulsifier. This has previously been shown to work well for pheromone applications (Atterholt et al., 1999). Two exceptions to this rule were emulsions specifically prepared with different concentrations of Span 60® for the purpose of examining the dependence of rheology on emulsifier concentration. Each emulsion prepared and its components are listed in Table 1.

Table 1. List of Wax Emulsions Prepared.

Emulsion	Paraffin Wax % (w/w)	Soy Wax % (w/w)	Span 60® % (w/w)	TEA stearate % (w/w)	Water % (w/w)
1	30	–	4	–	66
2	30	–	2	–	68
3	30	–	6	–	64
4	–	30	4	–	66
5	30	–	–	4	66
6	–	30	–	4	66
7	30	–	2	2	66
8	–	30	2	2	66

Each ingredient was weighed and placed into a beaker that was tared on an analytical balance and then placed onto a hotplate. The hotplate was turned up to the highest setting and the wax was allowed to melt and the water to boil. The boiling point of water insured some consistency between emulsions. After the wax had fully melted, the beaker was placed back onto the balance and more water was added dropwise until the water lost due to boiling and evaporation was replaced. The mixture was then emulsified for one minute using a CAT X520D homogenizer with a T10 dispersing tool on setting one, which is 11,000 rpm (IMP, 2011). The emulsions were stored in wide-mouthed glass jars and allowed to cool overnight. All tests were run within three days of emulsion preparation in order to avoid ageing effects.

RHEOMETER

The rheometer used in this research was an Anton Paar® Physica Modular Compact Rheometer (MCR) 101. The MCR 101 is an air bearing system that can

perform precise measurements is both the rotational and oscillatory modes (Anton Paar, 2007). The rheometer was also equipped with a peltier temperature control unit that provided temperature control from -40 ºC to 200 ºC.

Many measurement systems are available for the MCR 101. The measurement system used in this research was a 50 mm diameter parallel plate system. The rheometer was controlled using a Windows® XP personal computer running Rheoplus/32 software version 3.40.

The Measurement system was verified and tested using PSTD1000VE viscoelastic standard at 25 ºC. The test procedure runs a frequency sweep while simultaneously changing the γ_A over a range within the LVE region for the standard. The results are then analyzed and compared to two of the viscoelastic standard's known properties. The first is a crossover point where G' = G" and the second is a zero shear viscosity where the viscosity plateaus at low frequency (Mezger, 2006). The results for both properties were within tolerance (6.3 % and 1.4 % respectively).

RHEOLOGICAL MEASUREMENTS

With a parallel plate system, a gap between the plates has to be chosen in order to accommodate the sample. The optimal gap for emulsions of this type is around 1.0 mm above the bottom plate (Mezger, 2006). Therefore, all rheological tests were performed at a 1.0 mm measurement position unless otherwise noted.

All test methods were verified using Cannon viscosity standards N350 and N4000. These two standards were chosen because they each represent a η at one end of the

spectrum expected from the emulsion samples. All tests had a relative error of roughly 5% or less.

Special care was taken when each emulsion was loaded onto the rheometer in order to minimize the effects of work softening (Kokini, 1981; Ma, 1995). Work softening, or shear breakdown, occurs when a shear is applied to a rested sample that results in a persistent decrease in the sample's viscosity (McNaught, 1997). To minimize these effects, the emulsion samples were removed from the glass jars in one stroke (with the wide-mouths making this process relatively easy), and deposited onto the rheometer's lower plate. When the upper plate was lowered to the trim position (25 μm above the measurement position) the sample filled up the entire gap. The extra sample around the edge of the plate was trimmed with a metal spatula and the upper plate was lowered to the measurement position.

Before any test is performed, a rest time is necessary to allow sample relaxation and temperature equilibration (Ma, 1995). The MCR 101 allows for the monitoring of normal force from a sample. When the sample is completely relaxed the normal force should read around 0 N (Kamerkar, 2010). This test was performed on the 30% paraffin wax emulsion with 4% Span 60®, and it was found that after 10 minutes the normal force was 0.47 N. There was no significant change after 15 minutes. Therefore, in order to avoid sample drying, 10 minutes was chosen as the rest time for all samples being tested.

The first test usually run on a sample of unknown rheology is a rotational CSR flow curve. Looking at this data allows one to proceed with the next test (Mezger, 2006). Rotational CSR tests were performed on the 30% paraffin wax emulsions with 4% Span 60® and 4% TEA stearate. These tests were performed with 30 measuring points, a $\dot{\gamma}$

logarithmic ramp from 1 to 100 s^{-1} and a measuring point duration profile of "no time setting". Selecting "no time setting" allows the instrument to choose when to take each data point. The instrument takes each data point when it has determined that the sample has reached a steady state at each $\dot{\gamma}$ (Kamerkar, 2010).

It was determined that Span 60® and TEA stearate emulsions possess a yield point. A CSS flow curve is the recommended way to analyze a sample possessing a yield point (Mezger, 2006). In this way, the yield point can be determined by increasing the stress until flow occurs. This is known as the stress to initiate flow method, or the static method, and is the most frequently used (DeKee at al., 1986; Steffe, 1992; Ma et al.; Tabilo-Munizaga et al. 2004). Continuing to increase the shear stress and measuring the shear rate generates a flow curve. This was performed on all emulsions with 60 measuring points, a τ linear ramp from 1 to 100 Pa, and a linear variable measuring point duration profile from 25 to 1 seconds. This test was performed in triplicate for all samples.

Some of the flow curves had to be truncated because at higher shear the sample was slipping out from between the plates. This shows up as a negative slope in the CSR curve, which can only be explained by sample loss (Mezger, 2006). Only the data before sample slippage was used in the flow curves.

In order to test the CSS method and set-up for slippage effects, replicate samples were run at gap settings of 1.0 mm and 0.5 mm (Yoshimura et al., 1988; Ma et al. 1994). Normally, the difference in the flow curves measured at these gap settings indicates the existence of slippage in measurements. The slippage can then be mathematically accounted for. However, the difference between samples at the two gap settings were not

significant as compared to the error of the measurements at the same gap setting, which was found to have a relative standard deviation of 32%. This was determined for yield points by performing nine replicate CSS tests on the 30% paraffin wax sample with 4% Span 60®.

Yield points are not material constants and are very dependent upon a number of factors, including slight differences in sampling, which can produce error (Nguyen, 2006; Mezger, 2006). The error found here could also be the result of instrumental effects from the smooth parallel plate system on this type of sample. These effects could include the onset of secondary flow, fluid fracture, edge effects and sample expulsion (Nguyen, 1992). Sample inhomogeneity could also be contributing to this error. Relative standard deviations of up to 61% for yield points have been reported in the literature (Nguyen, 2006).

A temperature sweep from 15 °C to 50 °C was performed on all emulsions in triplicate at a strain rate of 5 s^{-1} to see how the dynamic viscosities (η) change with temperature. If any kind of structural hardening effects are taking place at these temperatures they are revealed by this test (Mezger, 2006).

Amplitude sweeps using controlled shear deformation (CSD) from $\gamma = 0.01\%$ to $\gamma = 100\%$ were performed on each of the emulsions at an angular frequency (ω) of 10 s^{-1}. The Rheoplus/32 software picked optimum amplitudes within the LVE range for running frequency sweeps on each emulsion listed in Table 2. The yield point (τ_y) of each emulsion and the limit of the LVE range were also determined by this method as well as information about the structural character of the emulsions before it yields to flow (Mezger, 2006). This was performed in triplicate for each sample. The resulting

optimum amplitudes for frequency sweeps were the same for each replicate of each sample.

Frequency sweeps using CSD from $\omega = 500\ s^{-1}$ to $\omega = 0.05\ s^{-1}$ were performed three times on all emulsions. The optimum amplitudes picked by the software from the amplitude sweeps were used for each emulsion sample. A list of these amplitudes can be found in Table 2. A frequency sweep gives information about the structural strength or "consistency" of the emulsions over time (Mezger, 2006).

Table 2. Shear Strain Amplitudes used in Frequency Sweeps.

Emulsion	γ_A (%)
1	0.05
2	0.5
3	0.1
4	0.1
5	0.5
6	0.1
7	0.5
8	0.1

SOFTWARE AND CALCULATIONS

The Rheoplus/32 software version 3.40 has a number of built-in data analysis and evaluation methods (*Instruction Manual*, 2007). A number of these methods were used in this research.

All replicate sample data was averaged using Microsoft Excel. A confidence interval was calculated for each averaged test with a confidence level of 95%. All rotational CSS data was averaged from one data point before the yield point (τ_y) for each

replicate. This was done because flow data before yielding has no direct meaning, and imprecision in this data when averaged produced nonsensical results.

The τ_y of each rotational CSS replicate was determined by the "stress to initiate flow" method (DeKee at al., 1986; Steffe, 1992; Ma et al.; Tabilo-Munizaga et al. 2004). A number of methods exist to evaluate this parameter. For example, the HB model fitting with no given regression parameters is an indirect method that attempts to determine τ_y through extrapolation to the y-axis by curve fitting the data (Nguyen, 1992). This method produces greater variability in τ_y than more direct methods and it can even be difficult to extract any meaningful yield point data from HB model fittings (Nguyen, 2006). The method generally accepted as the most reliable is known as the one tangent method (Nguyen, 2006; Mezger, 2006). This method is called the "Yield Stress II" method by the Rheoplus/32 software and is a direct method. It determines the yield point by calculating the bending point in a logarithmic plot of a τ vs. γ curve. A regression is then performed and checked for the point with the largest distance to the regression line which is reported as the yield point (τ_y) (*Instruction Manual*, 2007). This was performed on all replicates, then the results were averaged for each emulsion.

To generate Herschel/Bulkley fittings for the averaged CSS data, the "Herschel-Bulkley I" regression analysis method was used in the software. The HB model was chosen because it has been found to work well for emulsions (Nguyen, 1992; Ma, 1995). The average τ_y previously calculated for each emulsion was manually entered as a given regression parameter before running each analysis. Only the data from one point before the τ_y to the truncated part was selected for analysis. Selecting all of the data before the

truncation caused calculation errors with the correlation ratios. Herschel/Bulkley regressions were performed on all samples in this manner.

The amplitude sweeps were evaluated with two different analyses. The first was the "LVE Range" analysis. This produces the limiting value of the LVE region (γ_L) and an optimum amplitude within the LVE range for running frequency sweeps (*Instruction Manual*, 2007). The second was an analysis method called "Yield-Tangent Method/G' over TAU" which produces τ_y by calculating the bending point in a logarithmic plot of a G' vs. τ curve.

RESULTS AND DISCUSSION

CSR VS. CSS

The CSR and CSS flow curves for the 30% paraffin wax emulsion with 4% Span 60® were compared, as they ideally should overlap (Mezger, 2006). They are actually quite different, as shown in Figure 3. This difference could be due to a hysteresis in the sample. In other words, the sample was changed significantly before the data points were collected in the CSR test.

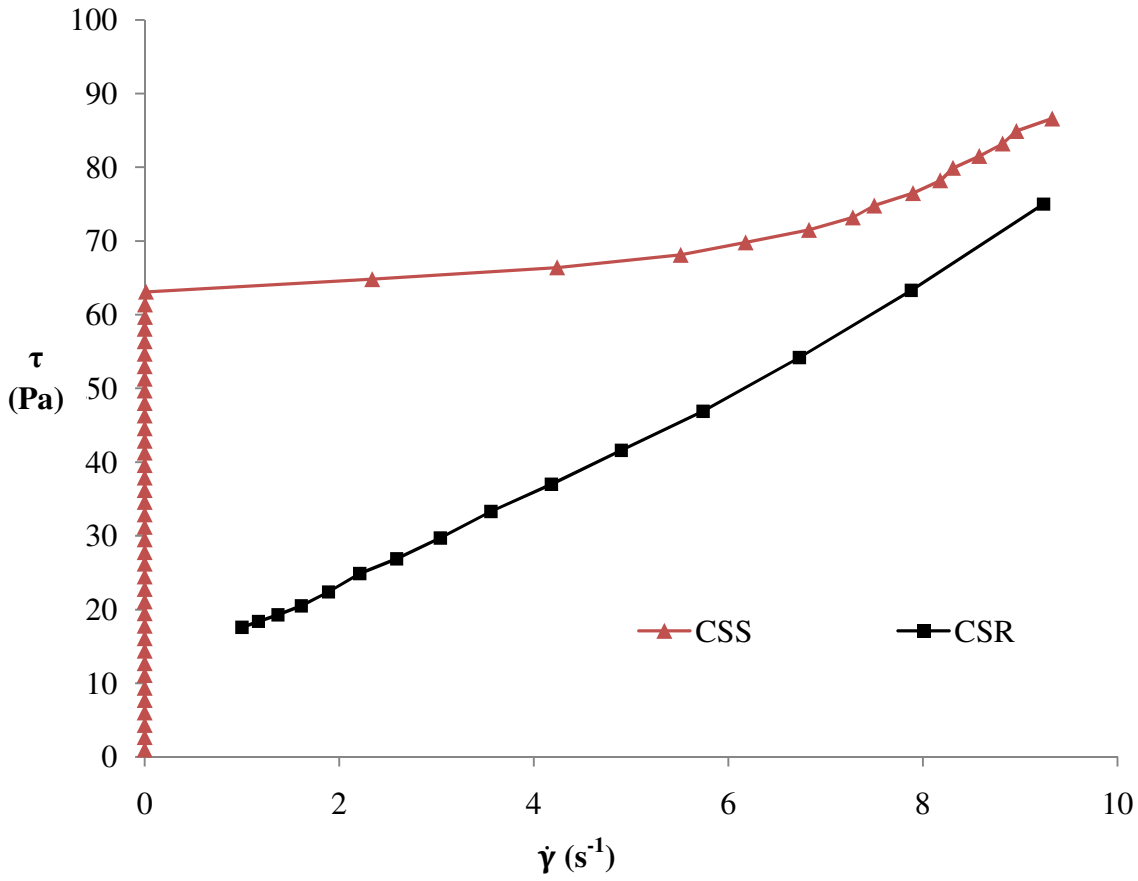

Figure 3. Comparison of CSR and CSS Curves for 30% Paraffin Wax Emulsion with 4% Span 60®.

Conversely, the CSR and CSS curves for the 30% paraffin wax emulsion with 4% TEA stearate, when compared, are quite close, apart from some separation at the beginning of the curves, as shown in Figure 4.

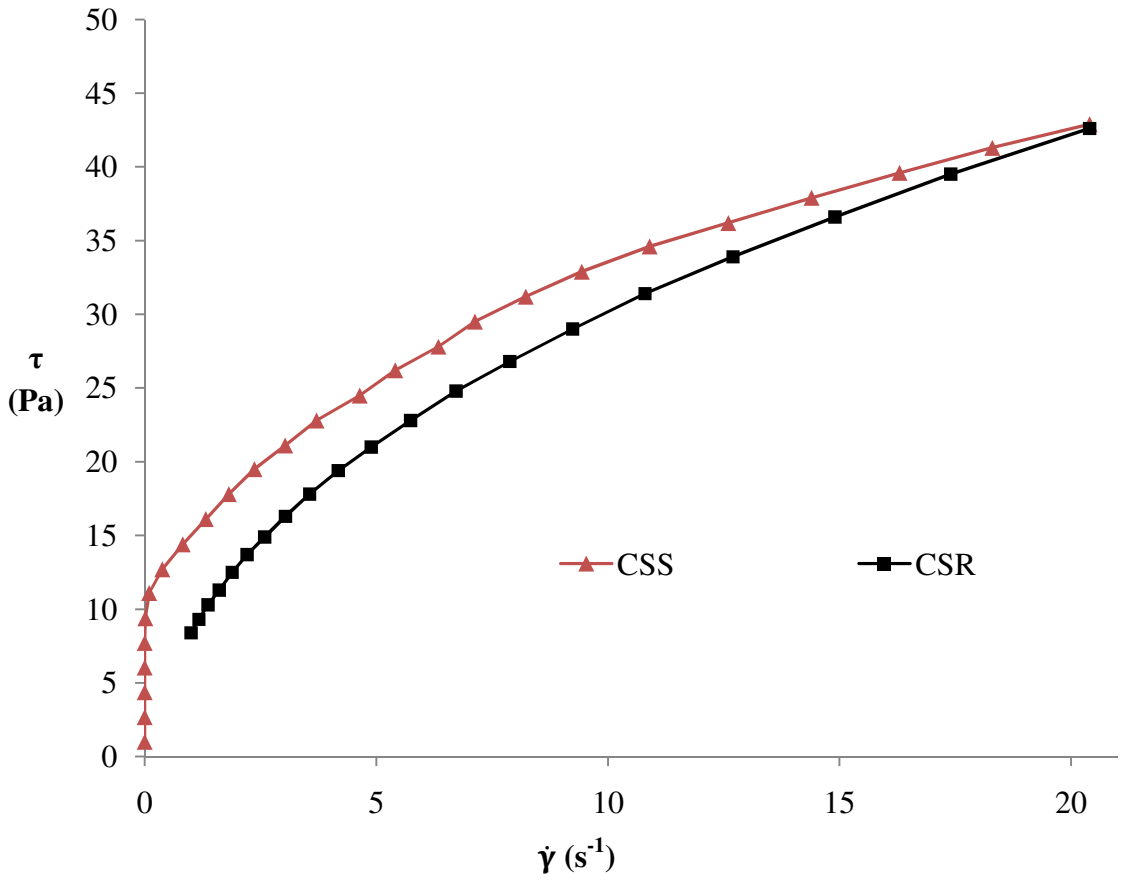

Figure 4. Comparison of CSR and CSS Curves for 30% Paraffin Wax Emulsion with 4% TEA Stearate.

To determine when one should ideally take data points, a "startup of shear" test was performed on the 30% paraffin wax emulsion with 4% Span 60®, with $\dot{\gamma} = 0.1\ s^{-1}$ (Kamerkar, 2010; Mezger, 2006). A "startup of shear" test is a transient test with a fixed

shear rate that is applied instantaneously to a sample and the stress response is measured. This detects the characteristic response time for the sample (Kamerkar, 2010). The results of this test are shown in Figure 5.

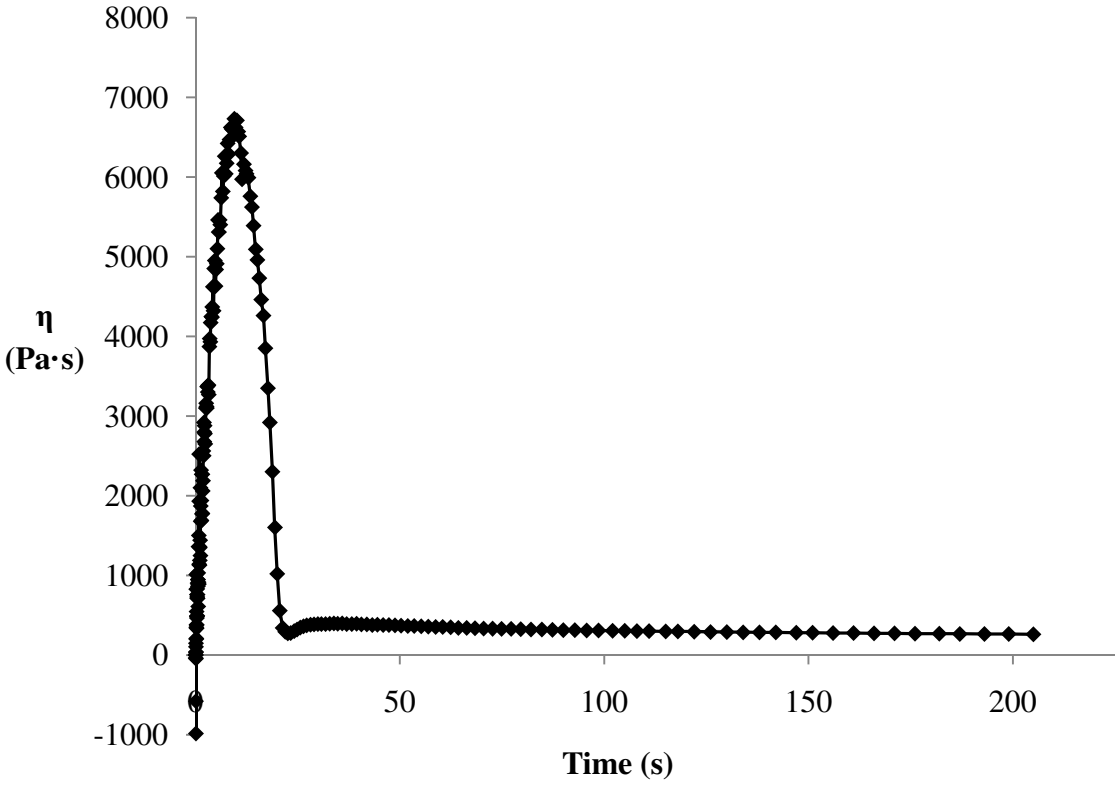

Figure 5. Startup of Shear Test Results for 30% Paraffin Wax Emulsion With 4% Span 60®

According to the results of this test, the 30% paraffin wax emulsion with 4% Span 60® has stabilized after 60 s^{-1}. Therefore, a second CSR test was performed on this emulsion with 30 measuring points, a $\dot{\gamma}$ logarithmic ramp from 1 to 100 s^{-1} and a

logarithmic variable measuring point duration profile from 60 to 1 seconds. The resulting curves are shown in Figure 6 below.

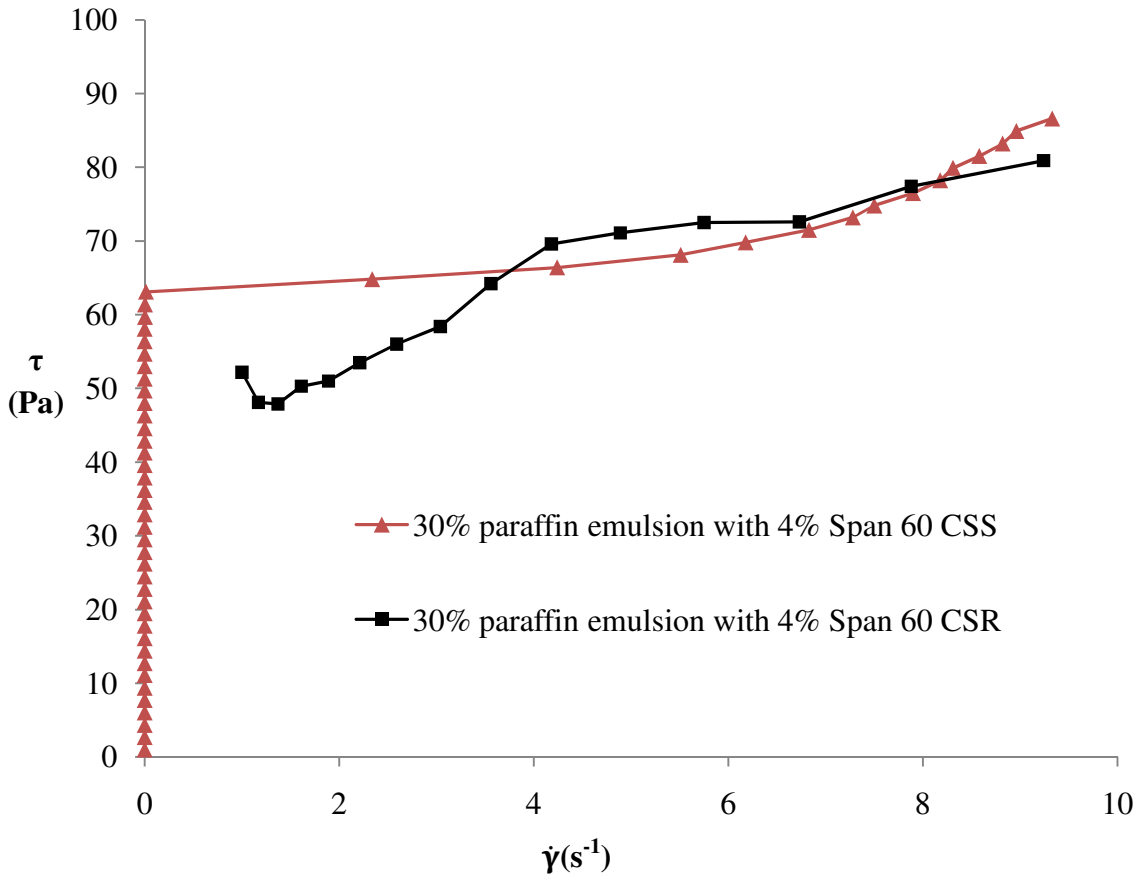

Figure 6. Comparison of Second CSR and CSS Curves for Paraffin Wax Emulsions with 4% Span 60®

This second CSR curve (Figure 6) is closer to the CSS curve than the first one (Figure 3), but there is quite a bit of noise obscuring the trend. It would appear that the hysteresis is preventing the CSR test from producing good data (Lipták, 2003). Because of this and

the fact that these emulsions have yield points (τ_y), it was decided that they would only be tested using the CSS method.

EFFECTS OF EMULSIFIER CONCENTRATION

The flow parameters from the HB regression analysis applied to the average flow curves for the emulsions with different Span 60© concentrations are listed in Table 3. These fitted curves are displayed in Figure 10 along with each curve's 95% confidence interval.

Table 3. Herschel/Bulkley Flow Parameters for 30% Paraffin Wax Emulsions at 25 °C vs. Emulsifier Concentration. Herschel/Bulkley model: $\tau = \tau_y + k \cdot \dot{\gamma}^n$

Span 60® % (w/w)	Yield Point τ_y (Pa)	Consistency k (Pa·s^n)	Flow Index n	Correlation Ratio r^2
2	54.8	2.31×10^0	3.58×10^{-1}	0.965
4	54.3	1.44×10^0	1.31×10^0	0.993
6	53.9	1.03×10^0	1.56×10^0	0.995

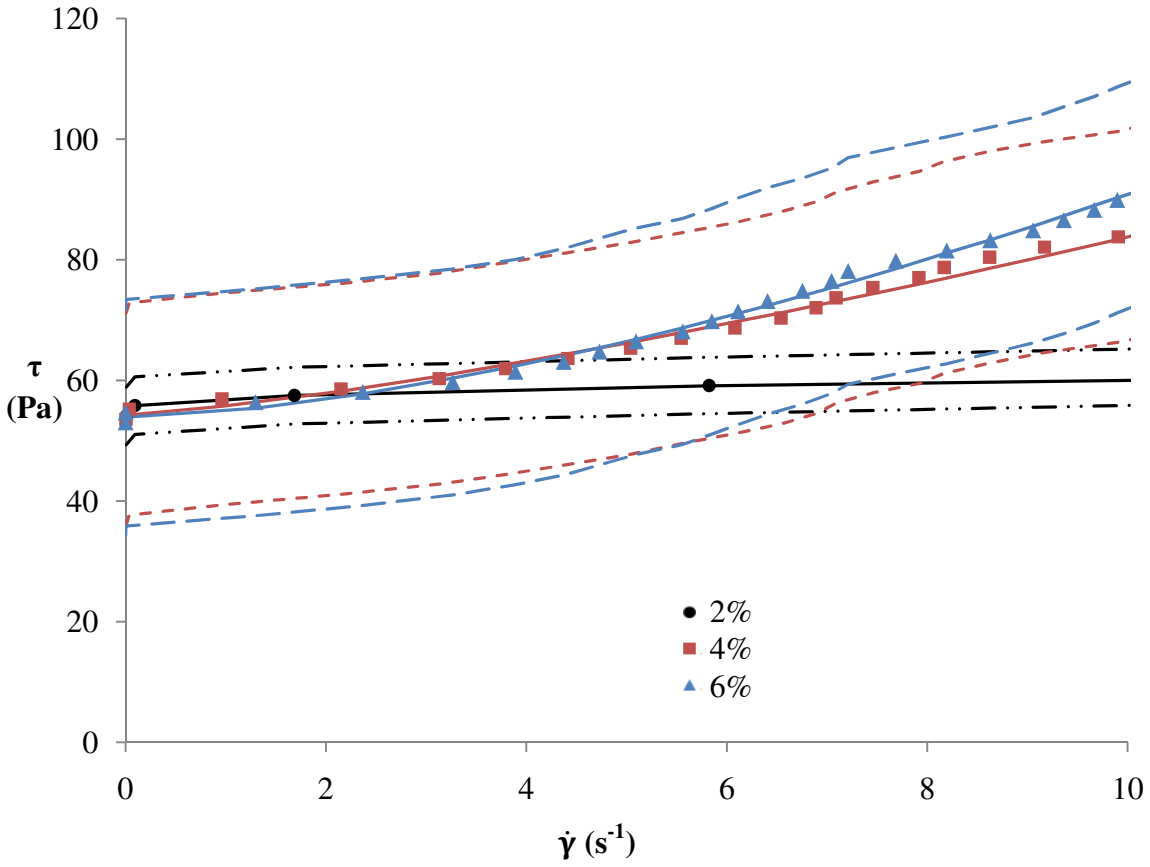

Figure 7. Flow Curves with Herschel/Bulkley Fittings and 95% Confidence Intervals for 30% Paraffin Wax Emulsions at 25 °C vs. Emulsifier Concentration.

The 4% and 6% Span 60® emulsions have a Herschel/Bulkley flow index (n) greater than one. This is because the slopes of the flow curves increase with increasing shear rate. Normally this would be an indication of shear-thickening behavior. However, in the case of some emulsions, this is due to a reduction of droplet size caused by droplet subdivision resulting from the shear forces. This subdivision causes an increase in volume-specific surface area resulting in increased interactions between the droplets (Mezger, 2006). Droplet subdivision can produce a tendency towards creaming under shear. Creaming is the migration of the wax to the surface of the emulsion leading to tacky behavior (Mezger, 2006).

Actually, all of the emulsions show a rapid drop in viscosity (η) after yielding giving way to a second region approaching nearly Newtonian behavior, as can be seen by looking at the viscosity curves in Figure 8 below (Mezger, 2006; Kamerkar, 2010). Each curve is approaching an infinite shear viscosity (η_∞). The infinite shear viscosity is the limit of the viscosity function as it approaches an infinite shear rate.

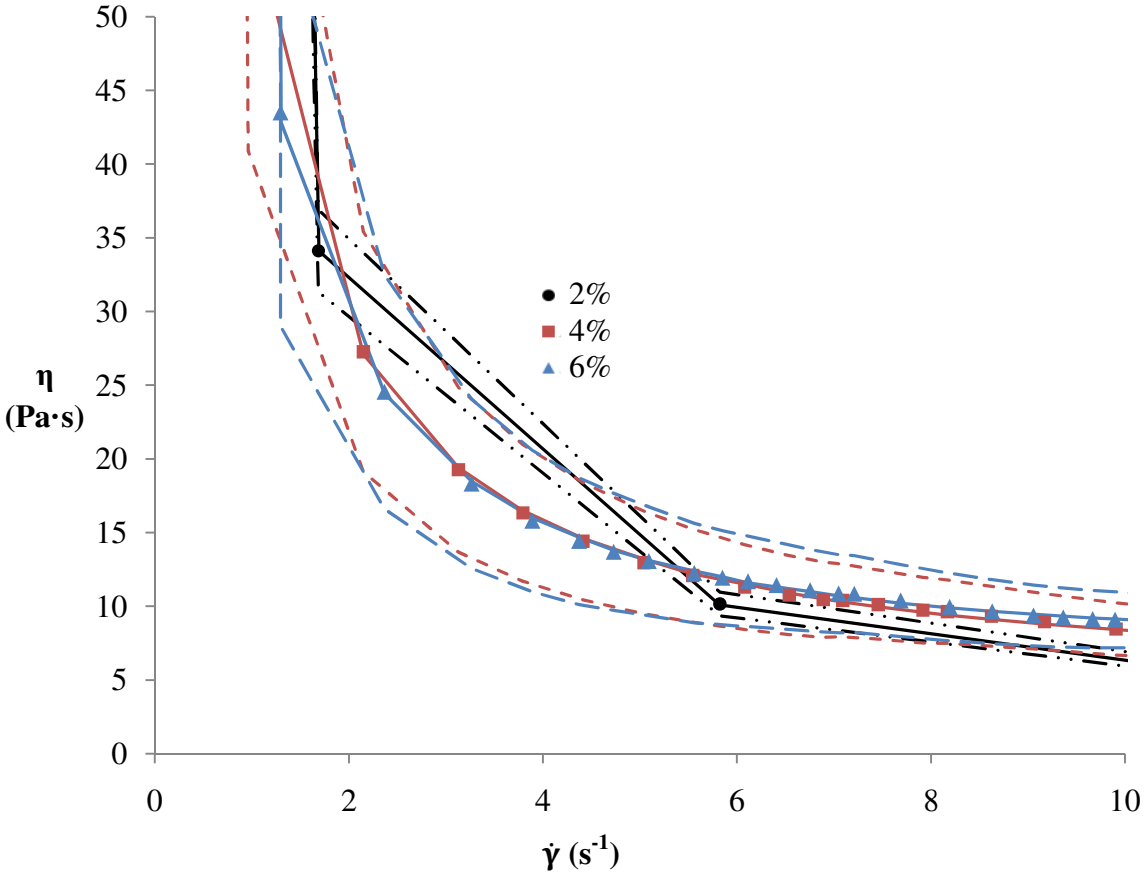

Figure 8. Viscosity Curves with Herschel/Bulkley Fittings and 95% Confidence Intervals for 30% Paraffin Wax Emulsions at 25 °C vs. Emulsifier Concentration.

Looking at the flow curve 95% confidence intervals there is no discernable difference between the 4% and 6% Span 60® emulsions. However, the 2% Span 60® emulsion shows shear-thinning behavior with a flow index less than one (Ma et al., 1995). The wax emulsions in this study are not truly emulsions (made of two immiscible liquids), but actually dispersions, because the waxes are solids over the temperature range of this study (Larson, 1998). However, these waxes have viscoelastic properties of their own. They are plastic (malleable) meaning that they can undergo non-reversible deformation (Mezger, 2006). If there is no creaming due to droplet subdivision to mask the effect, then droplet deformation could be responsible for the shear-thinning observed. This causes shear-thinning as the droplets deform into ellipsoids in the direction of flow. The decreased equatorial radii of the droplets produce a decrease in collision frequency between droplets (Mezger, 2011). This shear thinning will eventually give way to a η_∞ after all droplets have deformed completely (Mezger, 2006).

There is no appreciable difference in the yield points (τ_y) of these three emulsions, especially when taking the 95% confidence intervals into account. It would appear that within this Span 60® concentration range the τ_y does not change. This would mean that additional Span 60® above a concentration of 2% does not produce a significantly stronger three-dimensional network structure.

This difference in flow indices shows that to prevent shear-thinning, produce a quick transition from τ_y to η_∞, and to produce tackiness under shear, at least 4% Span 60® needs to be used. However, no significant difference in behavior is seen with the addition of more emulsifier.

The average temperature sweep curves for the emulsions with different Span 60© concentrations are displayed in Figure 9 along with each curve's 95% confidence interval. The averaged raw data for these curves can be found in Appendix A.

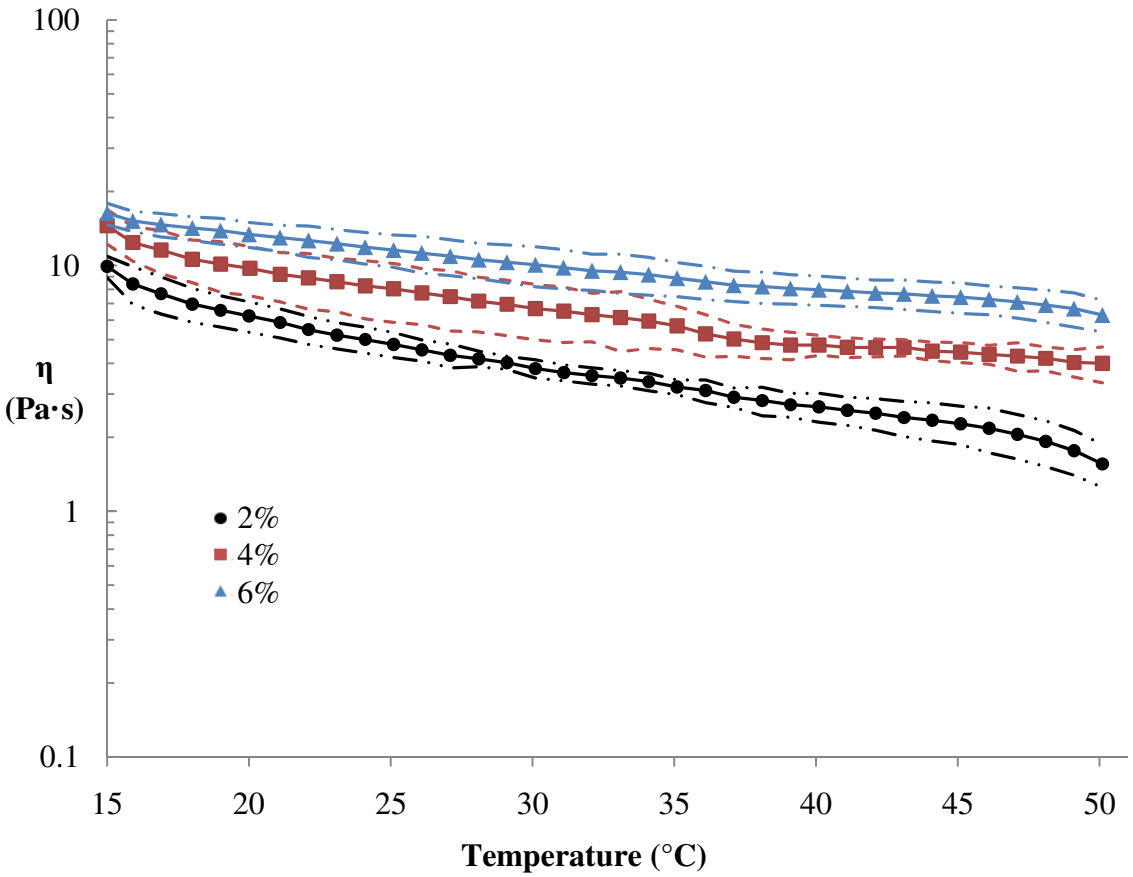

Figure 9. Temperature Sweep Curves with 95% Confidence Intervals for 30% Paraffin Wax Emulsions at 25 °C vs. Emulsifier Concentration.

Because every point in these temperature sweeps are taken well after the sample has yielded it can be assumed that the η at each point is approaching the η_∞ at that temperature. These emulsions all behave predictably, with η decreasing steadily with increase in temperature (Mezger, 2006).

With each increase in Span 60® concentration of 2% the η at each temperature increases by 67% ± 18% (mean ± standard deviation). This shows a direct relationship between emulsifier concentration and η_∞.

The parameters determined by oscillatory amplitude sweep for the emulsions of differing Span 60© concentrations are listed in Table 4.

Table 4. Oscillatory Amplitude Sweep Parameters for 30% Paraffin Wax Emulsions at 25 °C vs. Emulsifier Concentration.

Span 60® % (w/w)	Limit of the LVE Range γ_L (%)	Yield Point τ_y (Pa)
2	0.817	31.2
4	0.0988	49.9
6	0.196	41.7

The amplitude sweep CSD diagrams for the three emulsions are presented in Figures 10 through 12 with their 95% confidence intervals. All amplitude sweep CSS diagrams can be seen in Appendix B.

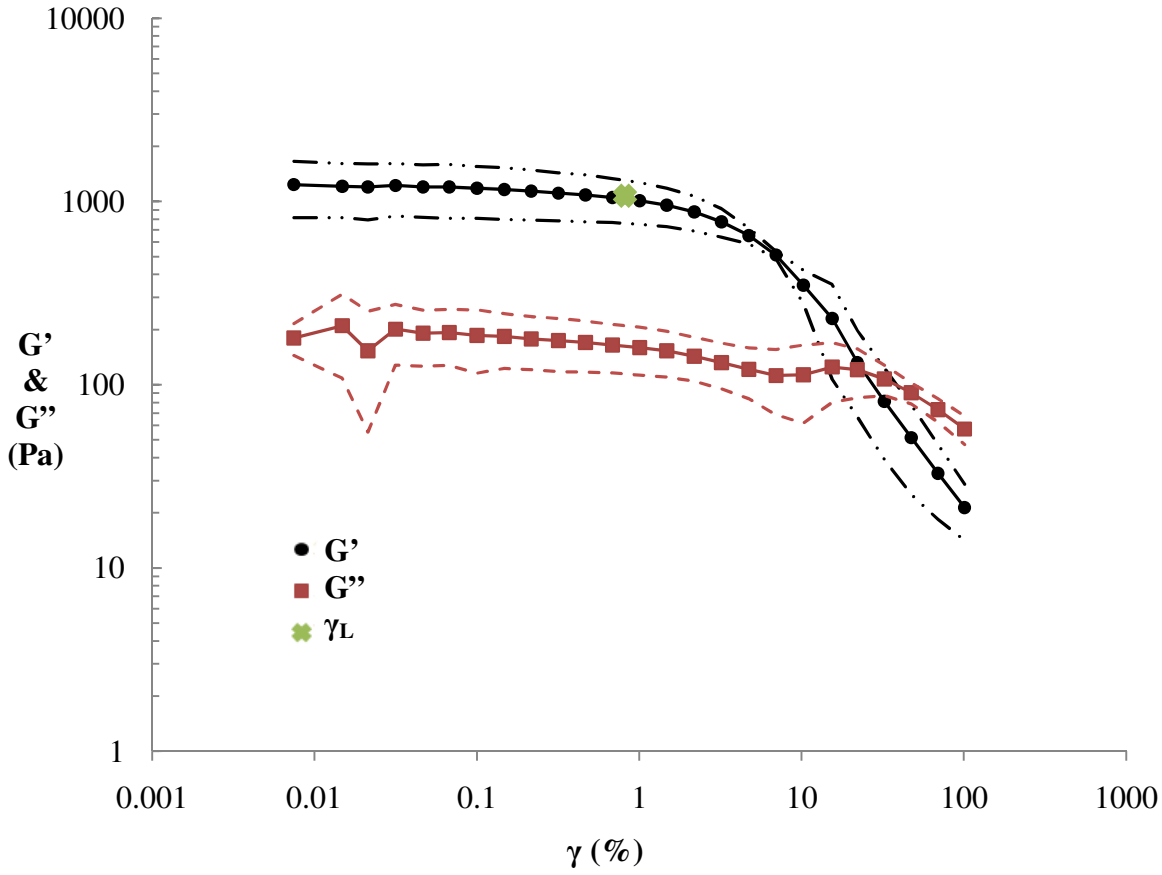

Figure 10. Amplitude Sweep (CSD) Diagram with 95% Confidence Intervals for 30% Paraffin Wax Emulsion with 2% Span 60®

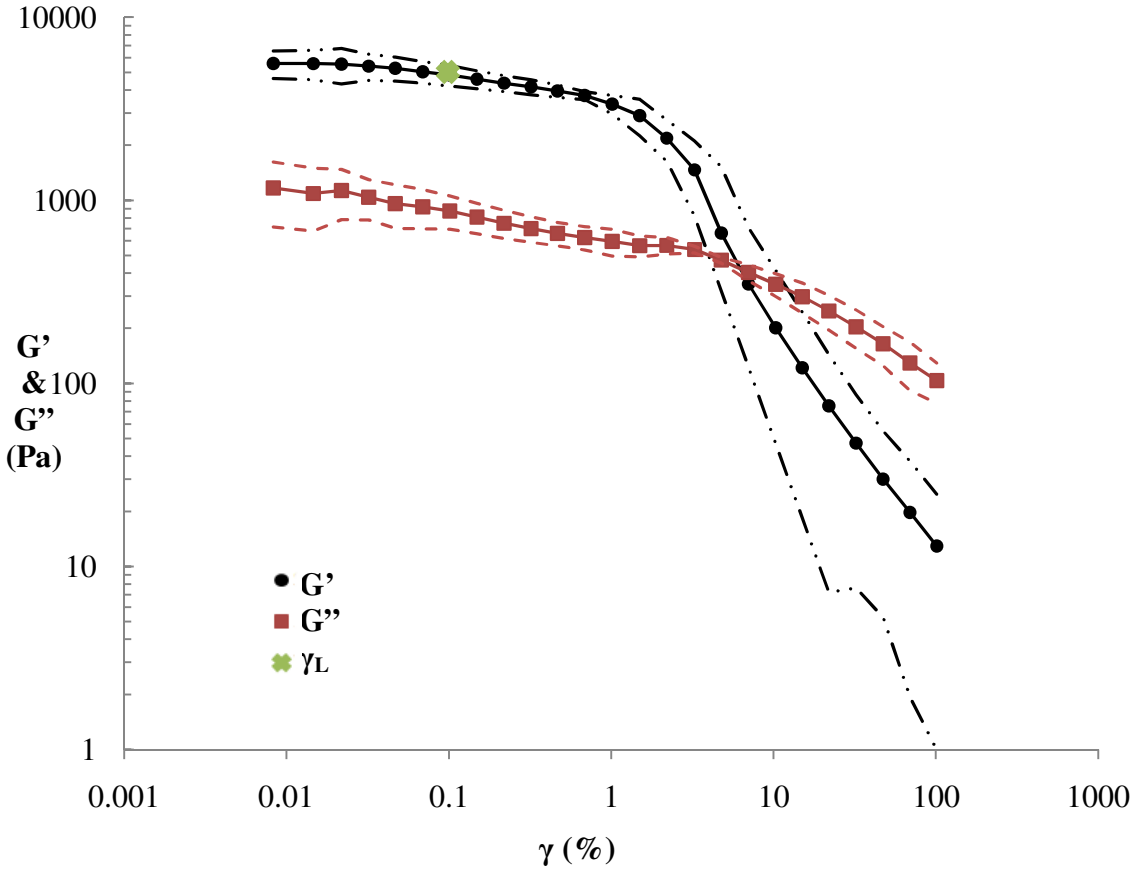

Figure 11. Amplitude Sweep (CSD) Diagram with 95% Confidence Intervals for 30% Paraffin Wax Emulsion with 4% Span 60®.

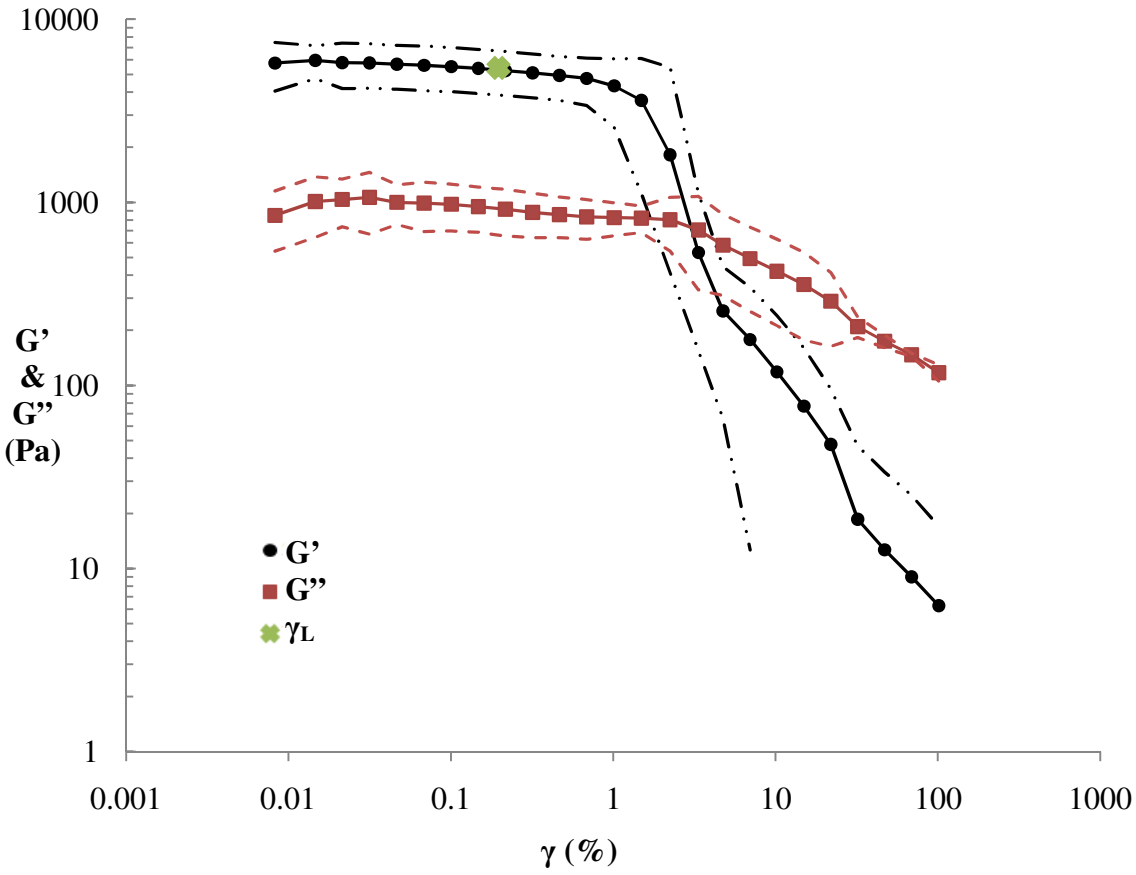

Figure 12. Amplitude Sweep (CSD) Diagram with 95% Confidence Intervals for 30% Paraffin Wax Emulsion with 6% Span 60®.

In the amplitude sweep for each emulsion, the storage modulus (G') is nearly an order of magnitude greater than the loss modulus (G") in the LVE region. This indicates a gel structural character producing stability at rest conditions and a yield point (Mezger, 2006). This confirms that all of these emulsions possess some shelf stability and will not flow at rest.

The γ_L values are the maximum strains that the samples can be subjected to and still return to their original shapes. In other words, it tells us how much the samples can

"jiggle". The 2% Span 60® emulsion is able to deform to a much greater extent than the other two due to a more flexible internal structure (Mezger, 2011). The 4% Span 60® emulsion would appear to have the most rigid internal structure.

Looking at the τ_y values it can be seen that the 4% Span 60® emulsion has the highest τ_y, denoting a stronger internal structure. This leads to the conclusion that 4% Span 60® is optimal for producing a three dimensional network structure. An excess of emulsifier in the 6% Span 60® emulsions actually reduces the strength and rigidity of the internal structure.

Every oscillatory τ_y is lower than the corresponding rotational τ_y. This is because the amplitude sweeps do not simulate a sample at rest or even in a slow motion state as they were carried out at a constant angular frequency of $\omega = 10\ s^{-1}$, which had already partially deformed these sensitive samples (Mezger, 2006). The range delimited by the two τ_y values can be treated as a "yield zone" where permanent deformation is occurring and the sample is going from a gel-like state to a liquid-like state.

The frequency sweep diagrams for the three emulsions of differing Span 60© concentrations and their 95% confidence intervals can be seen in figures 13, 14, and 15.

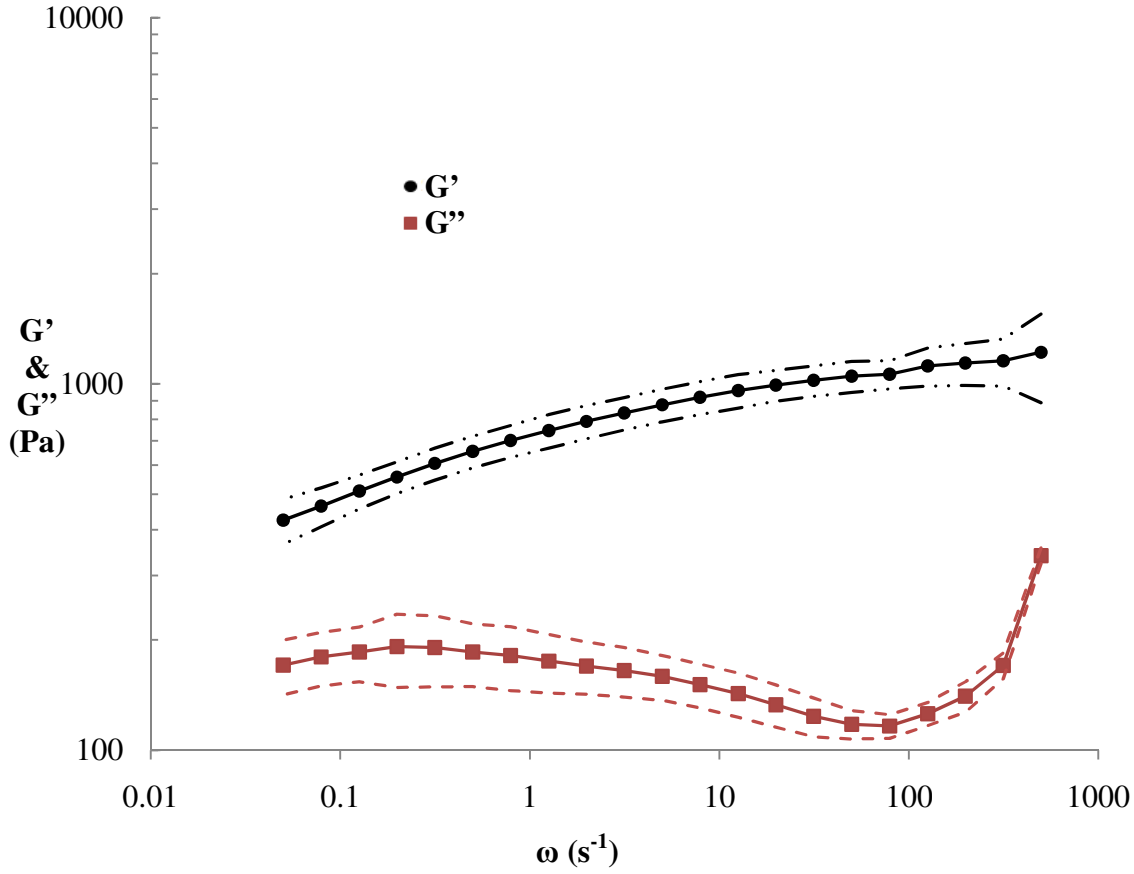

Figure 13. Frequency Sweep Diagram with 95% Confidence Intervals for 30% Paraffin Wax Emulsion with 2% Span 60®

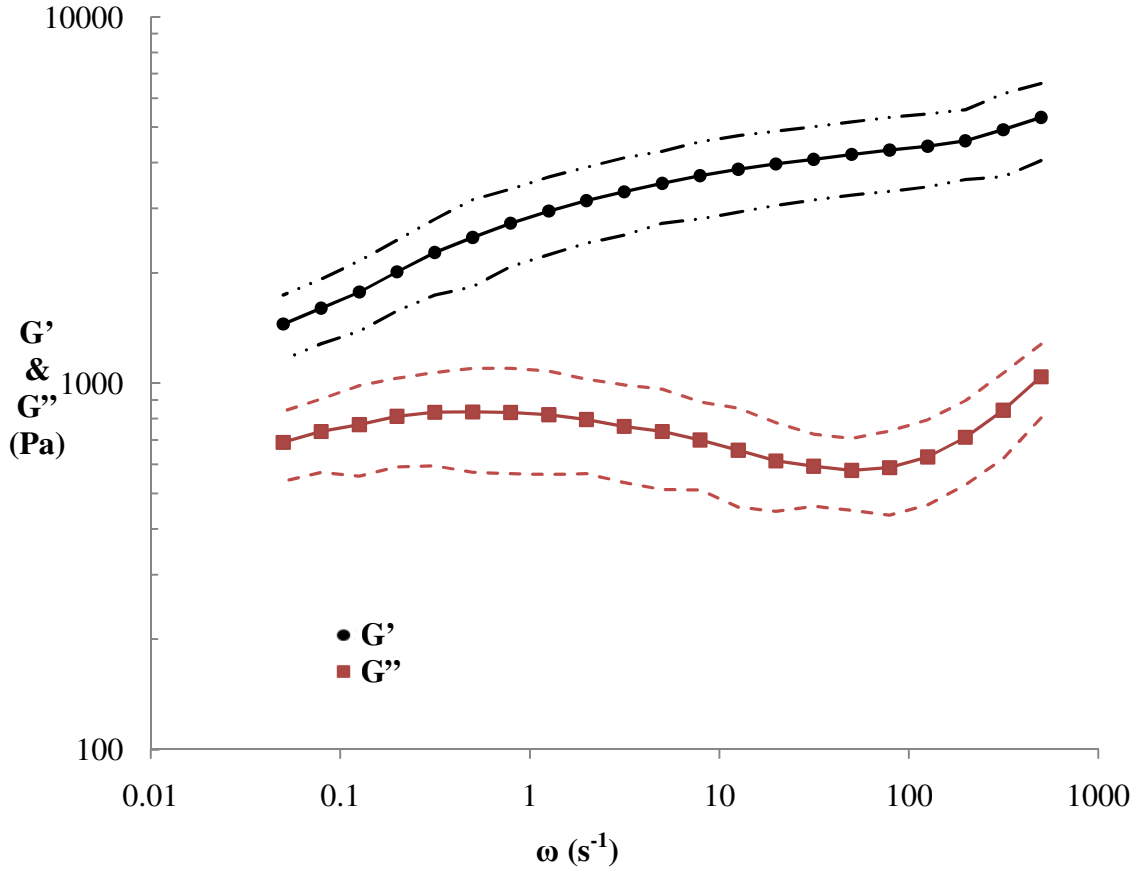

Figure 14. Frequency Sweep Diagram with 95% Confidence Intervals for 30% Paraffin Wax Emulsion with 4% Span 60®.

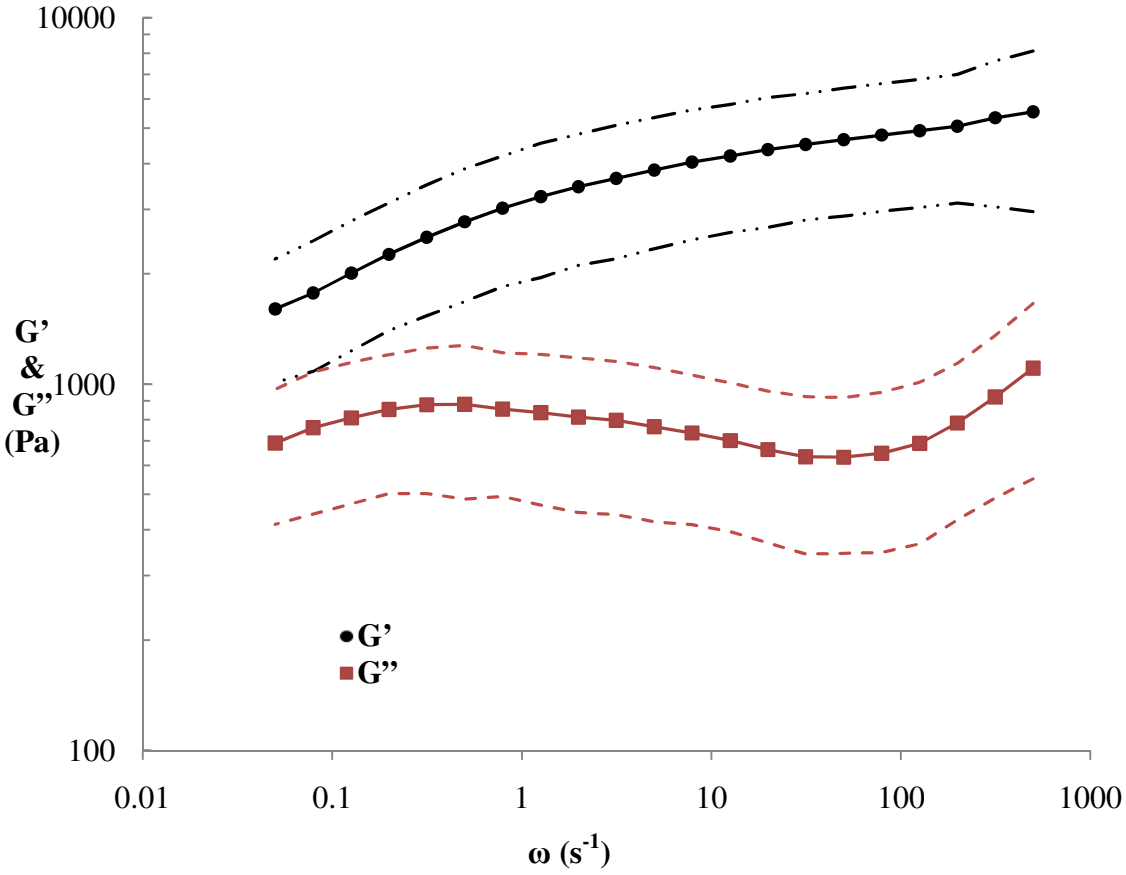

Figure 15. Frequency Sweep Diagram with 95% Confidence Intervals for 30% Paraffin Wax Emulsion with 6% Span 60®.

The frequency sweeps reveal that all three emulsions have similar viscoelastic properties and stability. All samples have G' higher than G" over the range of frequencies, denoting a gel-like character (Ma et al., 1995; Mezger, 2006). This can be attributed to the three dimensional networks formed between Span 60® molecules adsorbed to paraffin wax droplets.

Because they possess G'/G" higher than 1 Pa but lower than 10 Pa throughout the range of frequencies, and the moduli show frequency dependence, all of these emulsions

can be characterized as materials possessing weak gel-like behavior (Dapčević-Hadnađev, 2009; Nishinari, 2009). A "weak gel" may not be a true gel at all, but a "structured liquid" that, given enough time, will eventually flow at rest due to gravity. However, the flow may not occur within the timescale of conventional observation (Nishinari, 2009).

The magnitudes of the maximum G' are on the order of 10^3 Pa for the 4% and 6% Span 60® emulsions, which means that these gels possess a soft and yielding consistency that breaks down (flows) easily under shear stress (Ma et al., 1995). The 2% Span 60® emulsion has a maximum storage modulus magnitude of 10^2, meaning that it is very soft and yielding in consistency and even more susceptible to being broken down under shear stress. However, having G' >> 10 Pa means that all of these emulsions are stable under conditions where the shear stress has not been reached (Mezger, 2006).

At lower **ω** all emulsions still have G' > G" which means that they all have some long-term storage stability. However, the storage moduli (G') also show sloping at lower frequencies, denoting that over long periods of time some flow and creaming could occur (Mezger, 2006). This is weak gel-like behavior.

The magnitude of G' at the lowest frequency ($\omega = 0.05\ s^{-1}$) specifies the structural strength of an emulsion at rest; this is called the "gel strength" (Mezger, 2006). These magnitudes are listed in Table 5. The 2% emulsion is one order of magnitude lower in stability at rest than the other two. The difference between the 4% emulsion and the 6% emulsion is negligible as both values are well within the 95% confidence interval for both emulsions.

Table 5. Oscillatory Frequency Sweep Magnitudes of G' at the Lowest Frequency (ω = 0.05 s^{-1}) for 30% Paraffin Wax Emulsions at 25 °C vs. Emulsifier Concentration.

Span 60® % (w/w)	Magnitude of G' at ω = 0.05 s^{-1} (Pa)
2	395
4	1450
6	1650

Syneresis, (stiffing with time) will not occur with any of these samples according to this data. This is because the maximum G' is not more than one order of magnitude above the maximum G" for any of these emulsions (Mezger, 2006).

EFFECTS OF WAX AND EMULSIFIER TYPES

Span 60© Emulsions

The flow parameters from the HB regression analysis applied to the averaged flow curves for the 30% paraffin wax and 30% soy was emulsions with 4% Span 60® at 15 °C, 25 °C and 35 °C are listed in Table 6. These fitted curves are displayed in Figures 16 and 17 along with each curve's 95% confidence interval.

Table 6. Herschel/Bulkley Flow Parameters for 30% Paraffin Wax and Soy Wax Emulsions with 4% Span 60® vs. Temperature. Herschel/Bulkley model: $\tau = \tau_y + k \cdot \dot{\gamma}^n$

Wax Type	Temperature (°C)	Yield point τ_y (Pa)	Consistency k (Pa·s^n)	Flow Index n	Correlation Ratio r^2
Paraffin	15	60.9	3.14×10^{0}	1.03×10^{0}	0.988
Paraffin	25	54.3	1.44×10^{0}	1.31×10^{0}	0.993
Paraffin	35	47.7	6.85×10^{-3}	3.71×10^{0}	0.982
Soy	15	25.4	3.63×10^{0}	1.20×10^{0}	0.999
Soy	25	32.6	7.20×10^{-1}	1.58×10^{0}	0.995
Soy	35	22.0	1.31×10^{0}	1.26×10^{0}	0.964

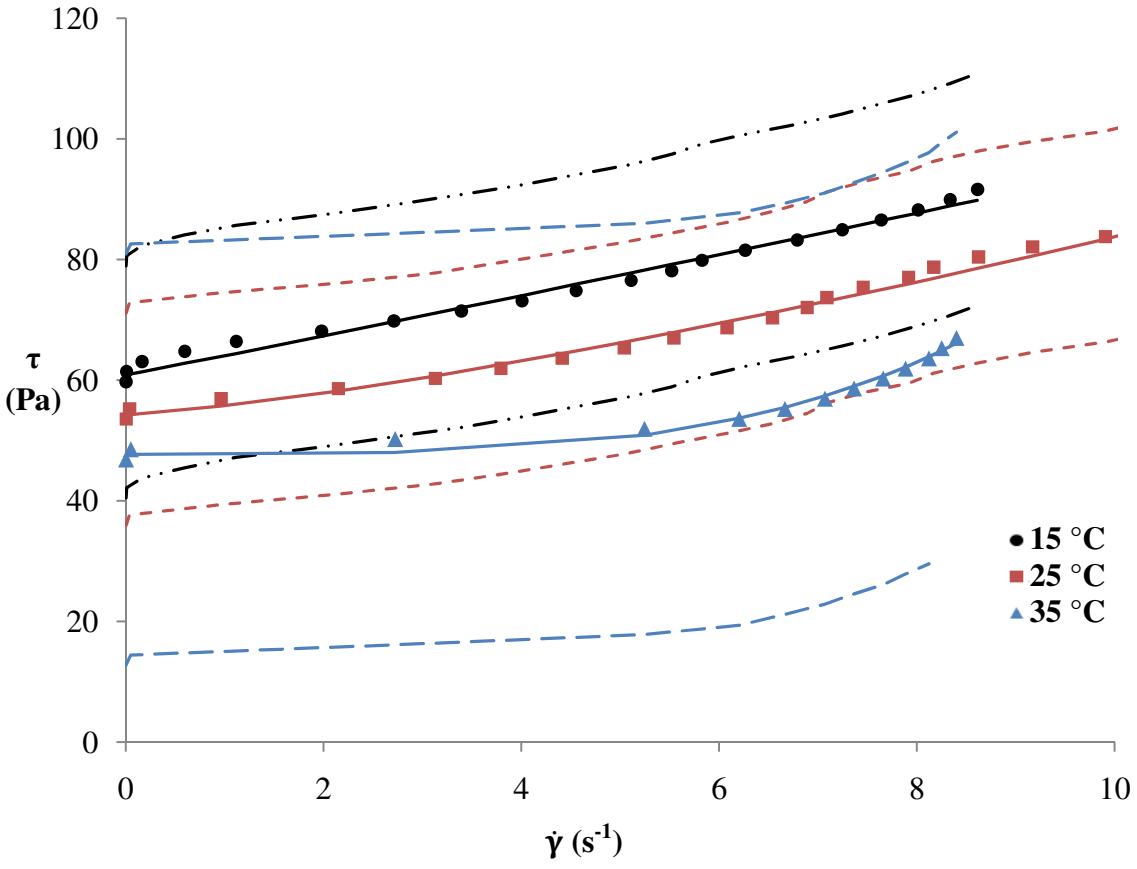

Figure 16. Flow Curves with Herschel/Bulkley Fittings and 95% Confidence Intervals for 30% Paraffin Wax Emulsion with 4% Span 60® at 15 °C, 25 °C and 35 °C.

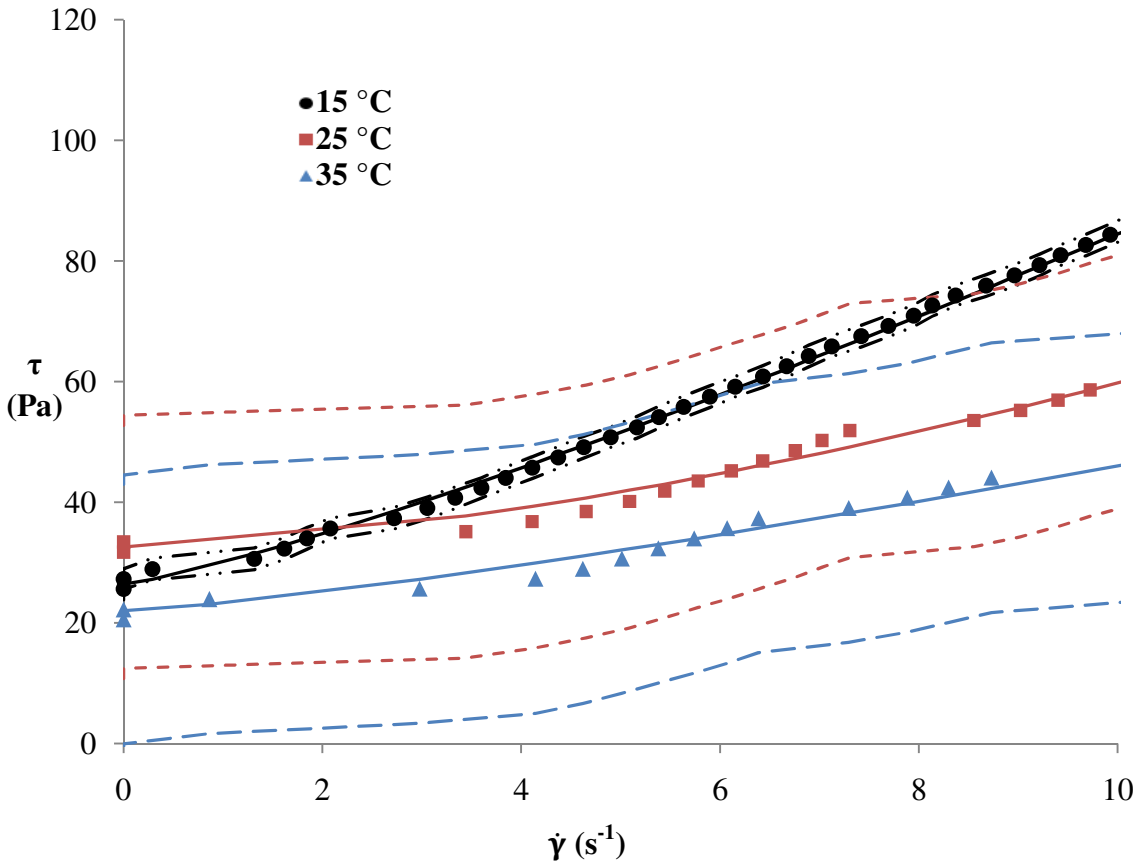

Figure 17. Flow Curves with Herschel/Bulkley Fittings and 95% Confidence Intervals for 30% Soy Wax Emulsion with 4% Span 60® at 15 °C, 25 °C and 35 °C.

As was seen with the 4% and 6% emulsions in the "Effects of Emulsifier Concentration" section, both of these emulsions at every temperature have a Herschel/Bulkley flow index (n) greater than one. Rather than being an indication of true shear-thickening, this denotes droplet subdivision leading to creaming and tackiness (Mezger, 2006). The paraffin wax emulsion shows temperature dependence with respect to flow index. The 15 °C curve shows almost perfect Bingham plastic behavior with a flow index of nearly one while at 25 °C there is a small increase. There is much greater increase at 35 °C, denoting a greater degree of subdivision leading to creaming. There is

no apparent temperature dependence within this temperature range for the soy wax emulsion.

All of these emulsions actually have a have a region of yielding and rapid thinning with a second region of nearly Newtonian behavior approaching an η_∞, as can be seen by looking at the viscosity curves in Figures 18 and 19 (Mezger, 2006; Kamerkar, 2010).

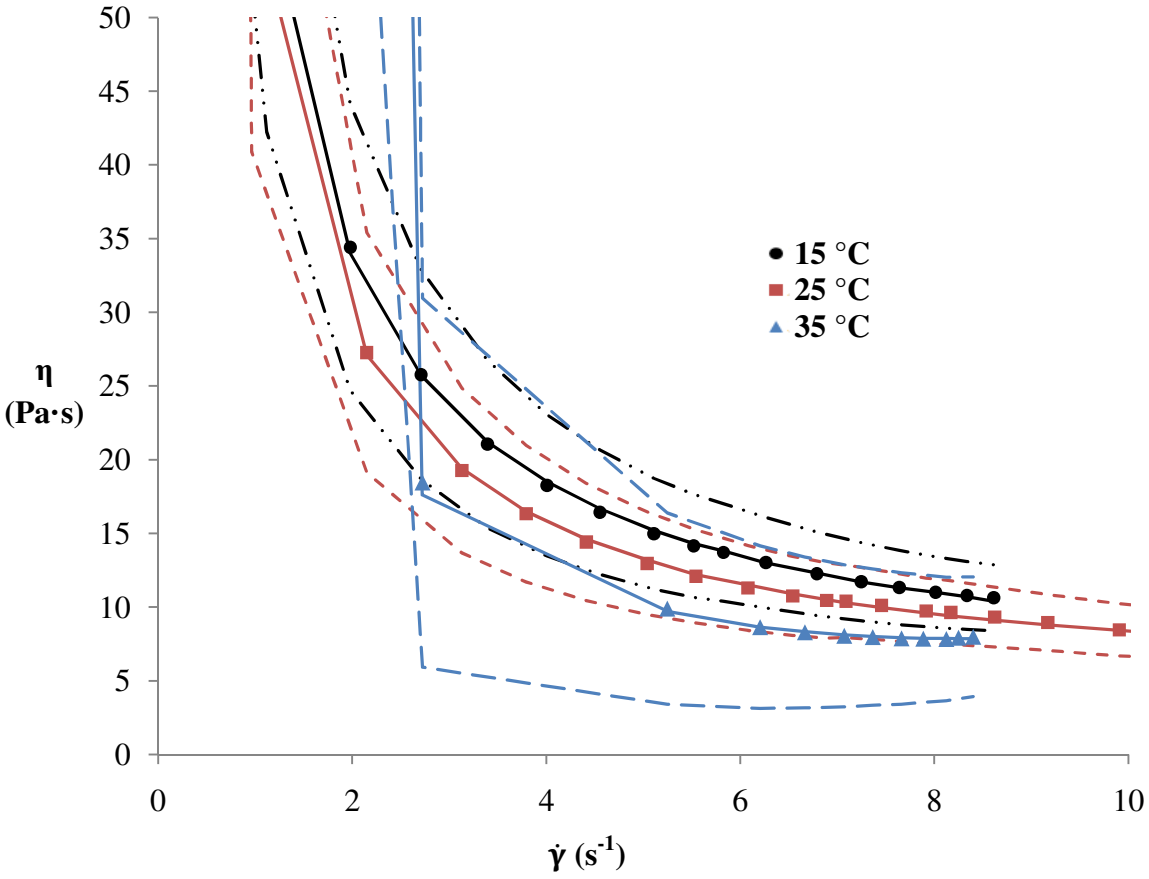

Figure 18. Viscosity Curves with Herschel/Bulkley Fittings and 95% Confidence Intervals for 30% Paraffin Wax Emulsion with 4% Span 60® at 15 °C, 25 °C, and 35 °C.

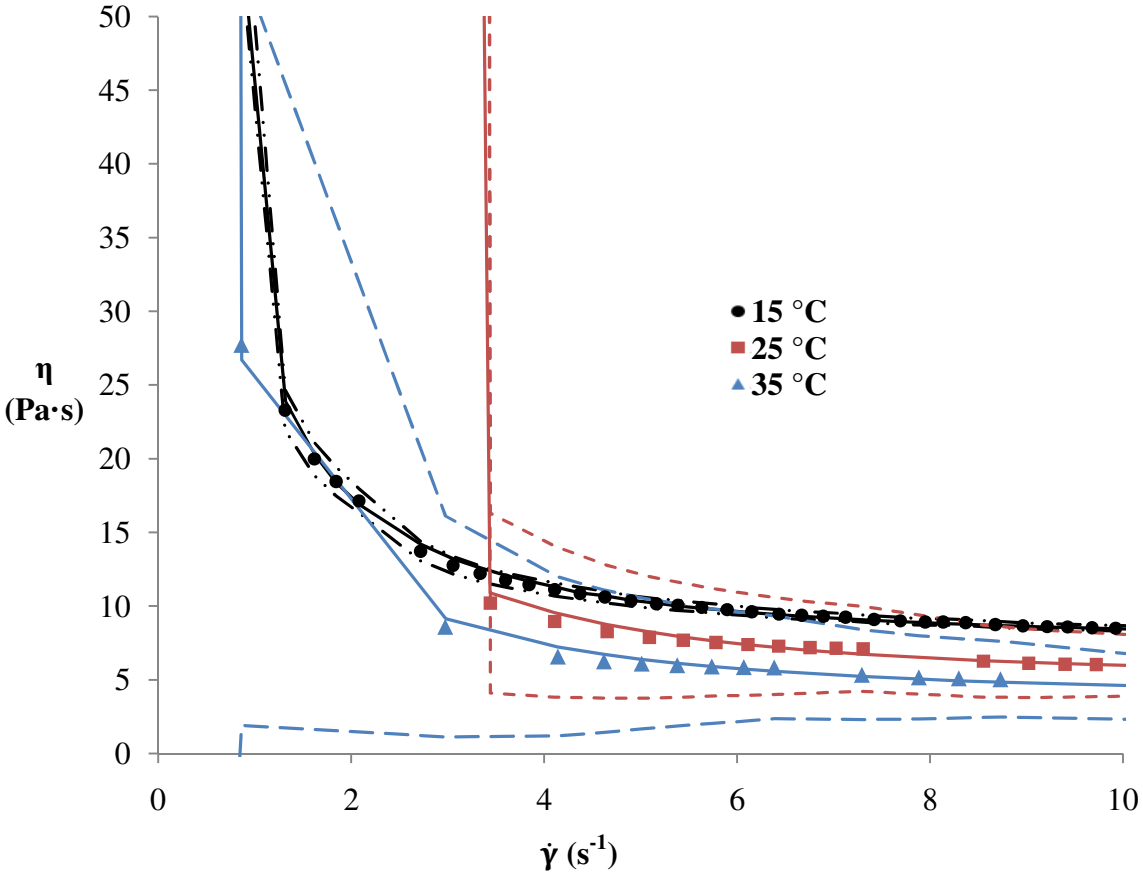

Figure 19. Viscosity Curves with Herschel/Bulkley Fittings and 95% Confidence Intervals for 30% Soy Wax Emulsion with 4% Span 60® at 15 °C, 25 °C, and 35 °C.

The τ_y for the paraffin emulsion at each temperature is well within every 95% confidence interval. The same is true for the soy wax emulsion. Therefore, no conclusions can be drawn as to the effect of temperature within this range on the τ_y of either emulsion, except that it would appear that the structures responsible for τ_y in both emulsions do not vary in strength to any great degree within this temperature range. However, it can be stated that the soy wax emulsion has an overall lower τ_y than the paraffin wax emulsion, indicating a weaker overall internal three-dimensional network structure before yielding (Mezger, 2006).

The temperature sweep curves for the 30% paraffin wax and soy wax emulsions with 4% Span 60® are displayed in Figure 20 along with each curve's 95% confidence interval. All temperature sweep averaged data can be found in Appendix A.

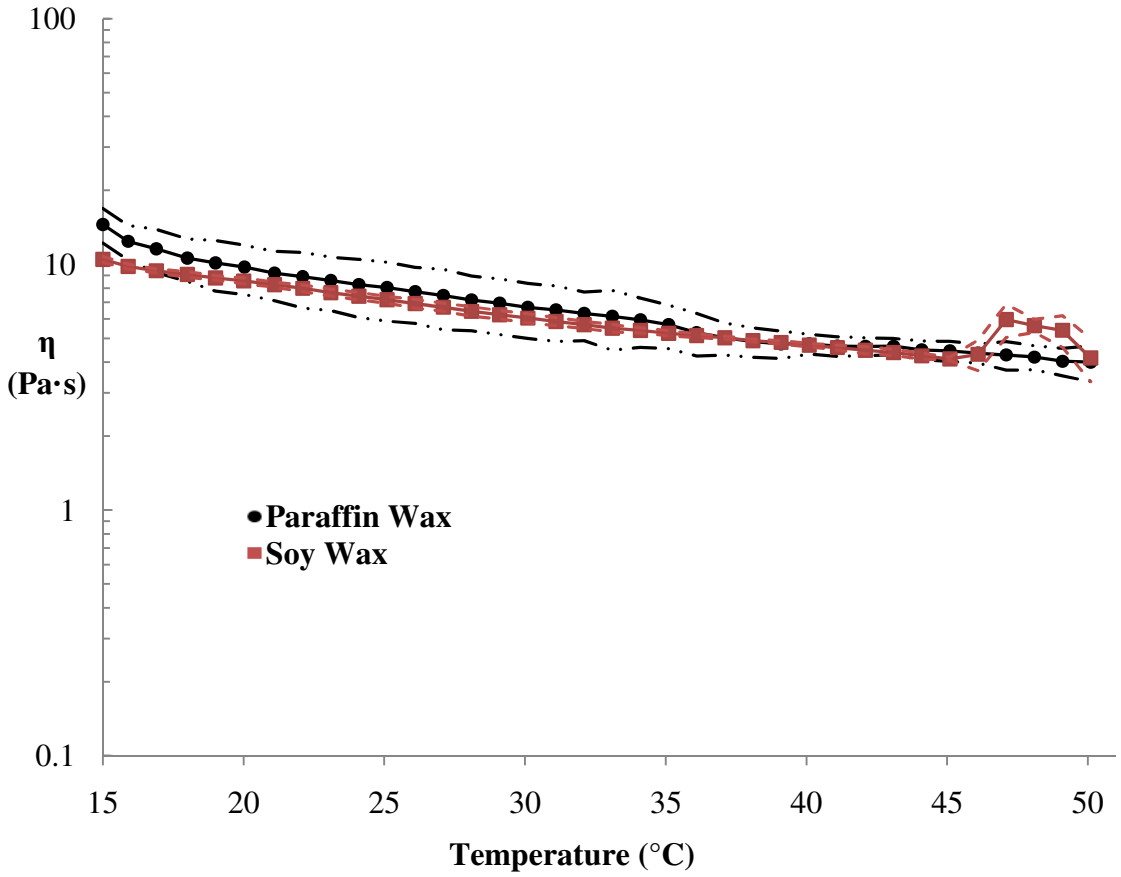

Figure 20. Temperature Sweep Curves for 30% Paraffin Wax and Soy Wax Emulsions with 4% Span 60®.

For the most part both emulsions behave predictably, with viscosity (η) decreasing steadily with increase in temperature. They both show similar η's at any given temperature until the soy wax emulsion has a sudden peak in viscosity between 45 °C and 50 °C. Some structural change like gelling is occurring at these higher

temperatures increasing the three-dimensional network structure strength, and then it goes away.

The parameters determined by oscillatory amplitude sweep for 30% paraffin wax and soy wax emulsions with 4% Span 60® are listed in Table 7.

Table 7. Oscillatory Amplitude Sweep Parameters for 30% Paraffin Wax and Soy Wax Emulsions with 4% Span 60® at 25 °C.

Wax Type	Limit of the LVE Range γ_L (%)	Yield Point τ_y (Pa)
Paraffin	0.0988	49.9
Soy	0.273	15.6

The amplitude sweep CSD diagrams for the two emulsions are presented in Figures 21 and 22 with their 95% confidence intervals. All amplitude sweep CSS diagrams can be seen in Appendix B

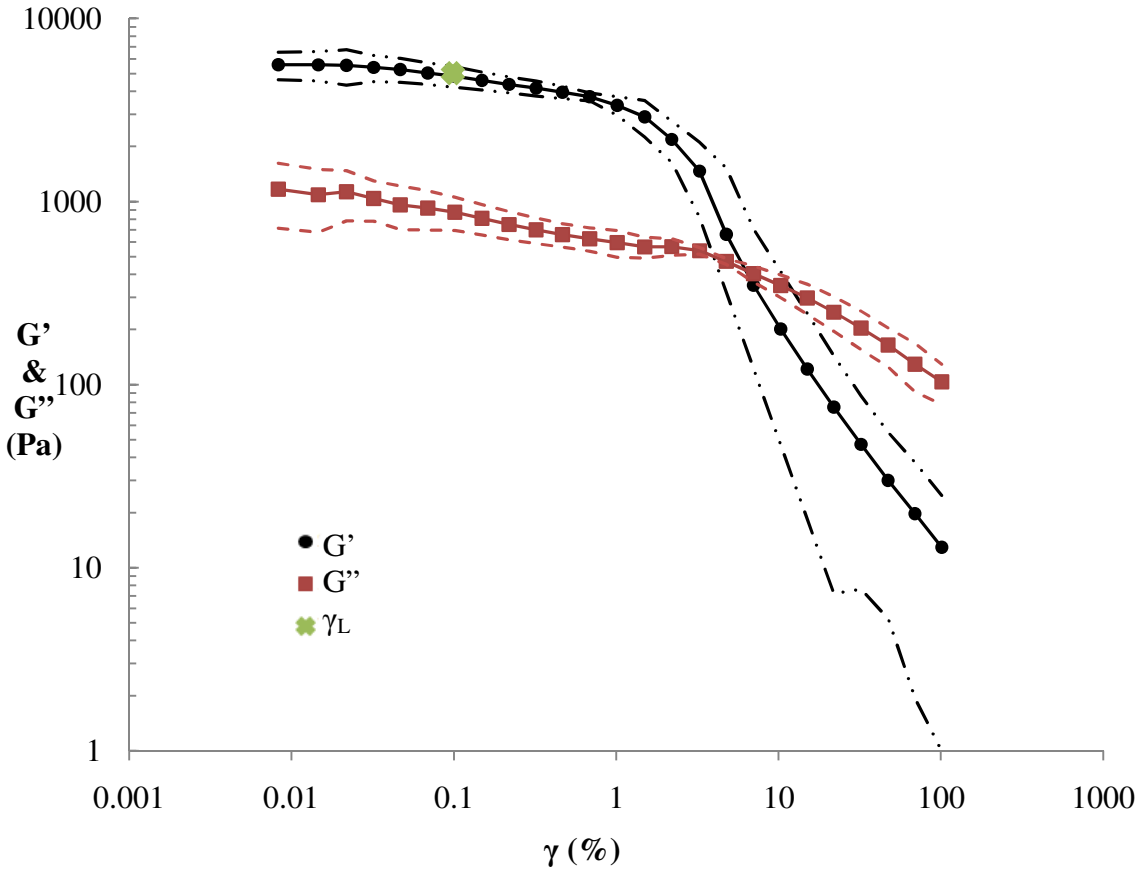

Figure 21. Amplitude Sweep (CSD) Diagram with 95% Confidence Intervals for 30% Paraffin Wax Emulsion with 4% Span 60®.

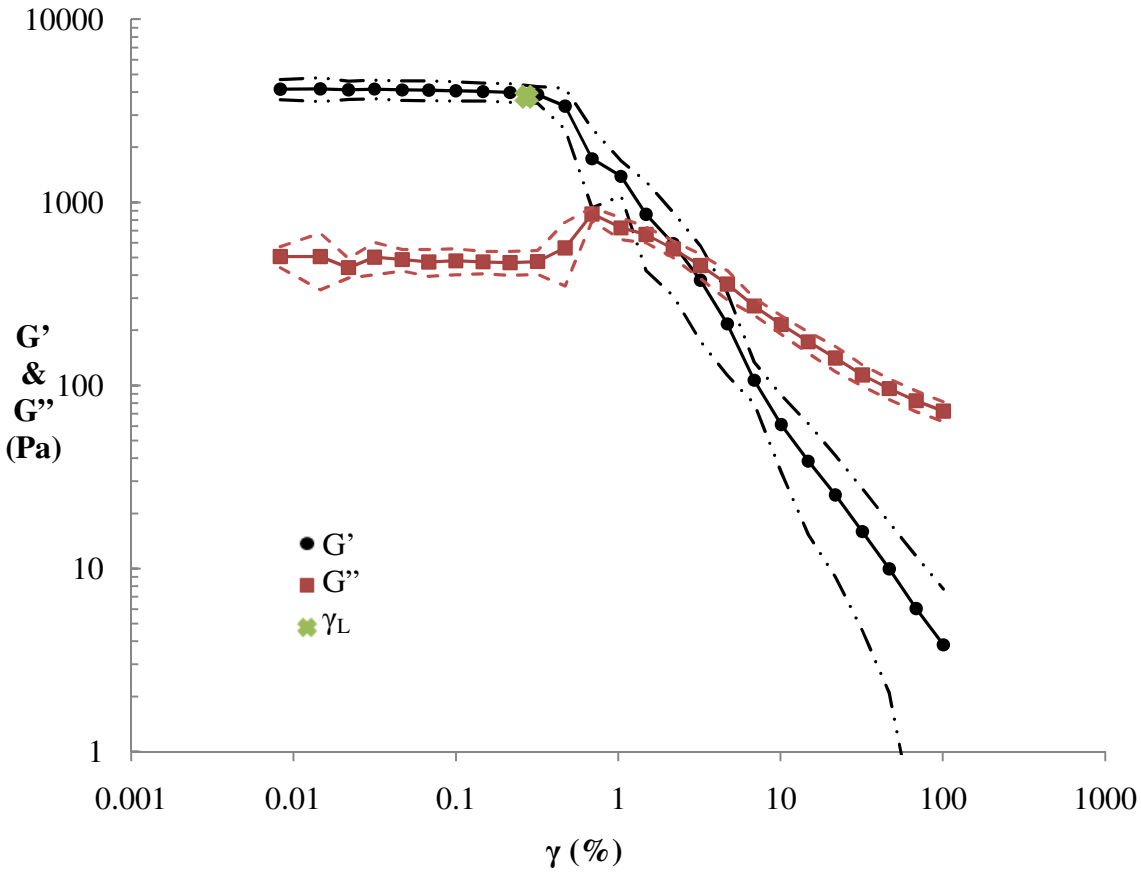

Figure 22. Amplitude Sweep (CSD) Diagram with 95% Confidence Intervals for 30% Soy Wax Emulsion with 4% Span 60®.

Both emulsions show gel character and have some shelf stability as indicated by each G' being nearly an order of magnitude higher than each G" in the LVE region. With the paraffin emulsion there is a significant range of γ between the γ_L and the point where the G' starts to rapidly dip towards the G". This denotes a gradual plastic deformation. This is not seen with the soy wax, which shows a much quicker transition denoting brittle behavior. The soy wax also shows a G" maxima between γ_L and the point where G' and G" cross over. This is because of the breaking down of a network of

superstructures before flowing. This breaking down of superstructures (possibly the disintegration of agglomerates) produces mesoscopic discontinuities, the propagation of which imparts brittle behavior (Mezger, 2011).

The paraffin wax emulsion shows a higher τ_y, denoting a stronger internal structure before shear than the soy wax emulsion. Both τ_y's are lower than the corresponding values determined by rotational CSS tests (producing a "yield zone"), but are within the 95% confidence intervals for each emulsion.

The frequency sweep diagrams for the paraffin wax and soy wax emulsions with 4% Span 60© and their 95% confidence intervals can be seen in figures 23 and 24.

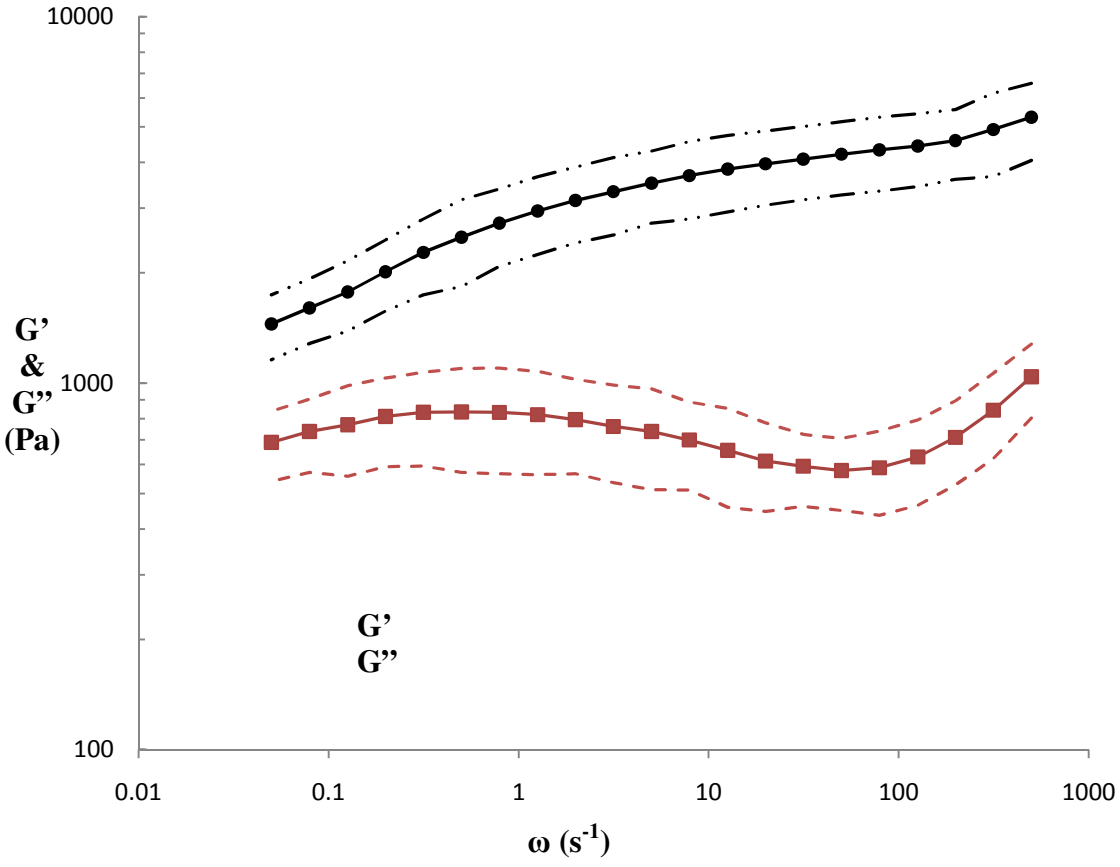

Figure 23. Frequency Sweep Diagram with 95% Confidence Intervals for 30% Paraffin Wax Emulsion with 4% Span 60®.

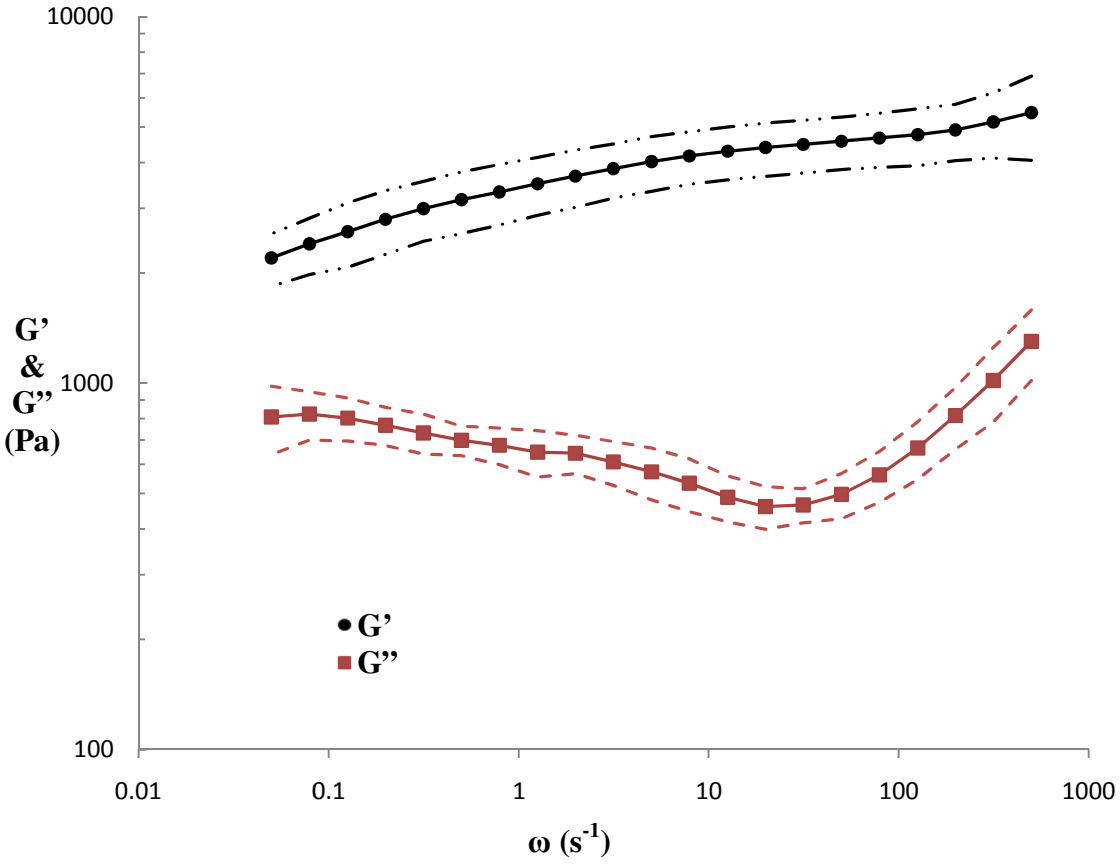

Figure 24. Frequency Sweep Diagram with 95% Confidence Intervals for 30% Soy Wax Emulsion with 4% Span 60®.

These two frequency sweep diagrams are very similar meaning that both emulsions have similar viscoelastic properties and stability. They possess G'/G" higher than 1 Pa but lower than 10 Pa throughout the range of frequencies, and the moduli show

frequency dependence. Because of this, both of these emulsions can be characterized as materials possessing weak gel-like behavior with no tendency towards syneresis.

Because the magnitudes of the maximum G' for both emulsions are on the order of 10^3 Pa they have a soft and yielding consistency. They have a measure of long-term storage stability with G' > G" at lower ω's.

The magnitudes of G' at the lowest frequency ($\omega = 0.05\ s^{-1}$) are listed in Table 8.

Table 8. Oscillatory Frequency Sweep Magnitudes of G' at the Lowest Frequency ($\omega = 0.05\ s^{-1}$) for 30% Paraffin Wax and Soy Wax Emulsions with 4% Span 60®.

Wax Type	Magnitude of G' at $\omega = 0.05\ s^{-1}$ (Pa)
Paraffin	1450
Soy	2200

These magnitudes of G' at the lowest frequency show that the soy wax emulsion has slightly higher gel strength than the paraffin emulsion.

TEA Stearate Emulsions

The flow parameters from the HB regression analysis applied to the averaged flow curves for the 30% paraffin wax and 30% soy was emulsions with 4% TEA stearate at 15 °C, 25 °C and 35 °C are listed in Table 9. These fitted curves are displayed in Figures 25 and 26 along with each curve's 95% confidence interval.

Table 9. Herschel/Bulkley Flow Parameters for 30% Paraffin Wax and Soy Wax Emulsions with 4% TEA Stearate vs. Temperature.
Herschel/Bulkley model: $\tau = \tau_y + k \cdot \dot{\gamma}^n$

Wax Type	Temperature (°C)	Yield point τ_y (Pa)	Consistency k (Pa·s^n)	Flow Index n	Correlation Ratio r^2
Paraffin	15	7.97	5.88×10^{0}	5.41×10^{-1}	0.983
Paraffin	25	5.79	5.25×10^{0}	5.19×10^{-1}	0.966
Paraffin	35	4.71	9.88×10^{-1}	5.94×10^{-1}	0.985
Soy	15	8.56	7.74×10^{0}	9.86×10^{-1}	0.999
Soy	25	15.3	3.66×10^{0}	1.18×10^{0}	0.995
Soy	35	32.8	6.12×10^{-1}	1.55×10^{0}	0.994

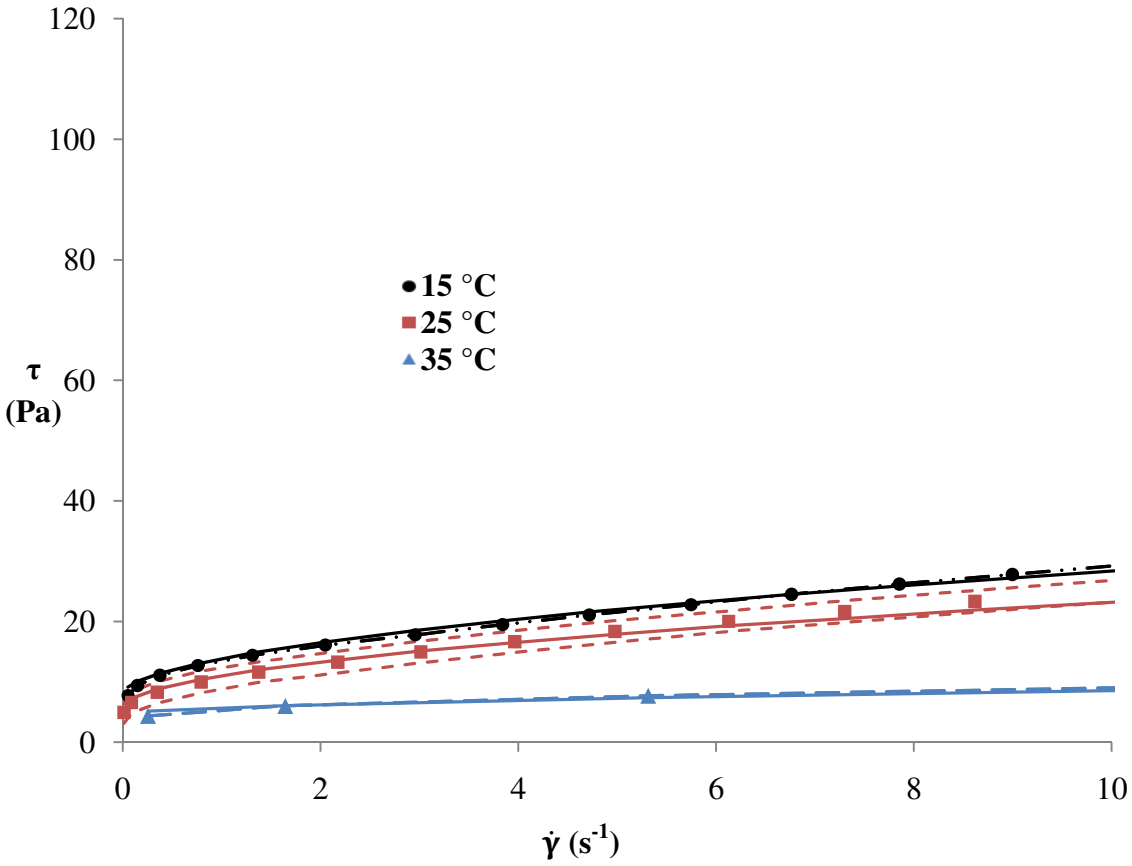

Figure 25. Flow Curves with Herschel/Bulkley Fittings and 95% Confidence Intervals for 30% Paraffin Wax Emulsion with 4% TEA Stearate at 15 °C, 25 °C and 35 °C.

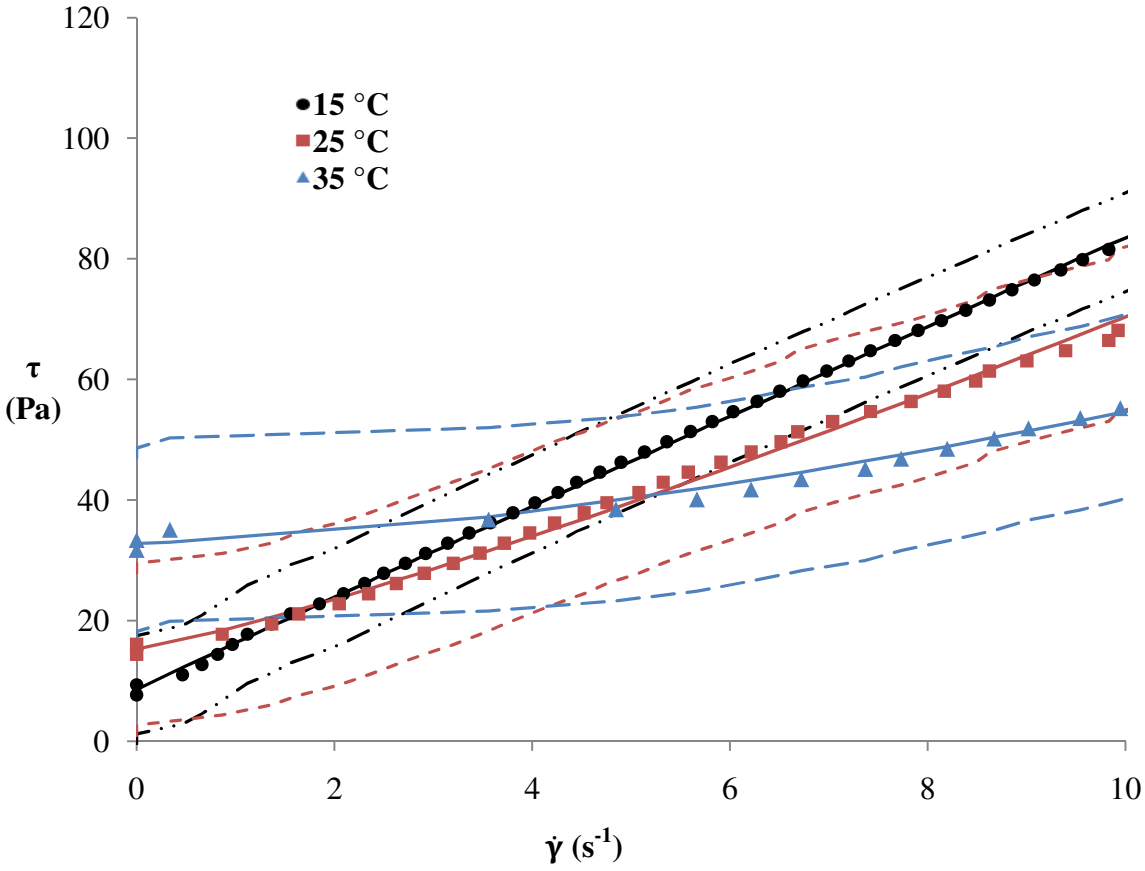

Figure 26. Flow Curves with Herschel/Bulkley Fittings and 95% Confidence Intervals for 30% Soy Wax Emulsion with 4% TEA Stearate at 15 °C, 25 °C and 35 °C.

The paraffin emulsion has a Herschel/Bulkley flow index less than one at all three temperatures. There appears to be no creaming due to droplet subdivision to mask the effect of droplet deformation responsible for the shear-thinning observed.

The soy wax emulsion shows more temperature dependant behavior with a flow index near one at 15 °C and 25 °C, and a flow index above one at 35 °C. This means that at 15 °C and 25 °C, either there is very little droplet deformation and droplet breakup leading to creaming, or the two effects have nearly balanced each other out. While at

35 °C an internal change has occurred causing creaming due to droplet breakup to become more prevalent. Both emulsions quickly plateau at each temeperature approaching an η_∞, as can be seen by looking at the viscosity curves in Figures 27 and 28.

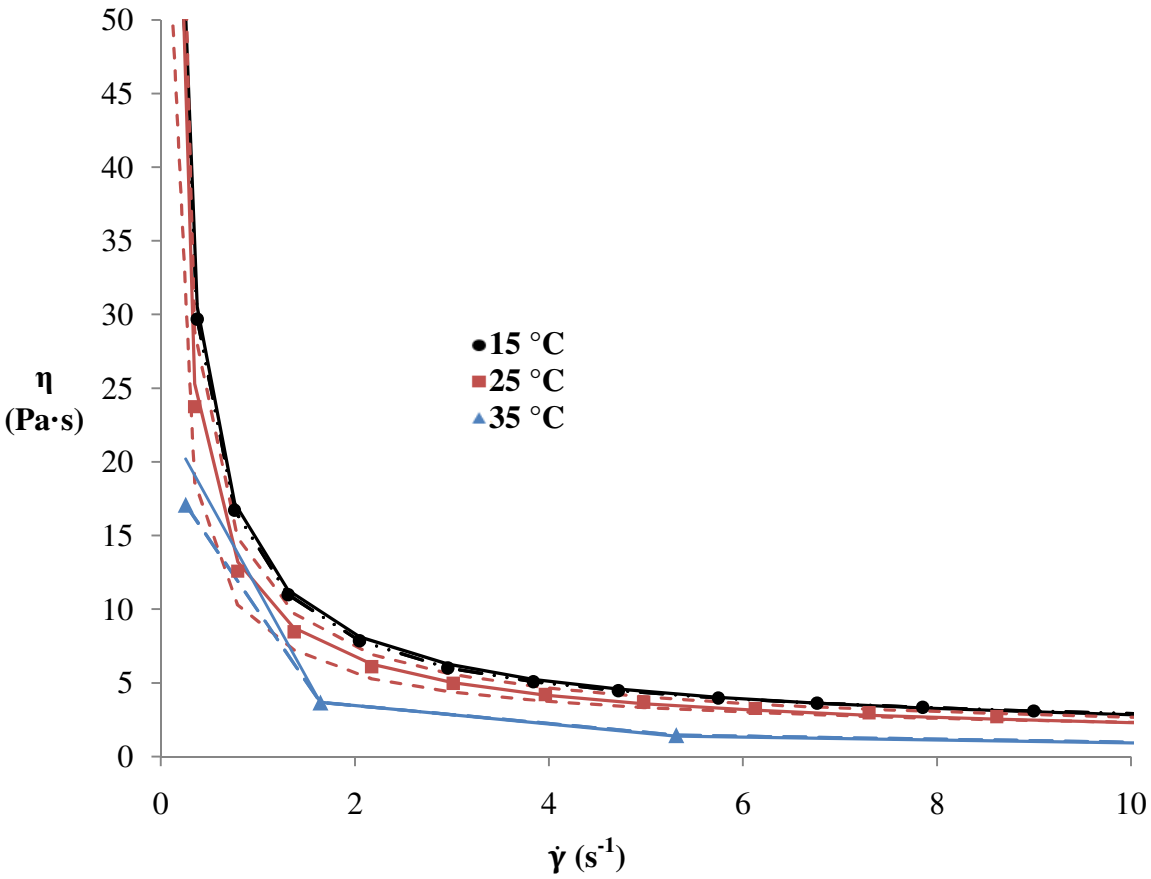

Figure 27. Viscosity Curves with Herschel/Bulkley Fittings and 95% Confidence Intervals for 30% Paraffin Wax Emulsion with 4% TEA Stearate at 15 °C, 25 °C, and 35 °C.

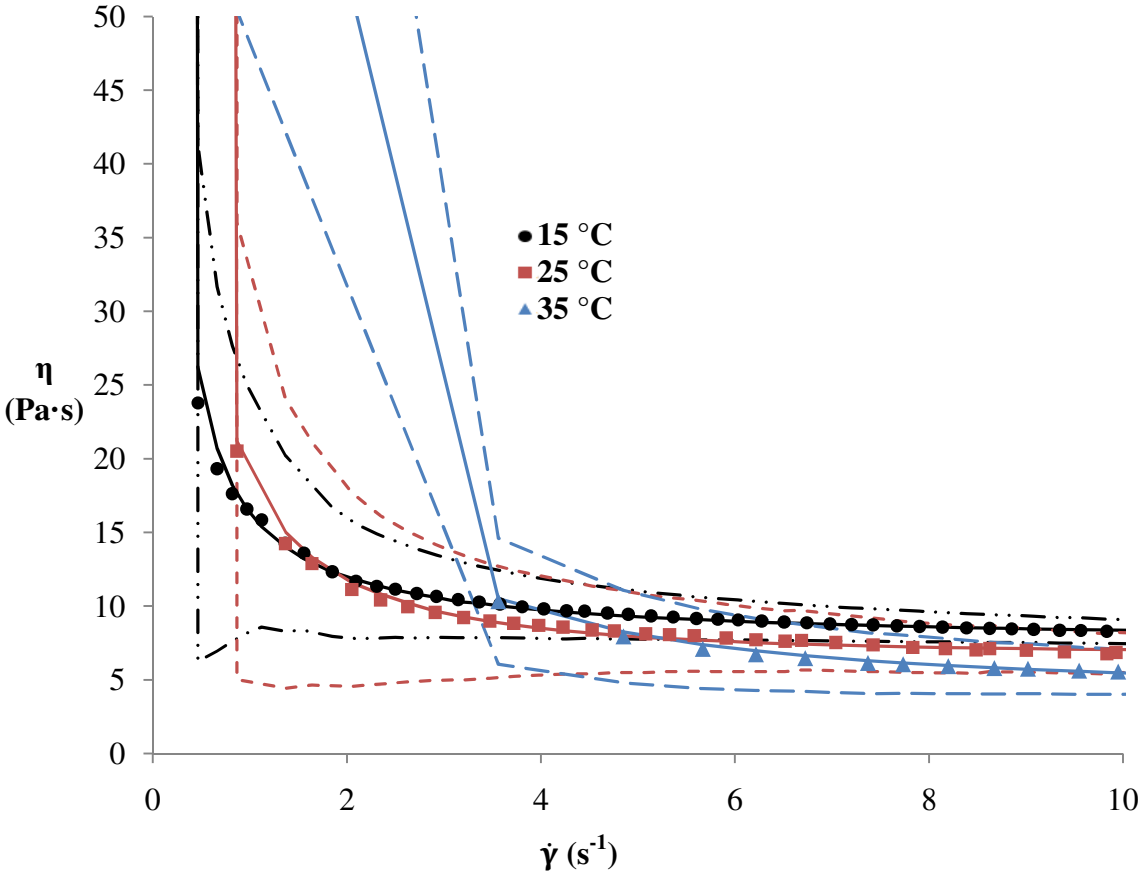

Figure 28. Viscosity Curves with Herschel/Bulkley Fittings and 95% Confidence Intervals for 30% Soy Wax Emulsion with 4% TEA Stearate at 15 °C, 25 °C, and 35 °C.

The τ_y for the paraffin emulsion shows a temperature dependence with 95% confidence intervals that do not overlap, as shown in Figures 25. The τ_y decreases with increasing temperature as the three-dimensional network structure becomes softer. Because of overlapping 95% confidence intervals, as can be seen in Figure 26, no conclusions can be drawn about the soy wax emulsion τ_y's except that the τ_y at 35 °C it is higher than the other soy wax τ_y's as well as those for the paraffin wax emulsion. This is due to a structural change causing a stronger internal three-dimensional network structure as was also seen with the increase in flow index in Table 9.

The temperature sweep curves for the 30% paraffin wax and soy wax emulsions with 4% TEA stearate are displayed in Figure 29 along with each curve's 95% confidence interval.

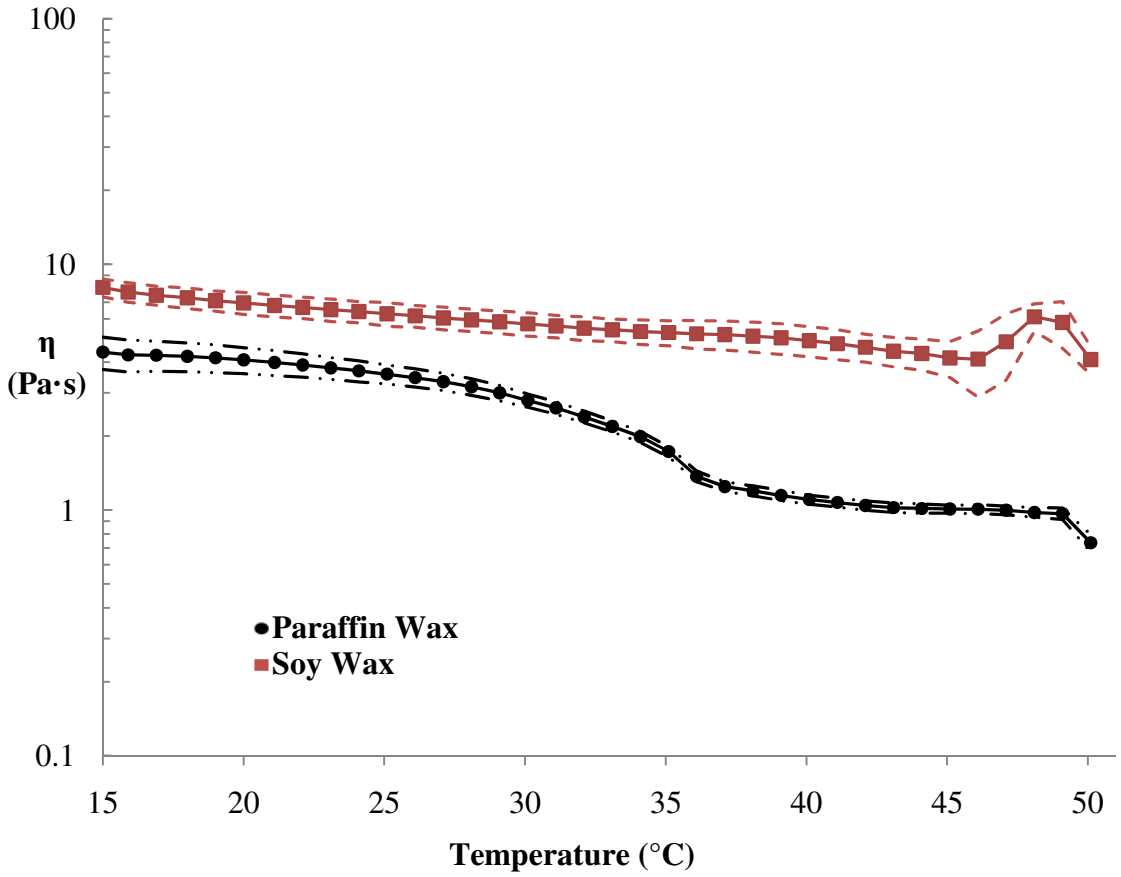

Figure 29. Temperature Sweep Curves for 30% Paraffin Wax and Soy Wax Emulsions with 4% TEA Stearate.

The two emulsions show very different behavior. This first thing of note is that the paraffin wax has a lower η at every temperature. Secondly, the soy wax emulsion shows a similar η peak as with Span 60© between 45 °C and 50 °C denoting a structural change. The third difference is that the paraffin wax shows a slow transition in the

middle of the temperature range possibly due to the gradual loss of some internal structure like hydrogen bonding (Mezger, 2011). This produces a rapid drop in η starting at around 25 °C, ending around 36 °C and leveling off.

The parameters determined by oscillatory amplitude sweep for 30% paraffin wax and soy wax emulsions with 4% TEA stearate are listed in Table 10.

Table 10. Oscillatory Amplitude Sweep Parameters for 30% Paraffin Wax and Soy Wax Emulsions with 4% TEA Stearate at 25 °C.

Wax Type	Limit of the LVE Range γ_L (%)	Yield Point τ_y (Pa)
Paraffin	1.12	4.23
Soy	0.393	14.1

The amplitude sweep CSD diagrams for the two emulsions are presented in Figures 30 and 31 with their 95% confidence intervals.

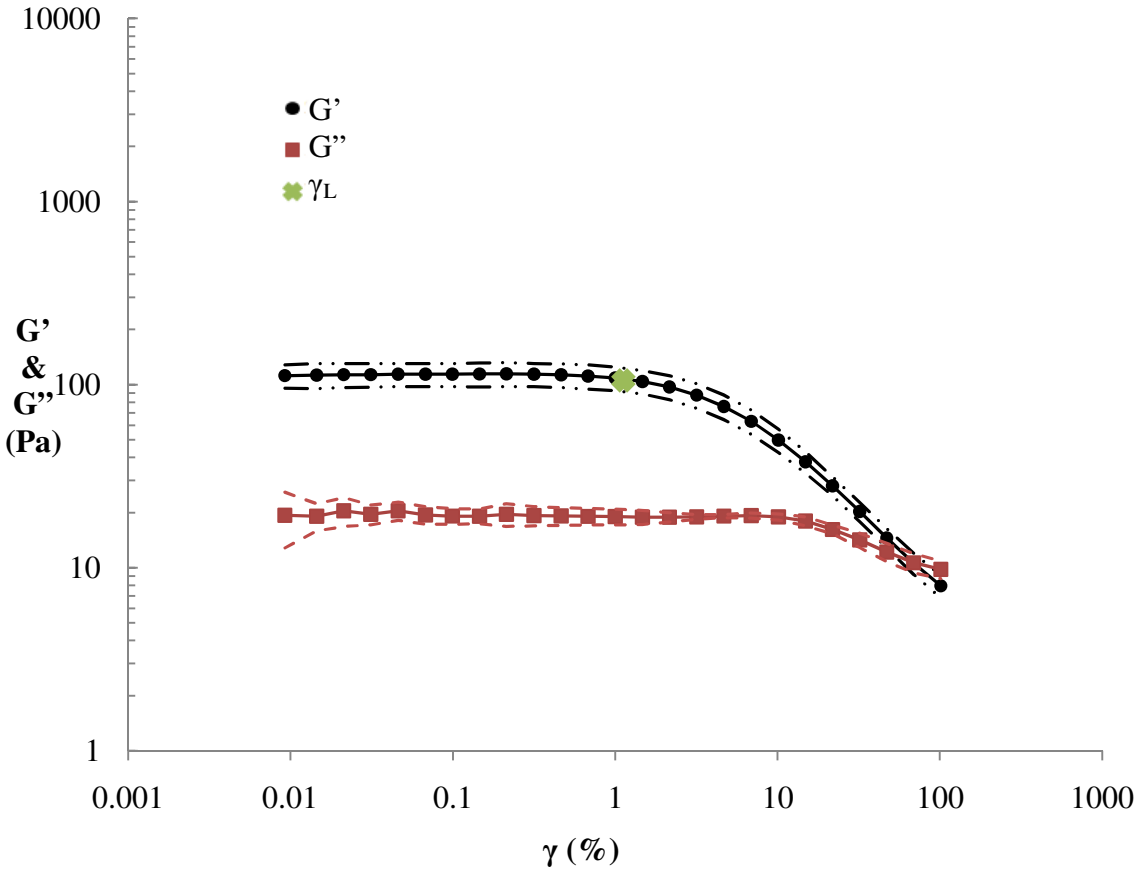

Figure 30. Amplitude Sweep (CSD) Diagram with 95% Confidence Intervals for 30% Paraffin Wax Emulsion with 4% TEA Stearate.

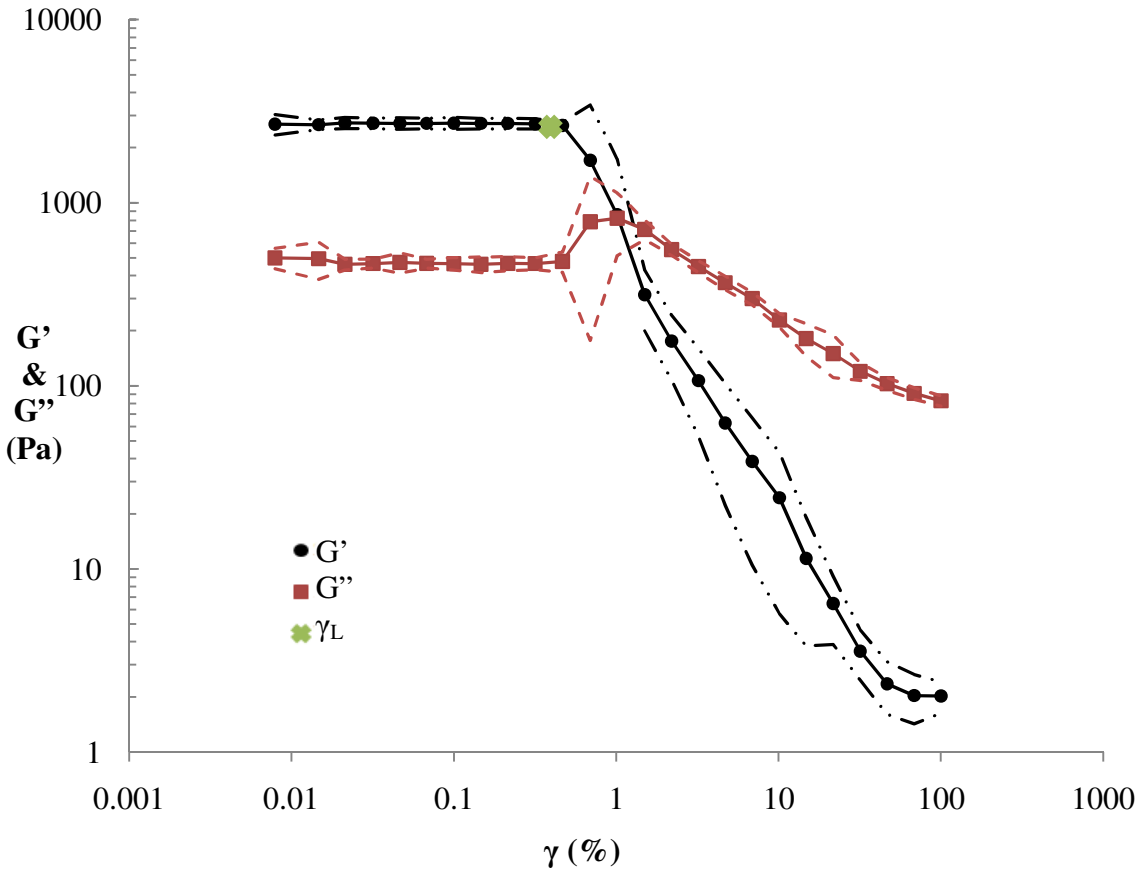

Figure 31. Amplitude Sweep (CSD) Diagram with 95% Confidence Intervals for 30% Soy Wax Emulsion with 4% TEA Stearate.

These TEA stearate emulsions show gel character and have some shelf stability with each G' being nearly an order of magnitude higher than each G" in the LVE region. The magnitude of G' for the paraffin wax emulsion is a decade lower than the for the soy wax. This means that the density of the internal network structures for the paraffin wax emulsion is lower, making the paraffin wax emulsion more soft and yielding in consistency.

The soy wax emulsion shows a G" maxima between γ_L and the point where G' and G" cross over, denoting brittle behavior. The paraffin wax emulsion does not, as shown in Figure 30.

The soy wax emulsion shows a higher τ_y, denoting a stronger internal structure before shear than the paraffin wax emulsion, as can be seen in Table 10. Both emulsions have τ_y's that are very close to the corresponding values determined by rotational CSS tests.

The frequency sweep diagrams for the paraffin wax and soy was emulsions with 4% TEA stearate and their 95% confidence intervals can be seen in figures 32 and 33.

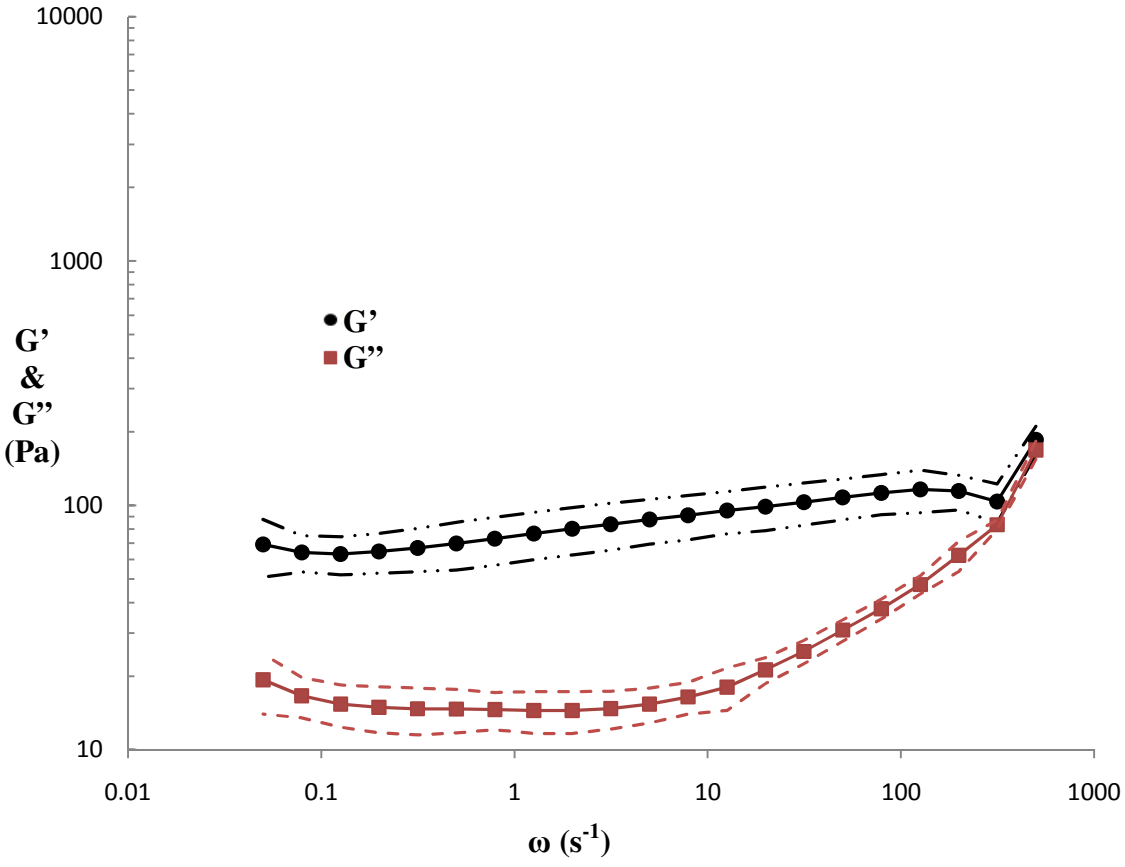

Figure 32. Frequency Sweep Diagram with 95% Confidence Intervals for 30% Paraffin Wax Emulsion with 4% TEA Stearate.

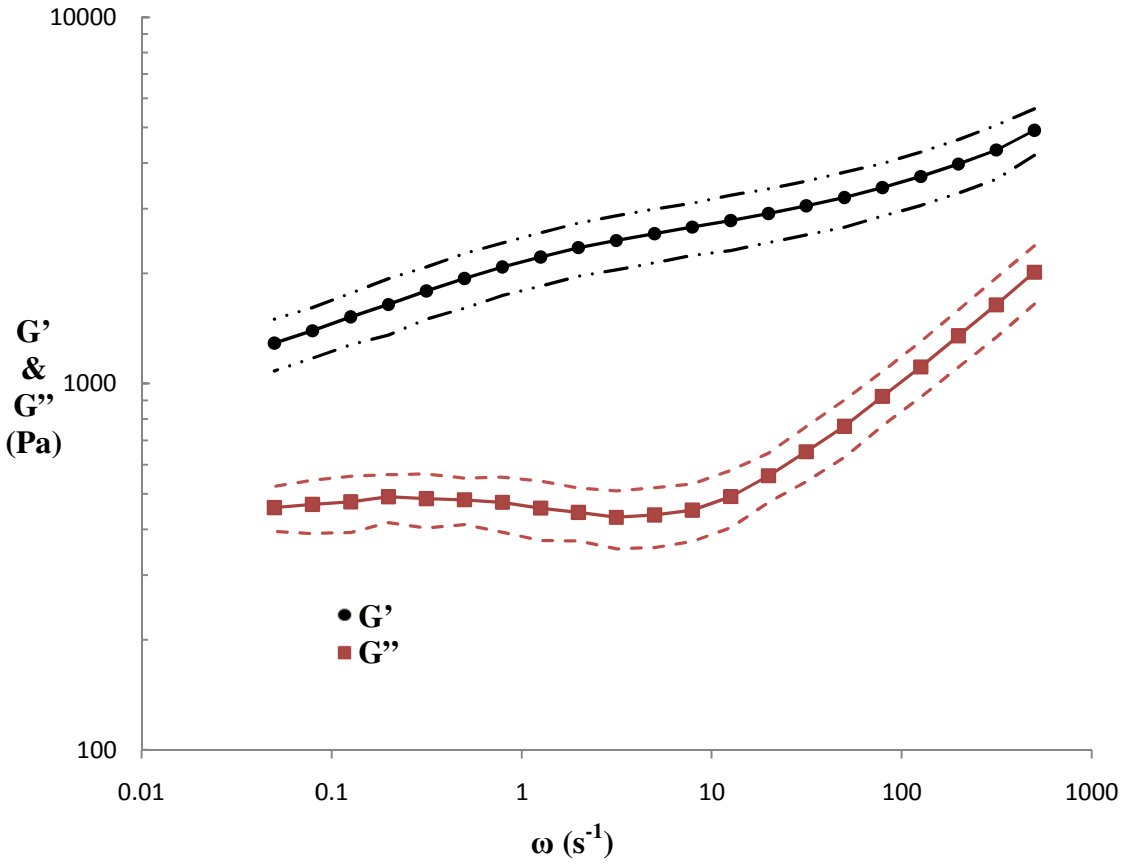

Figure 33. Frequency Sweep Diagram with 95% Confidence Intervals for 30% Soy Wax Emulsion with 4% TEA Stearate.

Both frequency sweeps possess G'/G" higher than 1 Pa but lower than 10 Pa throughout the range of frequencies and show frequency dependence denoting weak gel-like behavior. The paraffin wax emulsion shows a G'/G" near one at higher frequencies, as shown in Figure 32. This is not seen with the soy wax emulsion as can be seen in Figure 33. This means that the paraffin wax emulsion's short-term behavior is becoming fluid. The consequence of this is that a sudden deformation, like being dropped or sprayed, causes liquid-like behavior with the paraffin wax emulsion (Mezger, 2006).

For the soy wax emulsion, the magnitude of the maximum G' is on the order of 10^3 Pa, indicating a soft and yielding consistency. The paraffin wax emulsion has a maximum storage modulus magnitude of barely 10^2, meaning that it is extremely soft and yielding in consistency.

They both have a measure of long-term storage stability with G' > G" at lower ω's. The magnitudes of G' at the lowest frequency ($\omega = 0.05\ s^{-1}$) are listed in Table 11.

Table 11. Oscillatory Frequency Sweep Magnitudes of G' at the Lowest Frequency ($\omega = 0.05\ s^{-1}$) for 30% Paraffin Wax and Soy Wax Emulsions with 4% TEA Stearate.

Wax Type	Magnitude of G' at $\omega = 0.05\ s^{-1}$ (Pa)
Paraffin	69.2
Soy	1240

The two orders of magnitude difference shows that the soy wax emulsion has much higher gel strength than the paraffin emulsion.

Span 60© and TEA Stearate Mix Emulsions

The flow parameters from the HB regression analysis applied to the averaged flow curves for the 30% paraffin wax and 30% soy was emulsions with 2% Span 60© and 2% TEA stearate at 15 °C, 25 °C and 35 °C are listed in Table 12. These fitted curves are displayed in Figures 34 and 35 along with each curve's 95% confidence interval.

Table 12. Herschel/Bulkley Flow Parameters for 30% Paraffin Wax and Soy Wax Emulsions with 2% Span 60© and 2% TEA Stearate vs. Temperature.
Herschel/Bulkley model: $\tau = \tau_y + k \cdot \dot{\gamma}^n$

Wax Type	Temperature (°C)	Yield point τ_y (Pa)	Consistency k (Pa·s^n)	Flow Index n	Correlation Ratio r^2
Paraffin	15	39.5	6.36×10^{0}	3.55×10^{-1}	0.945
Paraffin	25	35.0	5.25×10^{0}	3.74×10^{-1}	0.980
Paraffin	35	20.0	4.94×10^{0}	4.84×10^{-1}	0.917
Soy	15	8.92	6.33×10^{0}	5.56×10^{-1}	0.920
Soy	25	6.35	3.86×10^{0}	7.04×10^{-1}	0.931
Soy	35	5.28	3.48×10^{0}	6.17×10^{-1}	0.860

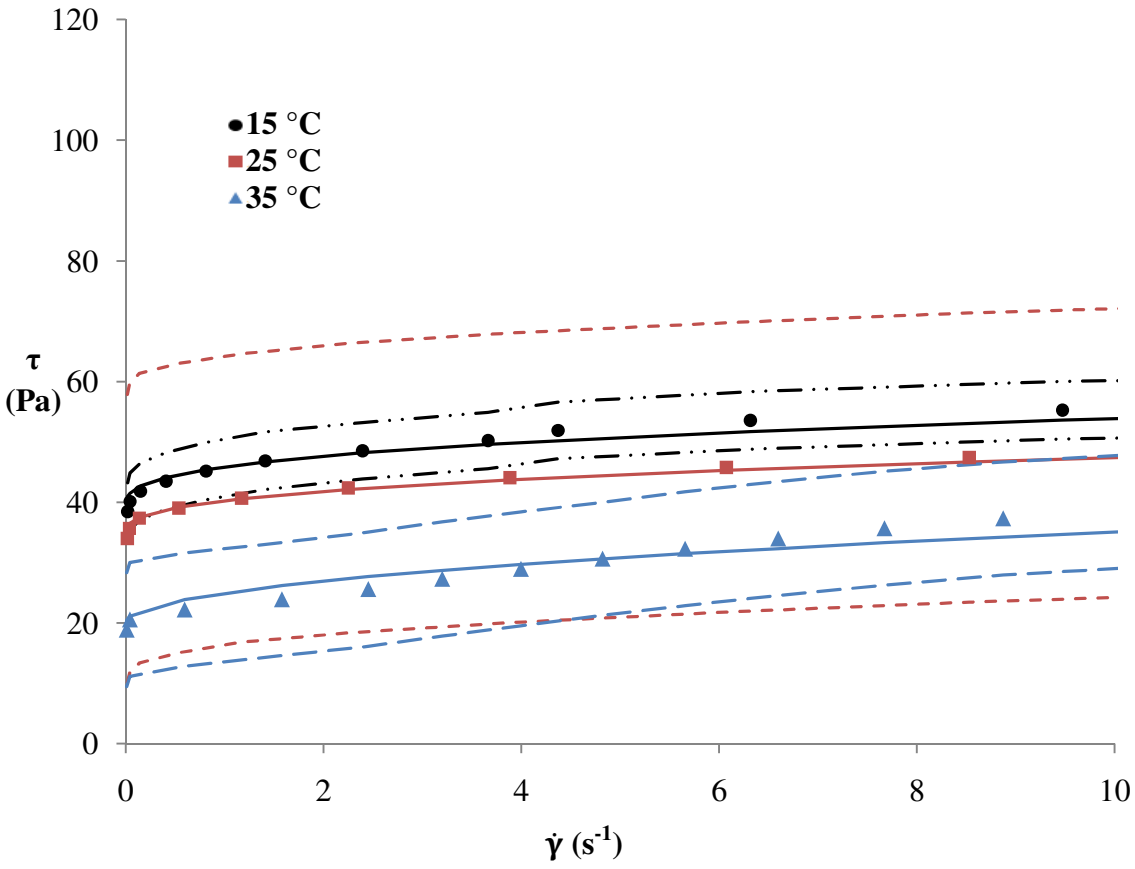

Figure 34. Flow Curves with Herschel/Bulkley Fittings and 95% Confidence Intervals for 30% Paraffin Wax Emulsion with 2% Span 60© and 2% TEA Stearate at 15 °C, 25 °C and 35 °C.

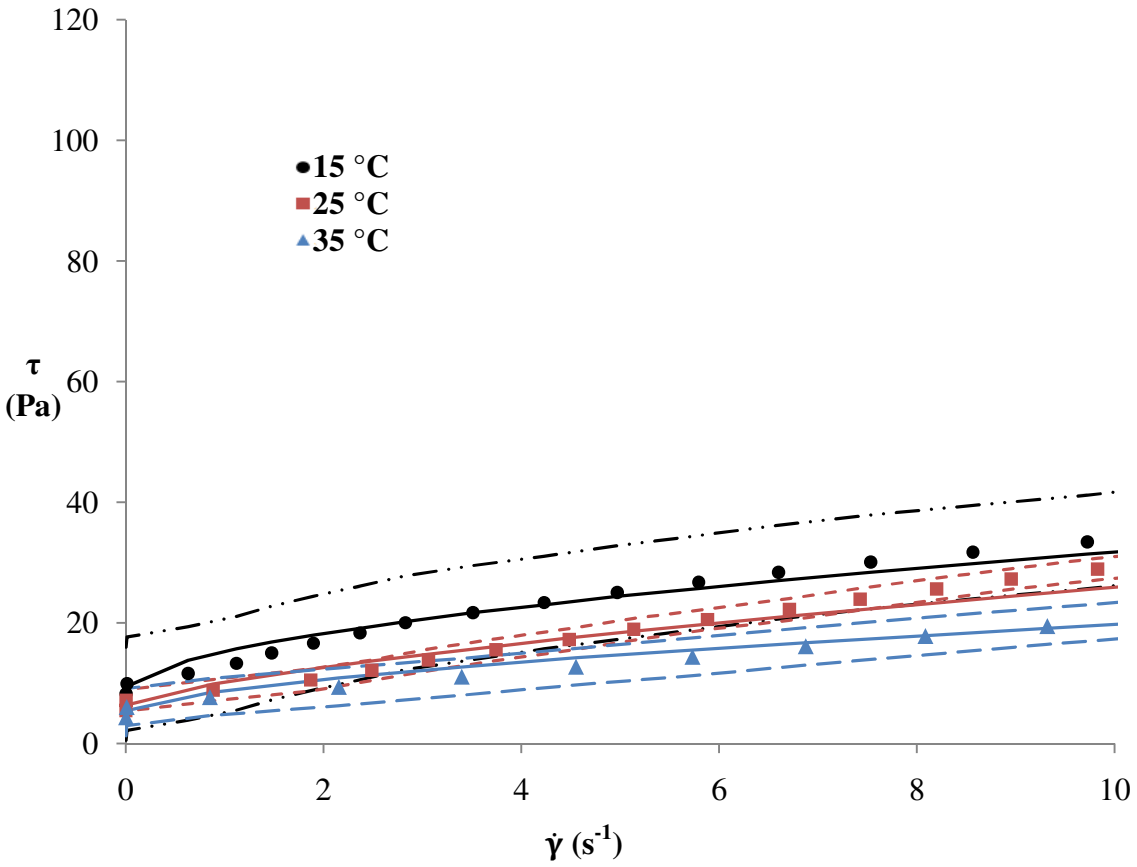

Figure 35. Flow Curves with Herschel/Bulkley Fittings and 95% Confidence Intervals for 30% Soy Wax Emulsion with 2% Span 60© and 2% TEA Stearate at 15 °C, 25 °C and 35 °C.

Both of the emulsions at every temperature display shear-thinning behavior, as their Herschel/Bulkley flow indexes are less than one. No significant creaming due to droplet subdivision appears to be occurring with either wax, and the standard behavior of shear-thinning due to droplet deformation is displayed. This could be expected as 2% Span 60© and 4% TEA stearate emulsions do not show droplet subdivision effects (with the exception of 4% TEA stearate with soy wax at 35 °C). In each case, the shear thinning should give way to a η_∞ as can be seen in the η curves in figures 36 and 37

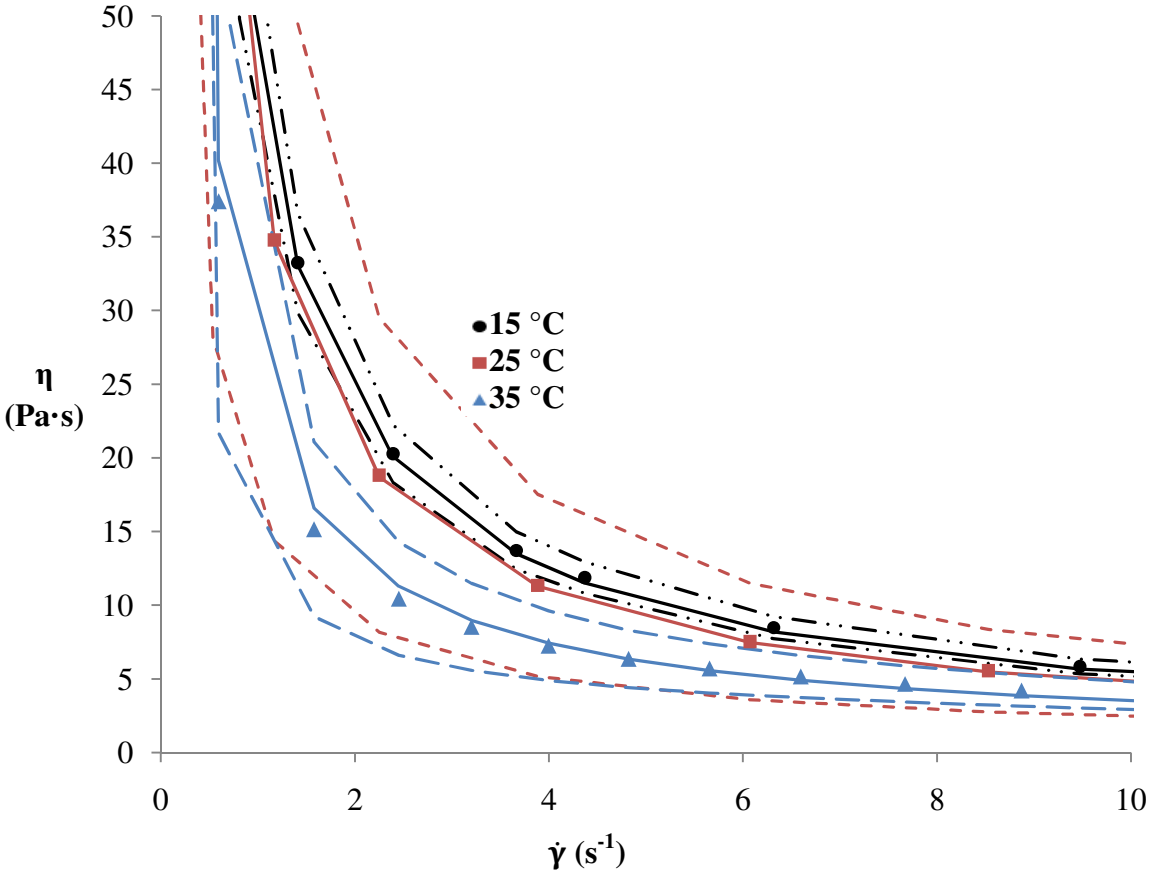

Figure 36. Viscosity Curves with Herschel/Bulkley Fittings and 95% Confidence Intervals for 30% Paraffin Wax Emulsion with 2% Span 60© and 2% TEA Stearate at 15 °C, 25 °C, and 35 °C.

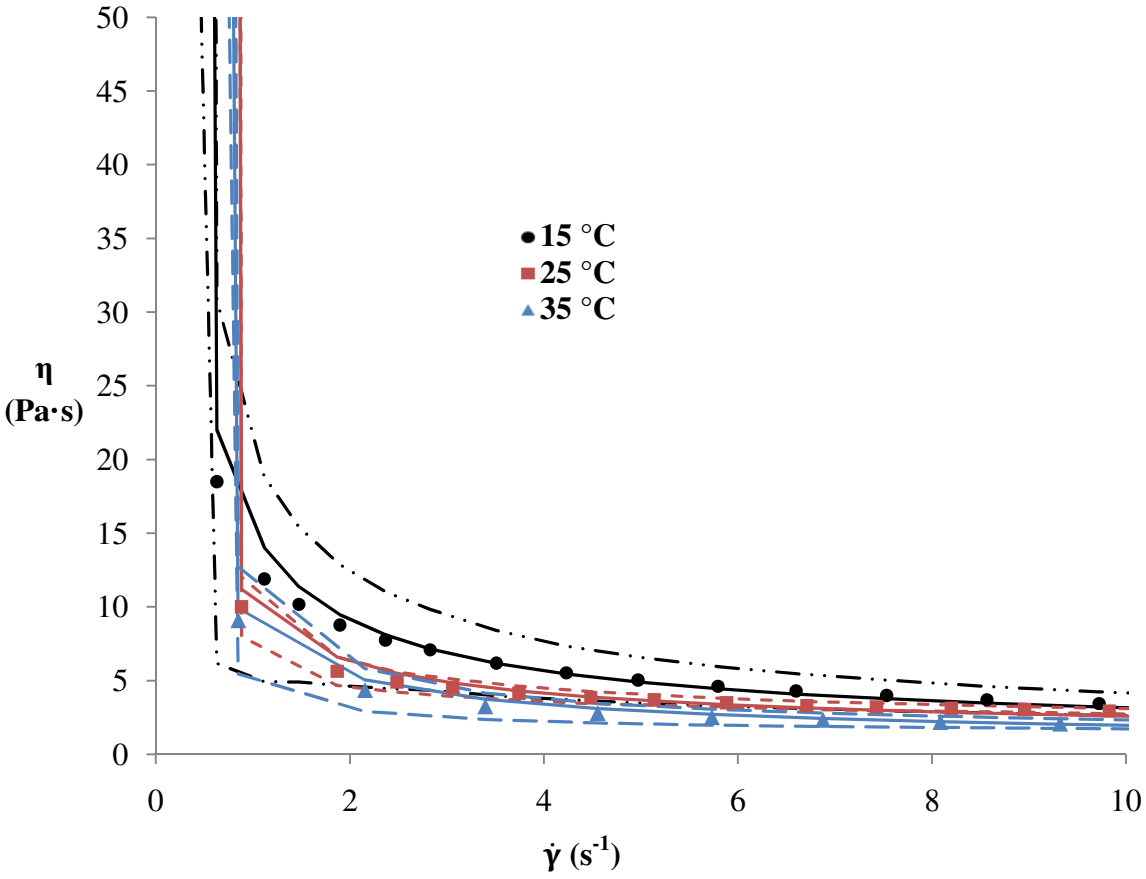

Figure 37. Viscosity Curves with Herschel/Bulkley Fittings and 95% Confidence Intervals for 30% Soy Wax Emulsion with 2% Span 60© and 2% TEA Stearate at 15 °C, 25 °C, and 35 °C.

Only two conclusions can be drawn from the data about τ_y's. The first is that the paraffin wax emulsion has a higher τ_y at 15 °C than at 35 °C. This is to be expected as the structure becomes softer at higher temperatures. The second is that overall the paraffin wax emulsion has a higher τ_y than the soy wax emulsion.

The temperature sweep curves for the 30% paraffin wax and soy wax emulsions with 2% Span 60© and 2% TEA stearate are displayed in Figure 38 along with each curve's 95% confidence interval.

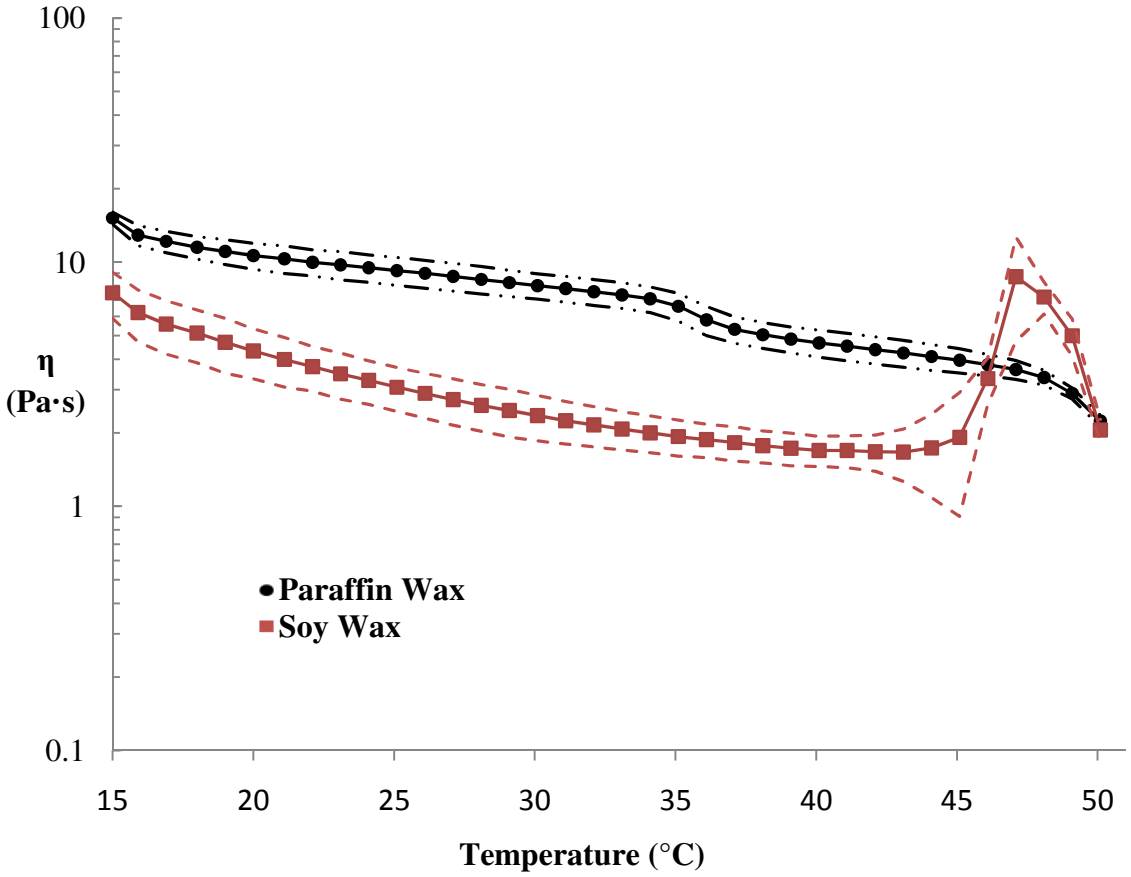

Figure 38. Temperature Sweep Curves for 30% Paraffin Wax and Soy Wax Emulsions with 2% Span 60© and 2% TEA Stearate.

In this case we see that the paraffin wax emulsion has an overall higher η at every temperature except between 45 °C and 50 °C where the soy wax emulsion produces a η peak. This peak is even more pronounced than with previous emulsions. The slow transition in the middle of the temperature range of the paraffin wax emulsion is also present, but to a lesser degree. This appears to be an effect of TEA stearate concentration.

The parameters determined by oscillatory amplitude sweep for 30% paraffin wax and soy wax emulsions with 2% Span 60© and 2% TEA stearate are listed in Table 13.

Table 13. Oscillatory Amplitude Sweep Parameters for 30% Paraffin Wax and Soy Wax Emulsions with 2% Span 60© and 2% TEA Stearate at 25 °C.

Wax Type	Limit of the LVE Range γ_L (%)	Yield Point τ_y (Pa)
Paraffin	1.02	35.7
Soy	0.411	5.04

The amplitude sweep CSD diagrams for the two emulsions are presented in Figures 39 and 40 with their 95% confidence intervals.

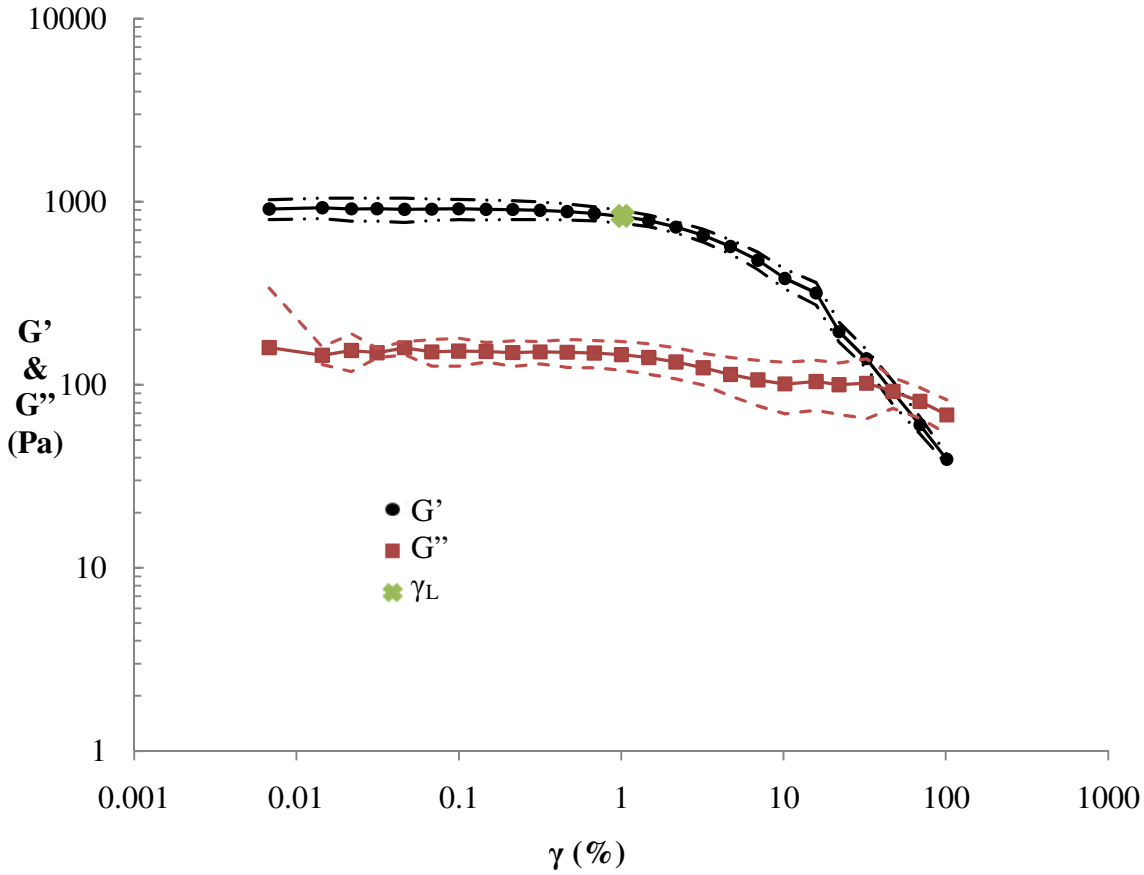

Figure 39. Amplitude Sweep (CSD) Diagram with 95% Confidence Intervals for 30% Paraffin Wax Emulsion with 2% Span 60® and 2% TEA Stearate

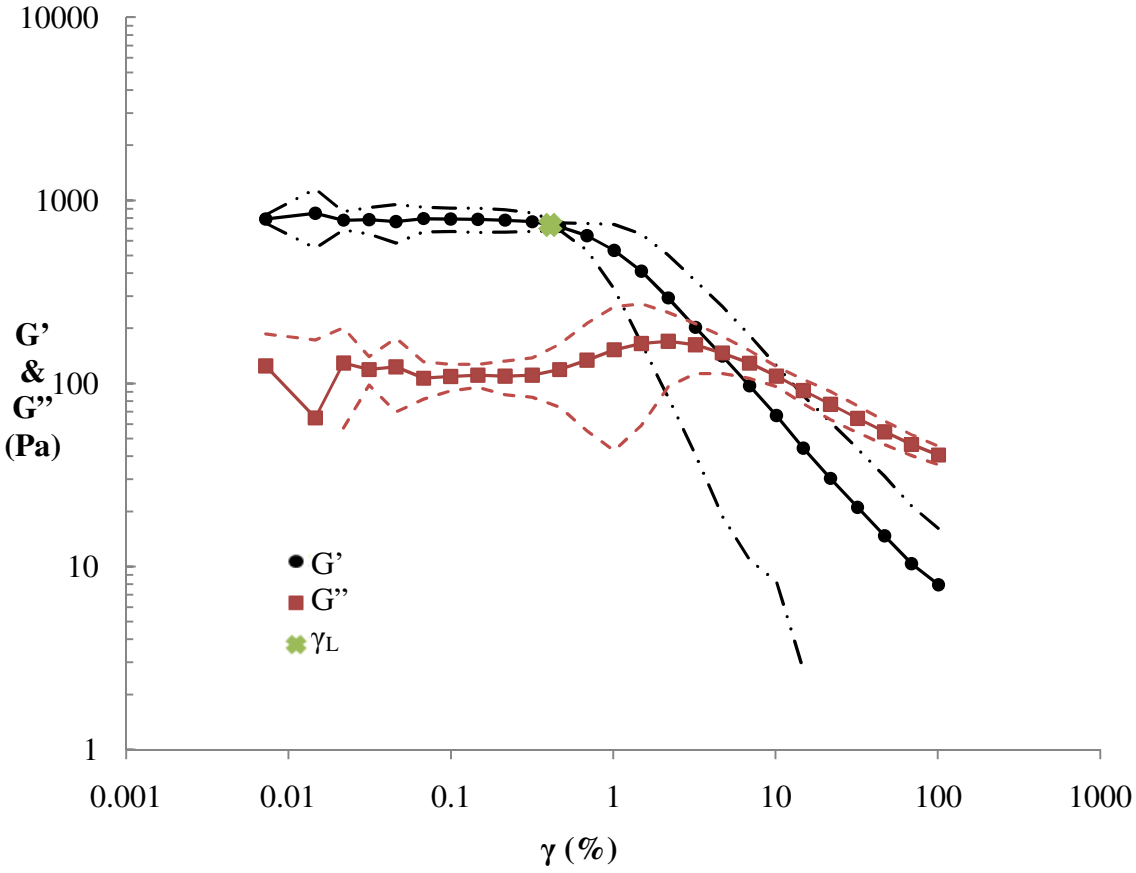

Figure 40. Amplitude Sweep (CSD) Diagram with 95% Confidence Intervals for 30% Soy Wax Emulsion with 2% Span 60® and 2% TEA Stearate.

As each G' is nearly an order of magnitude higher than each G" in the LVE region, these emulsions show gel character and have some shelf stability. The soy wax emulsion shows a G" maxima between γ_L and the point where G' and G" cross over. This indicates brittle behavior from the breaking down of a network of superstructures. The paraffin wax emulsion does not show this maxima as can be seen in Figure 39.

The paraffin wax emulsion has a stronger internal structure before shear as shown by the higher τ_y in Table 13. Both τ_y's are fairly close to the values produced by the rotational CSS tests.

The frequency sweep diagrams for the paraffin wax and soy was emulsions with 2% Span 60© and 2% TEA stearate and their 95% confidence intervals can be seen in figures 41 and 42.

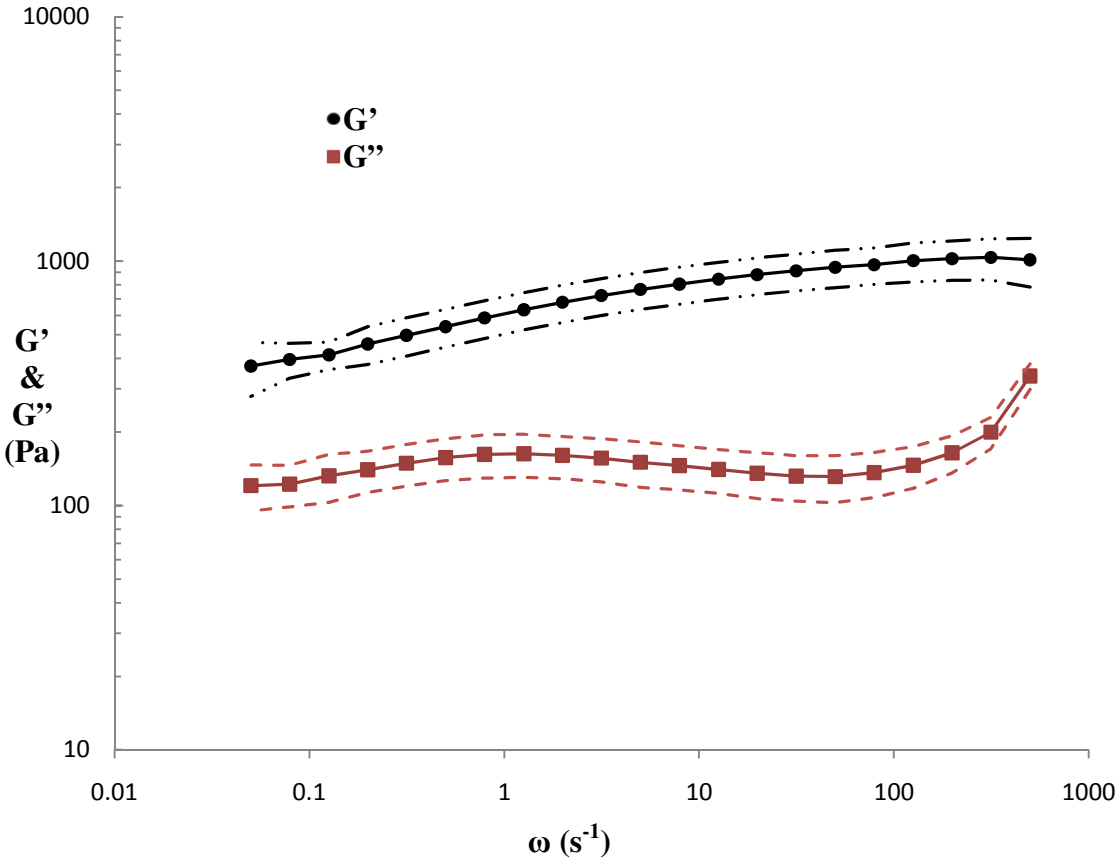

Figure 41. Frequency Sweep Diagram with 95% Confidence Intervals for 30% Paraffin Wax Emulsion with 2% Span 60© and 2% TEA Stearate.

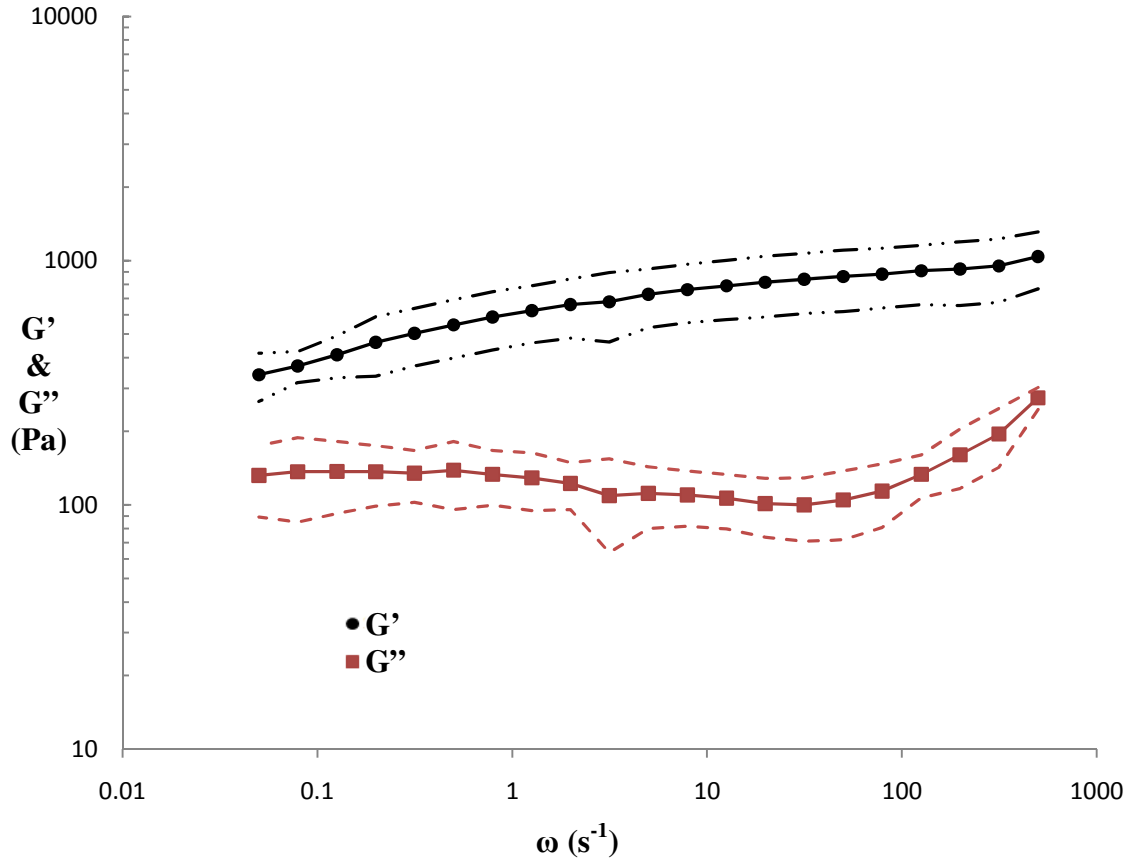

Figure 42. Frequency Sweep Diagram with 95% Confidence Intervals for 30% Soy Wax Emulsion with 2% Span 60© and 2% TEA Stearate.

Both emulsions display weak gel-like behavior and have a magnitude of the maximum G' on the order of 10^3 Pa indicating a soft and yielding consistency. They also both have a measure of long-term storage stability with G' > G" at lower ω's. The magnitudes of G' at the lowest frequency ($\omega = 0.05\ s^{-1}$) are listed in Table 14.

Table 14. Oscillatory Frequency Sweep Magnitudes of G' at the Lowest Frequency (ω = 0.05 s^{-1}) for 30% Paraffin Wax and Soy Wax Emulsions with 2% Span 60© and 2% TEA Stearate.

Wax Type	Magnitude of G' at ω = 0.05 s^{-1} (Pa)
Paraffin	372
Soy	341

There is no discernable difference in the gel strength for either of these emulsions as both values are inside the others 95% confidence interval.

Paraffin Wax Emulsions

The flow parameters from the HB regression analysis applied to the averaged flow curves for the 30% paraffin wax emulsions with each emulsifier at 15 °C, 25 °C and 35 °C are listed in Table 15. These fitted curves are displayed in Figure 43 along with each curve's 95% confidence interval.

Table 15. Herschel/Bulkley Flow Parameters for 30% Paraffin Wax Emulsions with 4% of Each Emulsifier vs. Temperature.
Herschel/Bulkley model: $\tau = \tau_y + k \cdot \dot{\gamma}^n$

Emulsifier	Temperature (°C)	Yield point τ_y (Pa)	Consistency k ($Pa \cdot s^n$)	Flow Index n	Correlation Ratio r^2
Span 60©	15	60.9	3.14×10^0	1.03×10^0	0.988
	25	54.3	1.44×10^0	1.31×10^0	0.993
	35	47.7	6.85×10^{-3}	3.71×10^0	0.982
TEA stearate	15	7.97	5.88×10^0	5.41×10^{-1}	0.983
	25	5.79	5.25×10^0	5.19×10^{-1}	0.966
	35	4.71	9.88×10^{-1}	5.94×10^{-1}	0.985
50-50 Mix	15	39.5	6.36×10^0	3.55×10^{-1}	0.945
	25	35.0	5.25×10^0	3.74×10^{-1}	0.980
	35	20.0	4.94×10^0	4.84×10^{-1}	0.917

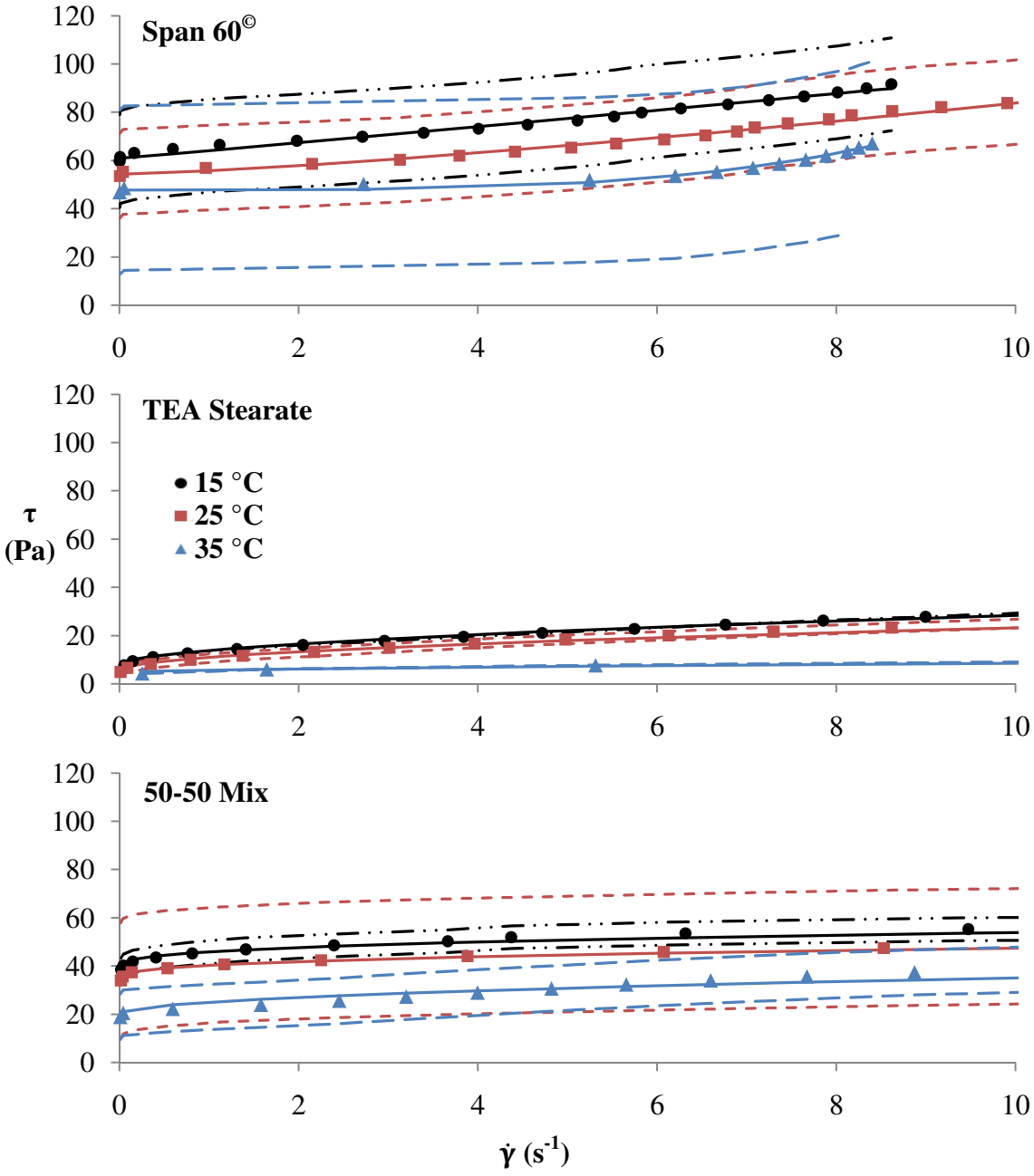

Figure 43. Flow Curves with Herschel/Bulkley Fittings and 95% Confidence Intervals for 30% Paraffin Wax Emulsions with 4% of Each Emulsifier at 15 °C, 25 °C and 35 °C.

The paraffin wax emulsion with 4% Span 60© is the only one that possesses a Herschel/Bulkley flow index greater than one, and at every temperature. This indicates droplet subdivision leading to creaming and tackiness only in this emulsion (Mezger, 2006). This effect increases at 35 °C. The 4% Span 60© emulsion also has the highest yield stresses at each temperature with the 4% TEA stearate emulsion having the lowest (an order of magnitude lower) and the 2% Span 60© and 2% TEA stearate emulsion predictably being in the middle. With the TEA stearate emulsion, the 95% confidence intervals are small enough to see that the yield stress decreases with increasing temperature and the flow index increases. This is probably true for all of these emulsions.

The temperature sweep curves for 30% paraffin wax emulsions with each emulsifier are displayed in Figure 44 along with each curve's 95% confidence interval.

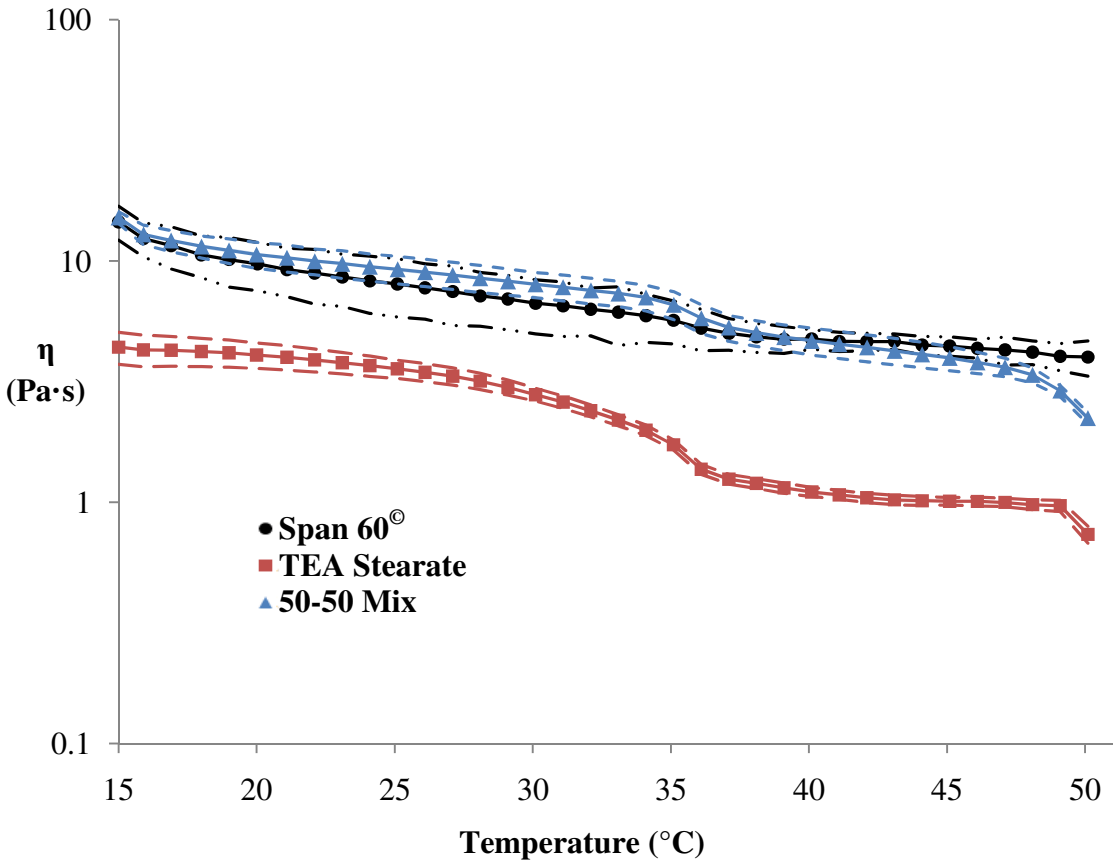

Figure 44. Temperature Sweep Curves for 30% Paraffin Wax Emulsions with 4% of Each Emulsifier.

The 4% Span 60© Emulsion and the 2% Span 60© and 2% TEA stearate emulsion show similar η's at all temperatures while the 4% TEA stearate emulsion is significantly lower at every temperature. The slow transition in the middle of the temperature range possibly due to the loss of hydrogen bonding becomes more evident as TEA stearate concentration increases.

The parameters determined by oscillatory amplitude sweep for 30% paraffin wax emulsions with each emulsifier are listed in Table 16.

Table 16. Oscillatory Amplitude Sweep Parameters for 30% Paraffin Wax Emulsions with Each Emulsifier at 25 °C.

Emulsifier	Limit of the LVE Range γ_L (%)	Yield Point τ_y (Pa)
Span 60©	0.0988	49.9
TEA Stearate	1.12	4.23
50-50 Mix	1.02	35.7

The amplitude sweep τ_y's for the paraffin wax emulsions are similar to the results from the rotational CSS tests. The 4% Span 60© emulsion has the highest value indicating the densest internal network structures. The 4% TEA stearate emulsion is the least dense and more soft and yielding in consistency. The 2% Span 60© and 2% TEA stearate emulsion is in the middle.

Each of these emulsions show a gradual plastic deformation without the breaking down of superstructures before yielding. This can be seen in Figures 35, 37 and 39 as the γ_L for each emulsion comes well before the point where the G' starts to rapidly dip towards G" (near the τ_y), and there is no G" maxima in this area.

The frequency sweep diagrams for the paraffin wax emulsions with each emulsifier can be seen in figure 45.

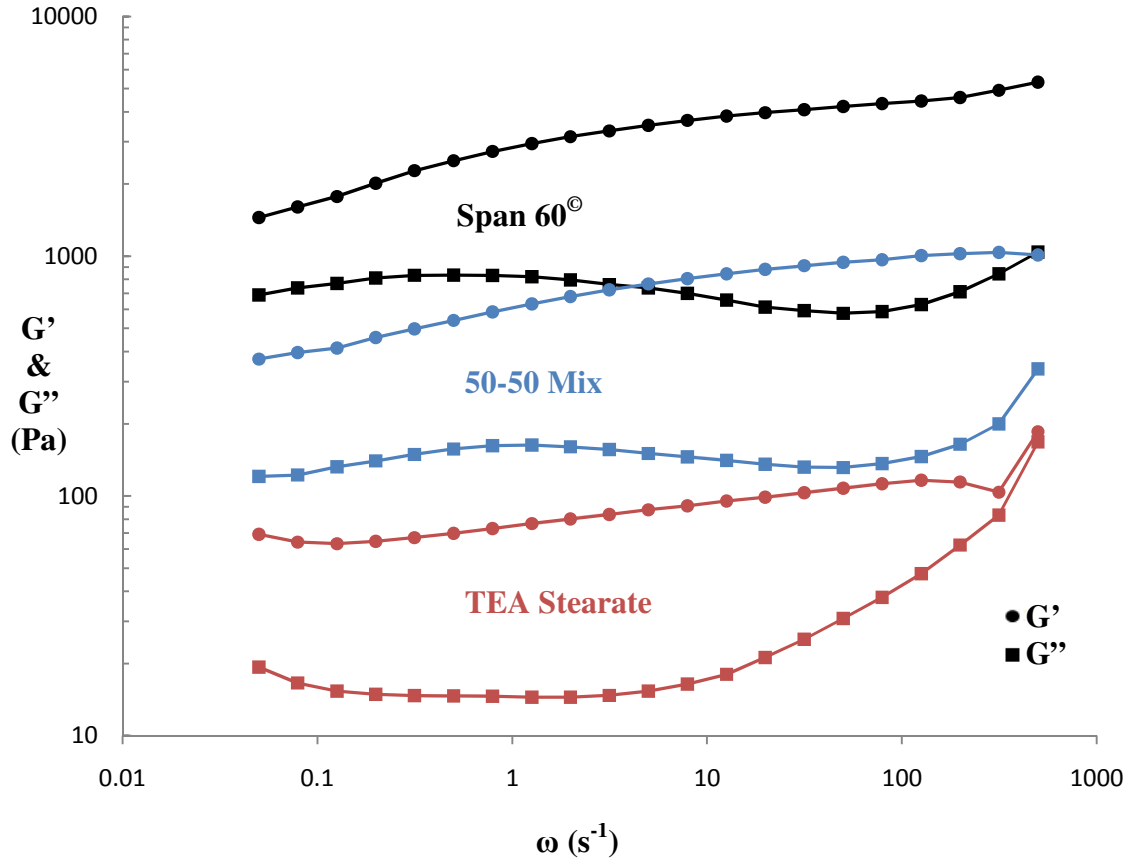

Figure 45. Frequency Sweep Diagrams for 30% Paraffin Wax Emulsions with Each Emulsifier.

All emulsions display weak gel-like behavior. They also all have a measure of long-term storage stability with G' > G" at lower ω's. The magnitude of the maximum G' for the 4% Span 60© emulsion is on the order of 10^3 Pa indicating a soft and yielding consistency. The 2% Span 60© and 2% TEA stearate emulsion is even softer with a G' maximum on the order of 10^2 Pa and the 4% TEA emulsion has a G' maximum on the order of 10^1 indicating an extremely soft and yielding consistency.

The magnitudes of G' at the lowest frequency ($\omega = 0.05\ s^{-1}$) are listed in Table 17.

Table 17. Oscillatory Frequency Sweep Magnitudes of G' at the Lowest Frequency (ω = 0.05 s^{-1}) for 30% Paraffin Wax Emulsions with Each Emulsifier.

Emulsifier	Magnitude of G' at ω = 0.05 s^{-1} (Pa)
Span 60©	1450
TEA Stearate	69.2
50-50 Mix	372

The gel strength of the 4% Span 60© emulsion is two orders of magnitude above that of the 4% TEA stearate emulsion, with the 2% Span 60© and 2% TEA stearate emulsion in the middle. With paraffin wax, 4% Span 60© forms a more stable, firmer and stronger emulsion; while 4% TEA stearate forms a more fluid-like, softer and weaker emulsion. The 2% Span 60© and 2% TEA stearate emulsion shows a gel strength comparable to that of a 2% Span 60© emulsion (Table 5). This shows that the TEA stearate does not contribute significantly to the three-dimensional structure strength of this emulsion.

Soy Wax Emulsions

The flow parameters from the HB regression analysis applied to the averaged flow curves for the 30% soy wax emulsions with each emulsifier at 15 °C, 25 °C and 35 °C are listed in Table 18. These fitted curves are displayed in Figure 46 along with each curve's 95% confidence interval.

Table 18. Herschel/Bulkley Flow Parameters for 30% Soy Wax Emulsions with 4% of Each Emulsifier vs. Temperature.
Herschel/Bulkley model: $\tau = \tau_y + k \cdot \dot{\gamma}^n$

Emulsifier	Temperature (°C)	Yield point τ_y (Pa)	Consistency k ($Pa \cdot s^n$)	Flow Index n	Correlation Ratio r^2
Span 60©	15	25.4	3.63×10^{0}	1.20×10^{0}	0.999
	25	32.6	7.20×10^{-1}	1.58×10^{0}	0.995
	35	22.0	1.31×10^{0}	1.26×10^{0}	0.964
TEA stearate	15	8.56	7.74×10^{0}	9.86×10^{-1}	0.999
	25	15.3	3.66×10^{0}	1.18×10^{0}	0.995
	35	32.8	6.12×10^{-1}	1.55×10^{0}	0.994
50-50 Mix	15	8.92	6.33×10^{0}	5.56×10^{-1}	0.920
	25	6.35	3.86×10^{0}	7.04×10^{-1}	0.931
	35	5.28	3.48×10^{0}	6.17×10^{-1}	0.860

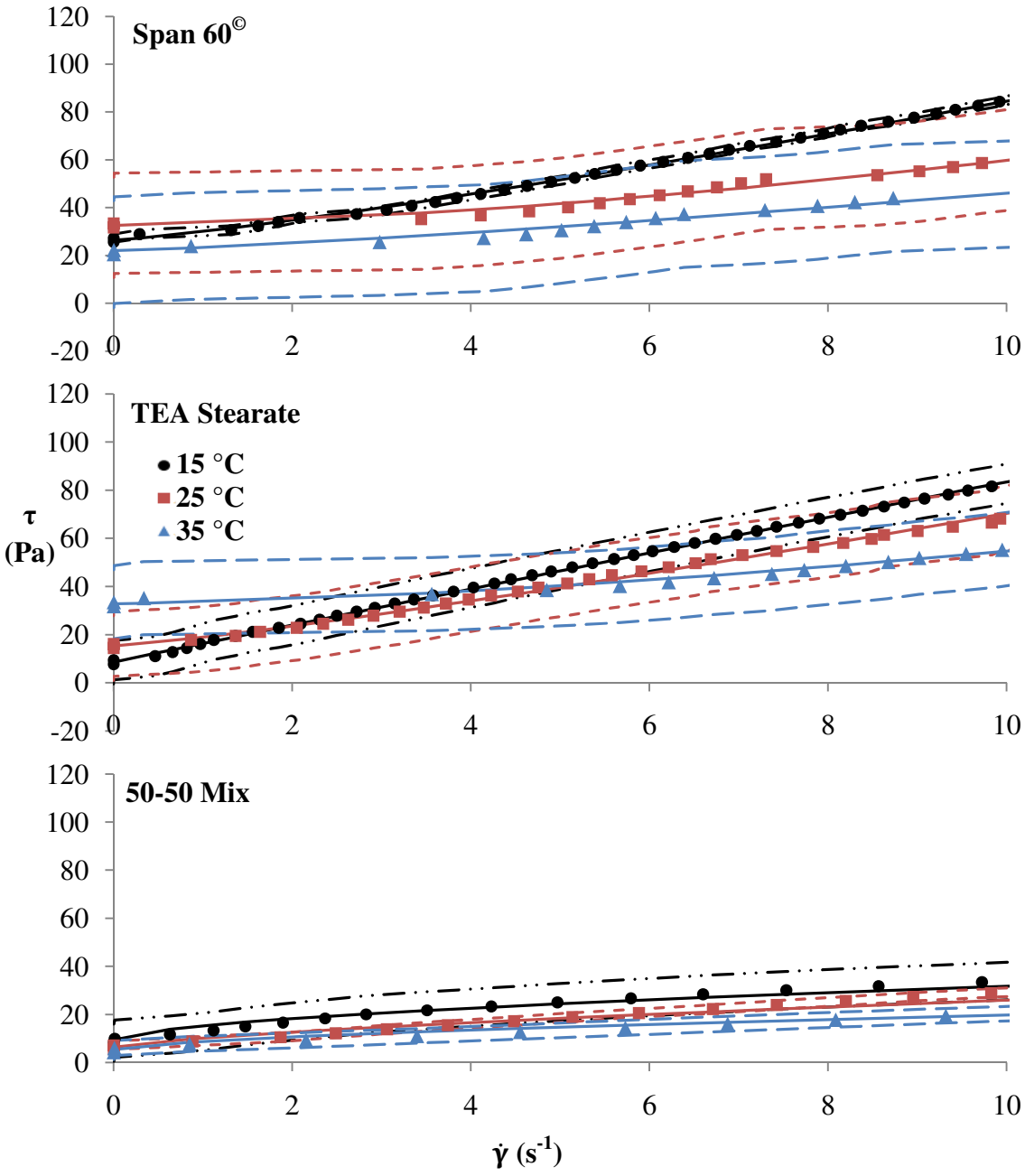

Figure 46. Flow Curves with Herschel/Bulkley Fittings and 95% Confidence Intervals for 30% Soy Wax Emulsions with 4% of Each Emulsifier at 15 °C, 25 °C and 35 °C.

The soy wax emulsion with 4% Span 60© is the only one that possesses a Herschel/Bulkley flow index (n) greater than one at every temperature. However, the TEA stearate emulsion also shows this behavior at 25 °C and 35 °C. Droplet subdivision appears to increase with temperature in this case.

The 4% Span 60© emulsion also has the highest yield stresses at each temperature except at 35 °C when the TEA stearate appears to go through some structural change producing a higher yield stress. The lowest yield stresses at 15 °C are TEA stearate and 50-50 mix emulsions which are practically the same. The 50-50 mix emulsion does not undergo the structural change that the pure TEA stearate emulsion does so it remains the lowest at all temperatures.

The temperature sweep curves for 30% soy wax emulsions with each emulsifier are displayed in Figure 47 along with each curve's 95% confidence interval.

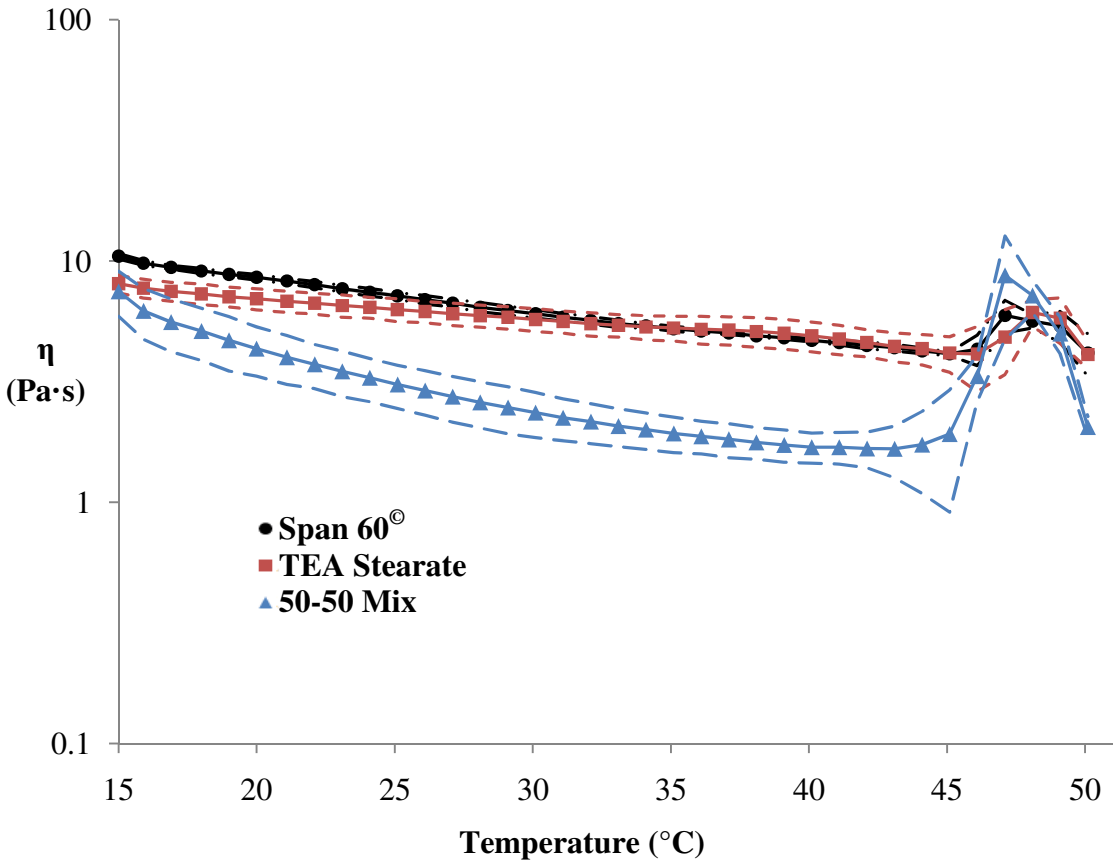

Figure 47. Temperature Sweep Curves for 30% Soy Wax Emulsions with 4% of Each Emulsifier.

The Span 60© and TEA stearate emulsions show similar η's over the entire range of temperatures. The 2% Span 60© and 2% TEA stearate emulsion drops to significantly lower η's above 15 °C. Between 45 °C and 50 °C there is a η peak in each emulsion, reaching a similar η in each emulsion at 47 °C. This appears to be an effect of the soy wax as each emulsion shows an identical maximum η when the confidence intervals are accounted for.

The parameters determined by oscillatory amplitude sweep for 30% soy wax emulsions with each emulsifier are listed in Table 19.

Table 19. Oscillatory Amplitude Sweep Parameters for 30% Soy Wax Emulsions with Each Emulsifier at 25 °C.

Emulsifier	Limit of the LVE Range γ_L (%)	Yield Point τ_y (Pa)
Span 60©	0.273	15.6
TEA Stearate	0.393	14.1
50-50 Mix	0.411	5.04

The amplitude sweep τ_y's for the soy wax emulsions are within the 95% confidence intervals for the results from the rotational CSS tests. The 4% Span 60© and 4% TEA stearate emulsions show similar values denoting similarity in internal network structure density. The 2% Span 60© and 2% TEA stearate emulsion shows a lower value indicating a less dense internal network structure and a more soft and yielding consistency.

Each of these emulsions show an abrupt yield and a G" maxima, both denoting brittle behavior due to the breaking down of a network of superstructures. This can be seen in Figures 22, 31 and 40.

The frequency sweep diagrams for the soy wax emulsions with each emulsifier can be seen in figure 48.

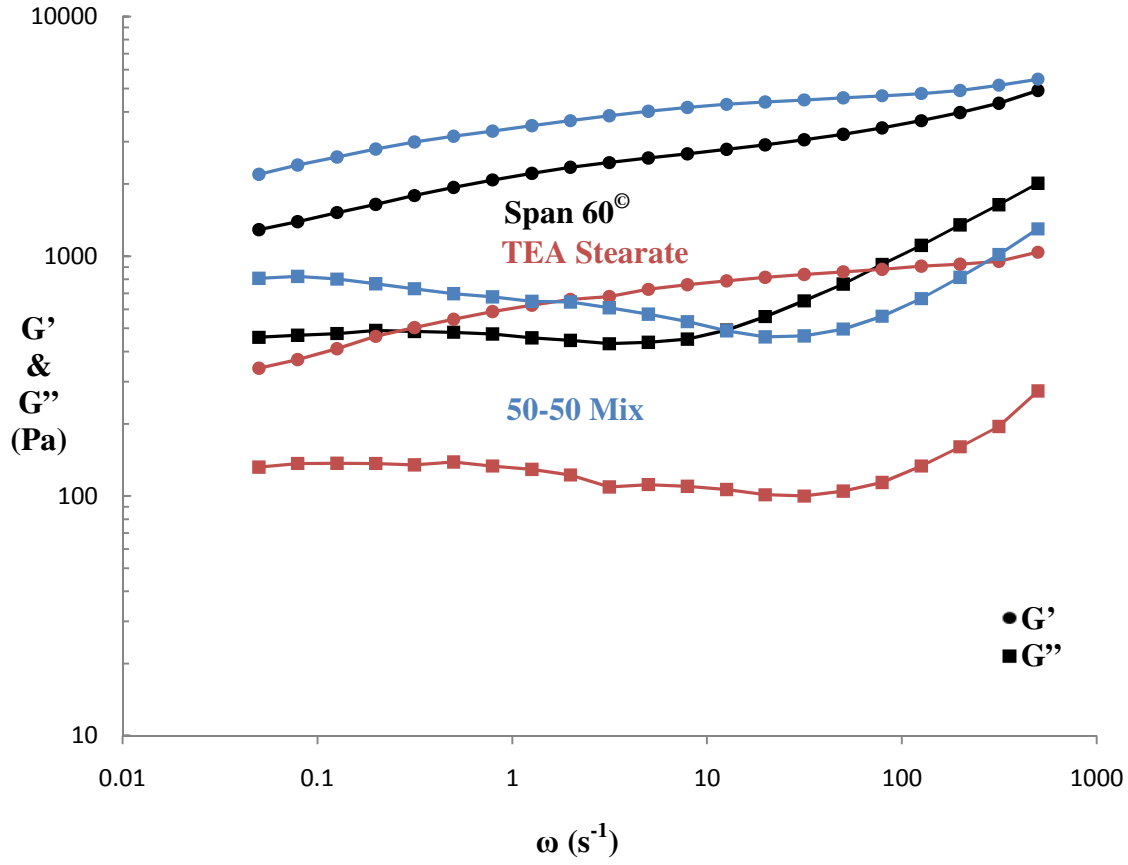

Figure 48. Frequency Sweep Diagrams for 30% Soy Wax Emulsions with Each Emulsifier.

These soy wax emulsions display weak gel-like behavior and possess a measure of long-term storage stability with G' > G" at lower ω's. The magnitudes of the maximum G' for all of the emulsions are on the order of 10^3 Pa indicating a soft and yielding consistency.

The magnitudes of G' at the lowest frequency ($\omega = 0.05\ s^{-1}$) are listed in Table 20.

Table 20. Oscillatory Frequency Sweep Magnitudes of G' at the Lowest Frequency (ω = 0.05 s^{-1}) for 30% Soy Wax Emulsions with Each Emulsifier.

Emulsifier	Magnitude of G' at ω = 0.05 s^{-1} (Pa)
Span 60©	2200
TEA Stearate	1240
50-50 Mix	341

The 4% Span 60© emulsion has the highest gel strength followed by the 4% TEA stearate emulsion. The 2% Span 60© and 2% TEA stearate emulsion has a gel strength one order of magnitude lower than the other two. Soy wax with 4% Span 60© produces the most stable, firm and strong emulsion; while 4% TEA stearate forms a slightly softer and weaker emulsion. The 2% Span 60© and 2% TEA stearate forms the most liquid-like, softest and weakest emulsion with soy wax. As with the paraffin wax emulsion the 2% Span 60© and 2% TEA stearate emulsion shows a gel strength comparable to that of a 2% Span 60© paraffin wax emulsion (Table 5). When these emulsifiers are mixed it would appear that TEA stearate does not contribute significantly to the three-dimensional structure strength of the emulsion produced.

CONCLUSIONS

The rheology of various wax formulations used for the controlled release of pest insect sex pheromones was tested and documented. All the emulsions were found to be suitable for use. It was found that all the emulsions are weak gels that have a yield point (τ_y) originating from an internal structure.

Testing different concentrations of Span 60© showed that 4% (w/w) emulsifier is an optimal concentration for these 30% (w/w) wax emulsions, as 6% (w/w) did very little to increase the stability and 2% reduced the stability. This agrees with the conclusions of unpublished psychorheological experiments performed prior to this research.

Paraffin wax was compared to soy wax and, while similar, showed slightly different properties. There was a structural transition involved with the 4% TEA stearate soy wax emulsion that made it increase in yield point (τ_y) between 25 °C and 35 °C. This could impact both production and distribution if these temperatures are involved.

All soy wax emulsions show a structural change around 40 °C to 50 °C under constant shear that increases the viscosity in that region. This might have an effect on production, but it is unlikely that temperatures will reach this high in the field during application.

The emulsifiers Span 60© and TEA stearate were also evaluated. The 4% Span 60© emulsions possessed a droplet subdivision effect leading to creaming under shear while the 4% TEA stearate and 2% Span 60© and 2% TEA stearate emulsions did not. There was one exception to this, as the transition seen in the soy wax emulsion with 4%

TEA stearate also produced this droplet subdivision effect at 35 °C. This shear creaming causes tackiness under shear.

The Span 60© emulsions have higher storage moduli (G') overall compared to all other emulsions, which denotes more elastic character. This means that they are more stable under most conditions. The paraffin wax emulsion, with TEA stearate was very soft and weak while the soy wax emulsion with TEA stearate was comparable to the Span 60© emulsions.

The 2% Span 60© and 2% TEA stearate emulsions show properties almost identical to the 2% Span 60© paraffin emulsion, except for viscosity under shear. This shows that the viscoelastic properties due to the three-dimensional internal structure of the emulsions are not being affected significantly by the TEA stearate, but come solely from the Span 60©. However, the viscosity is affected by the presence of TEA stearate, being higher overall with the paraffin wax and lower with the soy wax.

The data presented here will be of use in the production and application of these emulsions. Equations generated in this study can be used to predict the behavior of each of these emulsions under different conditions.

FUTURE STUDIES

A future study could be conducted, using the methods developed here, on wax formulation containing pheromones. Along with this study, it would elucidate the rheological differences encountered when the formulations are complete.

A controlled release study of soy wax formulations and formulations using TEA stearate and the mixture of Span 60© and TEA stearate would also be of use. That data would be complementary to what is presented here.

Frequency sweeps of these emulsions at even lower frequencies than presented here would tell much more about the storage stability of these emulsions. Thixotropy tests would also be of interest.

LITERATURE CITED

Ahmed, S. B.; Pfeiffer, D. G. Establishing a Mating Disruption Block in an Orchard or Vineyard. *Entomol. Exp. Applic.* 1993, *67*, 47-56.

Anton Paar GmbH. *Physica MCR: The Modular Rheometer Series;* Graz, Austria, 2007.

Atterholt, C. A. Controlled Release of Insect Sex Pheromones from Sprayable, Biodegradable Materials for Mating Disruption, Ph.D. Dissertation. The University of California-Davis, Davis, CA, 1996.

Atterholt, C. A.; Delwiche, M. J.; Rice, R. E.; Krochta, J. M. Controlled Release of Insect Sex Pheromones from Paraffin Wax and Emulsions. *Journal of Controlled Release.* 1999, *57,* 233-247.

Atterholt, C. A.; Delwiche, M. J.; Rice, R. E.; Krochta, J. M. Study of Biopolymers and Paraffin as Potential Controlled-release Carriers for Insect Pheromones. *J. Agric. Food Chem.*1998, *46,* 4429-4434.

Behle, R. W.; Cossé, A. A.; Dunlap, C.; Fisher, J.; Koppenhöfer, A. M. Developing Wax-Based Granule Formulations for Mating Disruption of Oriental Beetles (*Coleoptera*: *Scarabaeidae*) in Turfgrass. *Journal of Economic Entomology.* 2008, *101(6),* 1856-1863.

Bodenheimer, F. S. *Materialien zur Geschichte der Entomologie bis Linné*; W. Junk: Berlin, 1928.

Chemicalland21.com. SOYABEAN OIL. http://www.chemicalland21.com/industrialchem/organic/SOYABEAN%20OIL.htm (Accessed February, 27, 2011).

Dapčević-Hadnađev, T.; Hadnađev, M. S.; Aleksandra, M. T. Utilization of dynamic oscillatory measurements for agar threshold gel concentration and gel strength determination. *Food Processing, Quality and Safety*. 2009, *3-4*, 69-73.

DeKee, D.; Mohan, P.; Soong, D. S. Yield determination of styrene-butadiene styrene triblock copolymer solutions. *J. Macromolecular Science - Physics*. 1986, *B25 (1&2),* 153-169.

De Lame, F. M. Improving Mating Disruption Programs for the Oriental Fruit Moth, *Grapholita Molesta* (Busck): Efficacy of New Wax-Based Formulations and Effect of Dispenser Application Height and Density, M.S. Thesis. Michigan State University, East Lansing, MI, 2003.

European and Mediterranean Plant Protection Organization (EPPO). Mating disruption pheromones. In *EPPO Standards - Efficacy evaluation of plant protection products.* 2008, *38(3),* 322-325.

Fischbach, R.; Kokini, J. L. Effects of Aging and Mustard Flour on Rheological Properties of Model O/W Emulsion. *Journal of Food Science.* 1987, *52(6),* 1748-1749.

Instruction Manual: Rheoplus Software, Volume 3 – Analysis, Software Version: 3.0x; Anton Paar Germany GmbH: Ostfildern, Germany, 2007, 13-154.

IMP Innovative Solutions. CAT Homogenizers. http://www.imp.co.za/ImpAdmin/documents/IMPSA/Homogenisers.pdf (Accessed February 27, 2011).

Kamerkar, P.; Eickhoff, J. Anton Paar Rheology Academy. Presented at Anton Paar USA, Ashland, VA, November 9-11, 2010.

Kaye, G. W. C.; Laby, T. H. Mechanical properties of materials. In Kaye and Laby Tables of Physical and Chemical Constant; National Physical Laboratory. http://www.kayelaby.npl.co.uk/general_physics/2_2/2_2_1.html (February 27, 2011).

Kokini, J. L.; Dickie, A. An attempt to identify and model transient viscoelastic flow in foods. *J. Texture Studies.* 1981, *12,* 539-57.

Kung, H. C.; Goddard, E. D. Molecular association in fatty acid potassium soap systems II. *J. Colloid Interface Sci.* 1969, *29,* 242.

Larson, R. G. *The Structure and Rheology of Complex Fluids;* Oxford University Press: New York, NY, 1998, 263-279.

Lipták, B.G. *Instrument Engineers' Handbook, Volume One: Process Measurement and Analysis,* 2nd Ed.; Lipták Associates, Stamford, Connecticut, USA, 2003, 1628-1636.

Macosko, C. W. *Rheology Principles, Measurements, and Applications;* VCH Publishers, Inc.: New York, NY. 1994, 1-222.

Ma, L.; Barbosa-Cánovas, G. V. Rheological Characterization of Mayonnaise. Part II: Flow and Viscoelastic Properties at Different Oil and Xanthan Gum Concentrations. *Journal of Food Engineering*. 1995, *25,* 409-425.

Mansoori, G. A.; Barnes, H. L.; Webster, G. M. Petroleum Waxes. In *Fuels and Lubricants Handbook: Technology, Properties, Performance, and Testing;* Torten,

G. E.; Westbrook, S. R.; Shah, R. J. Eds.; ASTM International: Glen Burnie, MD, 2003, 525-556.

McNaught, A. D.; Wilkinson, A; *IUPAC Compendium of Chemical Terminology,* 2nd Ed.*;* Blackwell Scientific Publications, Oxford, UK, 1997, XML on-line corrected version: http://goldbook.iupac.org (Accessed February 27, 2011).

Meissner, H. E.; Atterholt, C. A.; Walgenbach, J. F.; Kennedy, G. G. Comparison of Pheromone Application Rates, Point Sources Densities, and Dispensing Methods for Mating Disruption of Tufted Apple Bud Moth (*Lepidoptera: Tortricidae*). *J. Econ. Entomol.* 2000, *93,* 820-827.

Mezger, T.G. *The Rheology Handbook: For Users of Rotational and Oscillatory Rheometers*. 2nd Revised Ed.; Vincentz Network GmbH & Co. KG: Hannover, Germany, 2006; pp 16-247.

Mezger T.G. Anton Paar USA's Rheology Seminar with Thomas Mezger. Presented at North Carolina State University, College of Textiles, Raleigh, NC, May 19, 2011.

Molnar, J. J.; Traxler, M.; Harris, C. K. Public Perceptions of Pesticides and Chemicals in Food. In *The Social Risks of Agriculture: Americans Speak Out on Food, Farming, and the Environment;* Wimberley, R. C., Ed.; Praeger Publishers: Westport, CT, 2002, 43-56.

National Center for Biotechnology Information (NCIB). PubChem Compound Database; http://pubchem.ncbi.nlm.nih.gov/ (Accessed February 27, 2011).

Nishinari, K. Some Thoughts on the Definition of a Gel. In *Gels: Structures, Properties, and Functions: Fundamentals and Applications;* Masayuki, T., Nishinari, K. Eds.; Progress in Colloid and Polymer Science, Vol. 136; Springer: Dordrecht, NL, 2009, 87-94.

Nguyen, Q. D.; Boger, D. V. Measuring the Flow Properties of Yield Stress Fluids. *Annual Review of Fluid Mechanics.* 1992, *24,* 47-88.

Nguyen, Q. D.; Akroyd, T.; De Kee, D. C.; Zhu, L. Yield Stress Measurements in Supensions: an Inter-laboratory Study. *Korea-Australia Rheology Journal.* 2006, *18(1),* 15-24.

Pal, R. Shear Viscosity Behavior of Emulsions of Two Immiscible Liquids. *Journal of Colloid and Interface Science.* 2000, *225*, 359-366.

Rechcigl, J. E.; Rechcigl, N. A. *Insect pest management: techniques for environmental protection;* CRC Press: Boca Raton, Fl, 1999, 124.

Rice, R. E.; Atterholt, C. A.; Delwiche, M. J.; Jones, R. A. Efficacy of Mating Disruption Pheromones in Paraffin Emulsion Dispensers. *IOBS WPRS Bull.* 1997, *20,* 151-161.

Sarpaki, A. A. Natural Insecticides and Insect Repellents in Antiquity: A Review of the Evidence. *Journal of Archaeological Science.* 1995, *22*, 705-710.

Shortening Flake; MSDS No. PLAIN415 [Online]; Golden Foods/Golden Brands: Louisville, KY, October 30, 2008. http://www.candlescience.com/library/pdf/GW415.pdf (accessed February 27, 2011).

Steffe, J. F. Yield stress: Phenomena and measurement. In *Advances in Food Engineering,* Singh R. P.; Wirakartakusumah M. A. Eds.; CRC Press, London, UK, 1992, 363-376.

Stenersen, J. *Chemical Pesticides: Mode of Action and Toxicology;* CRC Press: Boca Raton, Fl, 2004, 34-97.

Stern, V. M.; Smith, R.F.; van den Bosch, R.; Hagen, K. S. The Integrated Control Concept. *Hilgardia.* 1959, *29*, 81-101.

Tabilo-Munizaga, G.; Barbosa-Cánovas, G. V. Rheology for the Food Industry. *Journal of Food Engineering.* 2004, *67,* 147-156.

US Environmental Protection Agency. About Pesticides. http://www.epa.gov/pesticides/about/index.htm (Accessed July 25, 2010).

US Environmental Protection Agency. Integrated Pest Management (IPM) Principles. http://www.epa.gov/pesticides/factsheets/ipm.htm (Accessed February 26, 2011).

Wilkinson, J. B., *Modern Cosmeticology*; Chemical Publishing Co., Inc.: New York, NY, 1940, 15-16.

Yaron, I.; Gal-Or, B. On viscous flow and effective viscosity of concentrated suspensions and emulsions. *Rheologica Acta.* 1972, *11(3),* 241-252.

Yoshimura, A. S.; Prud'homme, R. K. Wall Slip Corrections for Couette and Parallel Disk Viscometers. *Journal of Rheology*. 1988, *32,* 53-67.

Zhu, S.; Heppenstall-Butler, M.; Butler, M. F.; Pudney, P. D. A.; Ferdinando, K. J.; Mutch, K. J. Acid Soap and Phase Behavior of Stearic Acid and Triethanolamine Stearate. *J. Phys. Chem. B.* 2005, *109,* 11753-11761.

APPENDIX A: TEMPERATURE SWEEP DATA

Table A-1. Averaged Temperature Sweep Data For All Emulsions.

Temperature (°C)	Paraffin Wax, 4% Span 60®, η (Pa·s)	Paraffin Wax, 2% Span 60®, η (Pa·s)
15	14.5	9.91
16	12.4	8.42
17	11.6	7.68
18	10.6	6.97
19	10.1	6.57
20	9.74	6.23
21	9.20	5.86
22	8.90	5.49
23	8.58	5.21
24	8.27	5.00
25	8.04	4.78
26	7.73	4.53
27	7.47	4.31
28	7.16	4.17
29	6.95	4.02
30	6.68	3.81
31	6.52	3.66
32	6.31	3.56
33	6.14	3.49
34	5.94	3.37
35	5.68	3.20
36	5.27	3.10
37	5.02	2.91
38	4.85	2.82
39	4.74	2.71
40	4.75	2.66
41	4.64	2.57
42	4.63	2.50
43	4.64	2.41
44	4.48	2.35
45	4.44	2.27
46	4.35	2.18
47	4.28	2.05
48	4.19	1.92
49	4.03	1.76
50	4.00	1.56

Table A-1. (continued)

Temperature (°C)	Paraffin Wax, 6% Span 60®, η (Pa·s)	Soy Wax, 4% Span 60®, η (Pa·s)
15	16.3	10.5
16	15.2	9.80
17	14.7	9.41
18	14.2	9.09
19	13.9	8.80
20	13.4	8.56
21	13.0	8.26
22	12.6	7.98
23	12.3	7.67
24	11.9	7.42
25	11.6	7.17
26	11.2	6.92
27	10.9	6.69
28	10.6	6.43
29	10.3	6.24
30	10.1	6.04
31	9.81	5.85
32	9.52	5.68
33	9.41	5.49
34	9.17	5.38
35	8.88	5.24
36	8.59	5.13
37	8.31	5.03
38	8.21	4.89
39	8.07	4.81
40	7.97	4.69
41	7.85	4.58
42	7.73	4.47
43	7.67	4.37
44	7.53	4.24
45	7.43	4.12
46	7.29	4.30
47	7.11	5.95
48	6.91	5.63
49	6.68	5.39
50	6.29	4.16

Table A-1. (continued)

Temperature (°C)	Paraffin Wax, 4% TEA Stearate, η (Pa·s)	Soy Wax, 4% TEA Stearate, η (Pa·s)
15	4.39	8.05
16	4.28	7.71
17	4.26	7.48
18	4.22	7.31
19	4.16	7.11
20	4.08	6.97
21	3.99	6.80
22	3.89	6.68
23	3.79	6.54
24	3.68	6.42
25	3.57	6.29
26	3.46	6.17
27	3.33	6.05
28	3.18	5.94
29	3.00	5.84
30	2.79	5.72
31	2.60	5.61
32	2.40	5.50
33	2.19	5.41
34	1.99	5.33
35	1.73	5.28
36	1.37	5.21
37	1.25	5.17
38	1.20	5.10
39	1.15	5.02
40	1.10	4.89
41	1.07	4.75
42	1.04	4.60
43	1.02	4.43
44	1.01	4.33
45	1.01	4.16
46	1.01	4.11
47	0.998	4.84
48	0.977	6.11
49	0.967	5.80
50	0.736	4.09

Table A-1. (continued)

Temperature (°C)	Paraffin Wax, 2% Span 60®, 2% TEA Stearate, η (Pa·s)	Soy Wax, 2% Span 60®, 2% TEA Stearate, η (Pa·s)
15	15.2	7.49
16	12.9	6.21
17	12.2	5.58
18	11.5	5.12
19	11.1	4.69
20	10.6	4.33
21	10.3	3.99
22	9.99	3.73
23	9.75	3.49
24	9.48	3.28
25	9.24	3.07
26	9.00	2.90
27	8.75	2.74
28	8.49	2.59
29	8.24	2.47
30	8.01	2.35
31	7.79	2.24
32	7.56	2.16
33	7.34	2.07
34	7.07	2.00
35	6.59	1.93
36	5.79	1.88
37	5.30	1.82
38	5.04	1.77
39	4.84	1.73
40	4.67	1.69
41	4.52	1.69
42	4.38	1.67
43	4.24	1.67
44	4.10	1.73
45	3.96	1.92
46	3.80	3.33
47	3.63	8.71
48	3.37	7.19
49	2.90	4.99
50	2.23	2.05

APPENDIX B: AMPLITUDE SWEEP CSS DIAGRAMS

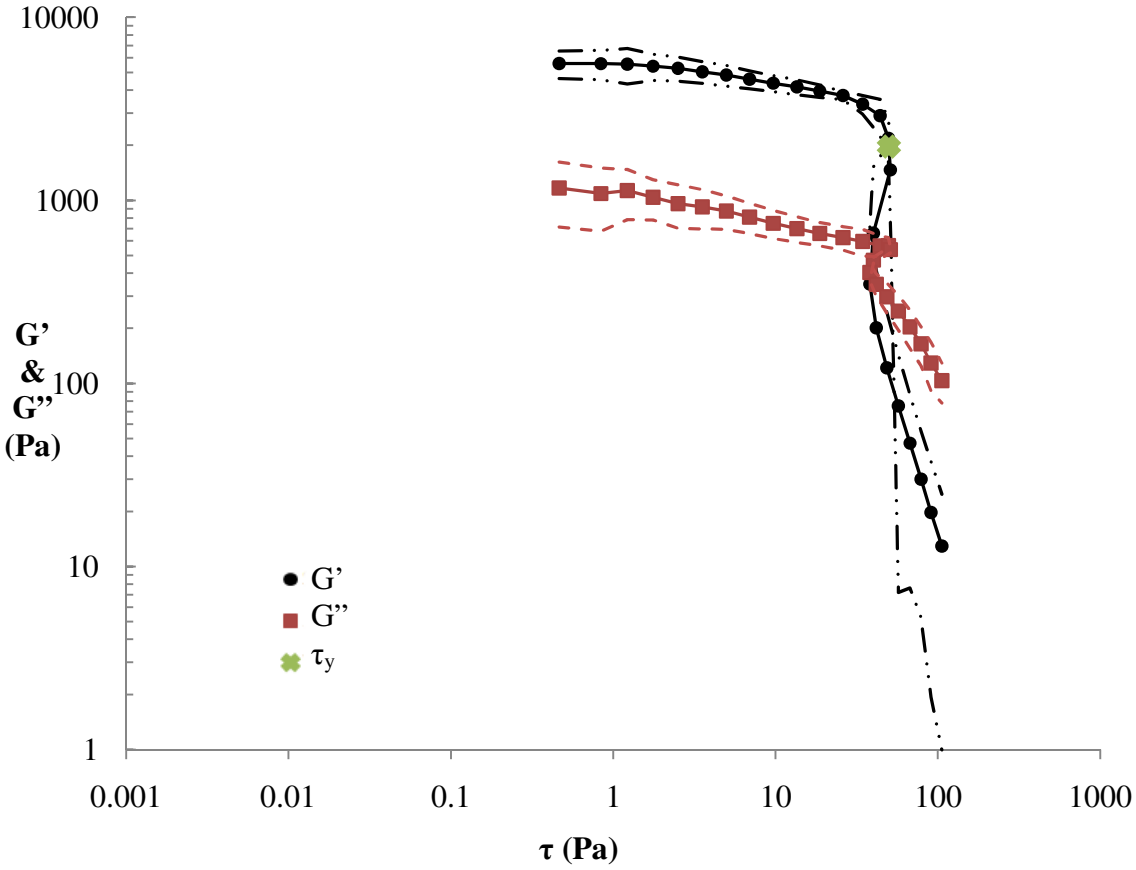

Figure B-1. Amplitude Sweep (CSS) Diagram with 95% Confidence Intervals for 30% Paraffin Wax Emulsion with 4% Span 60®.

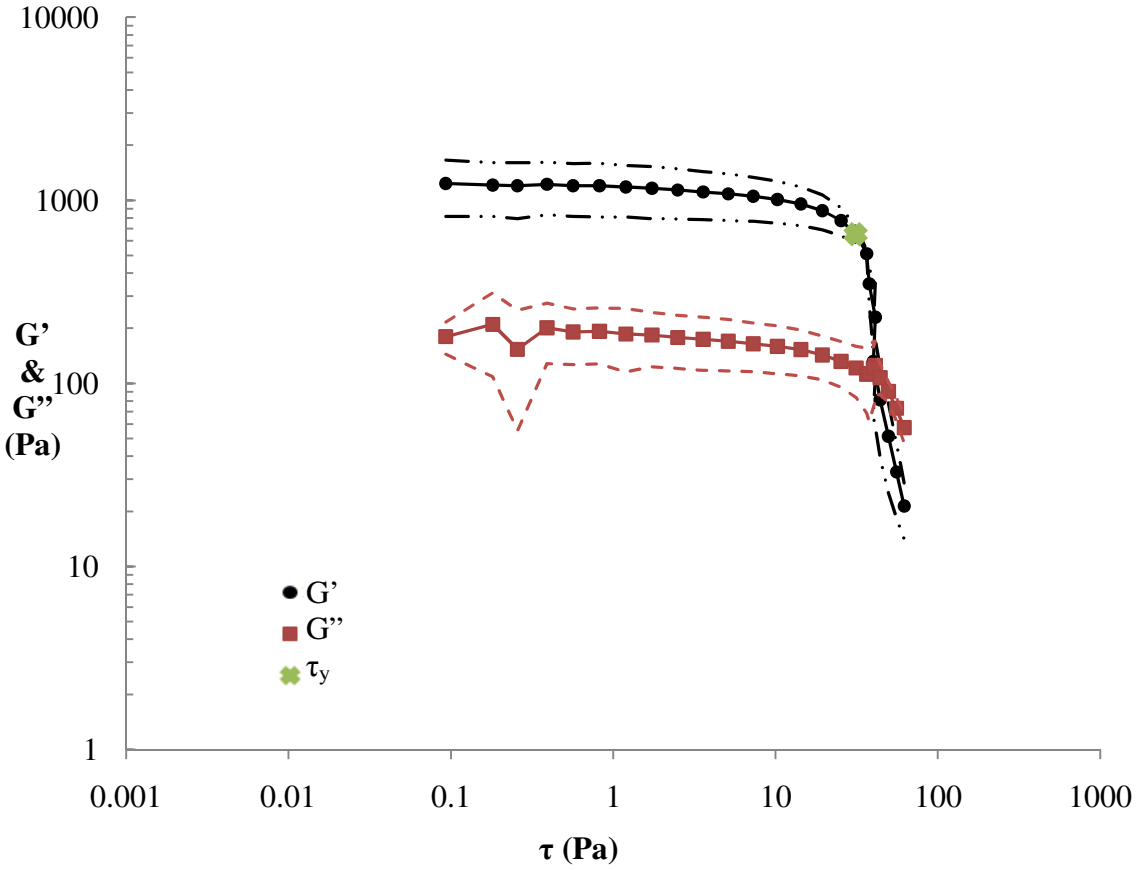

Figure B-2. Amplitude Sweep (CSS) Diagram with 95% Confidence Intervals for 30% Paraffin Wax Emulsion with 2% Span 60®

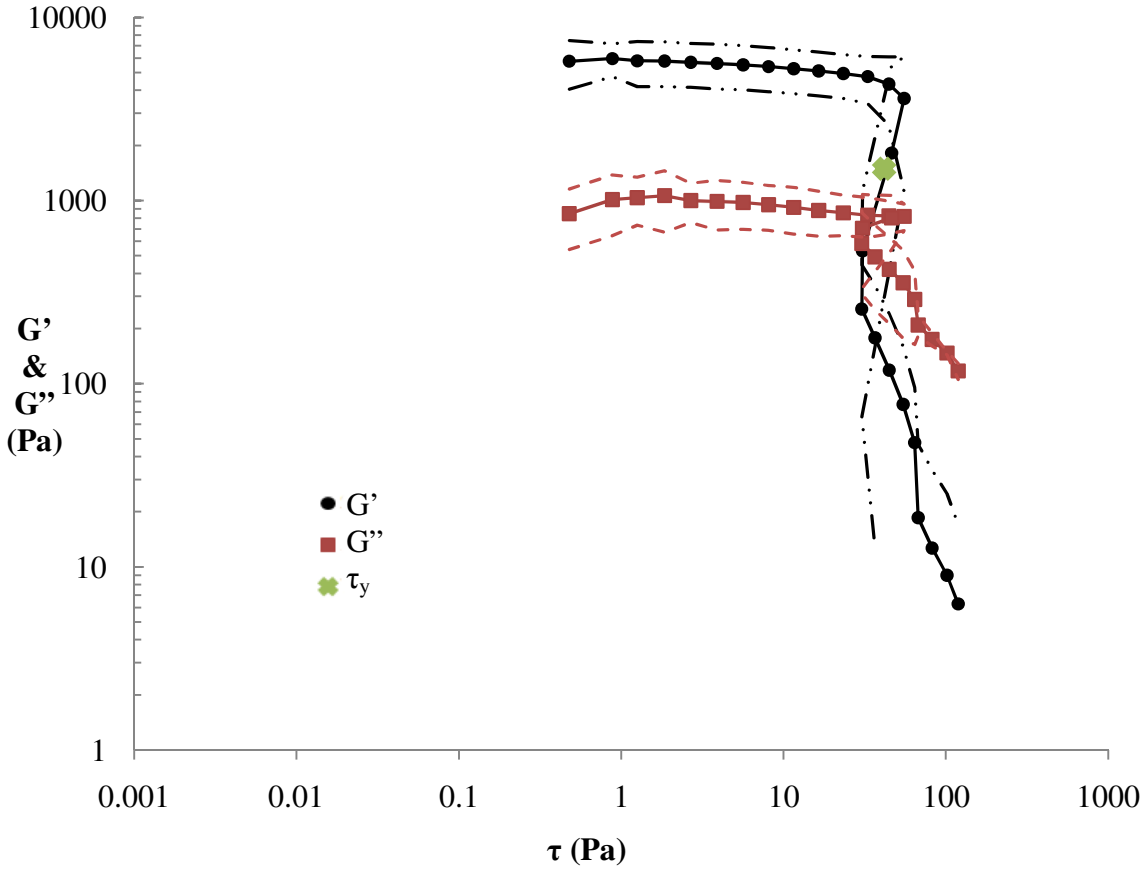

Figure B-3. Amplitude Sweep (CSS) Diagram with 95% Confidence Intervals for 30% Paraffin Wax Emulsion with 6% Span 60®.

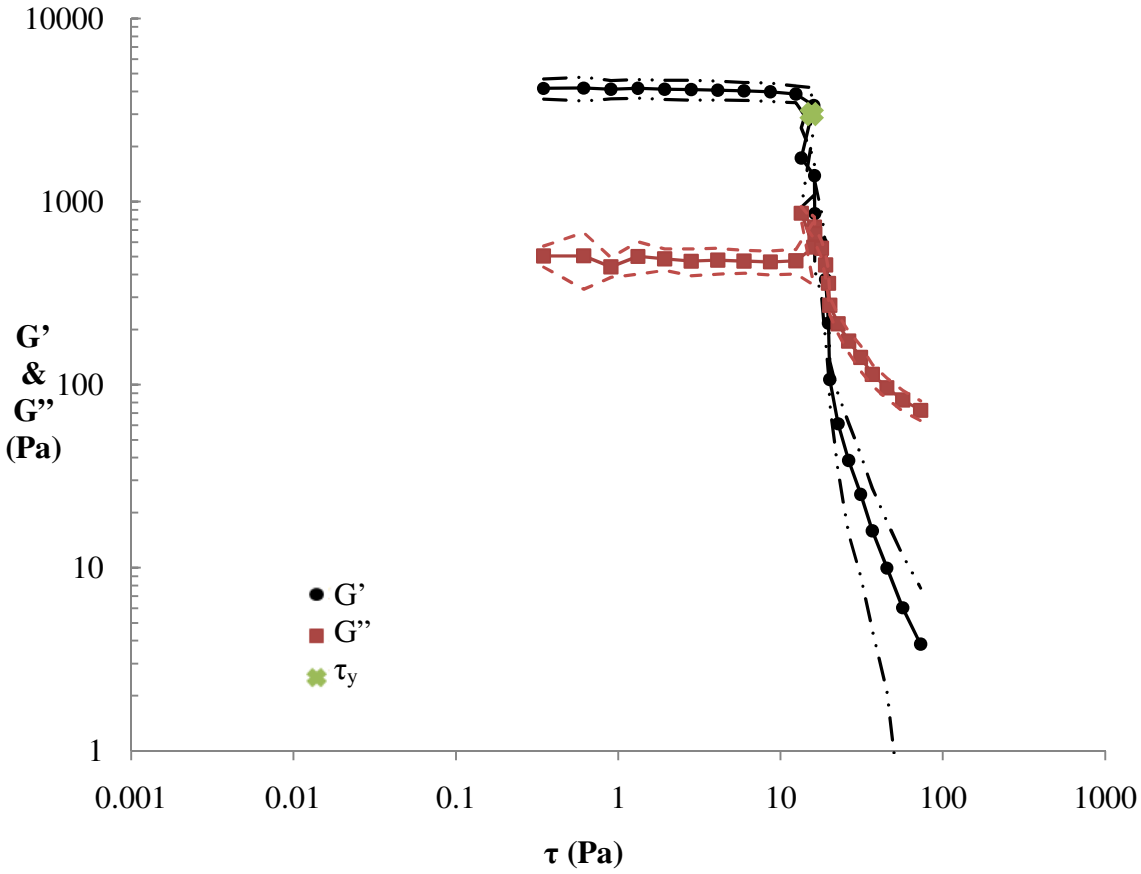

Figure B-4. Amplitude Sweep (CSS) Diagram with 95% Confidence Intervals for 30% Soy Wax Emulsion with 4% Span 60®

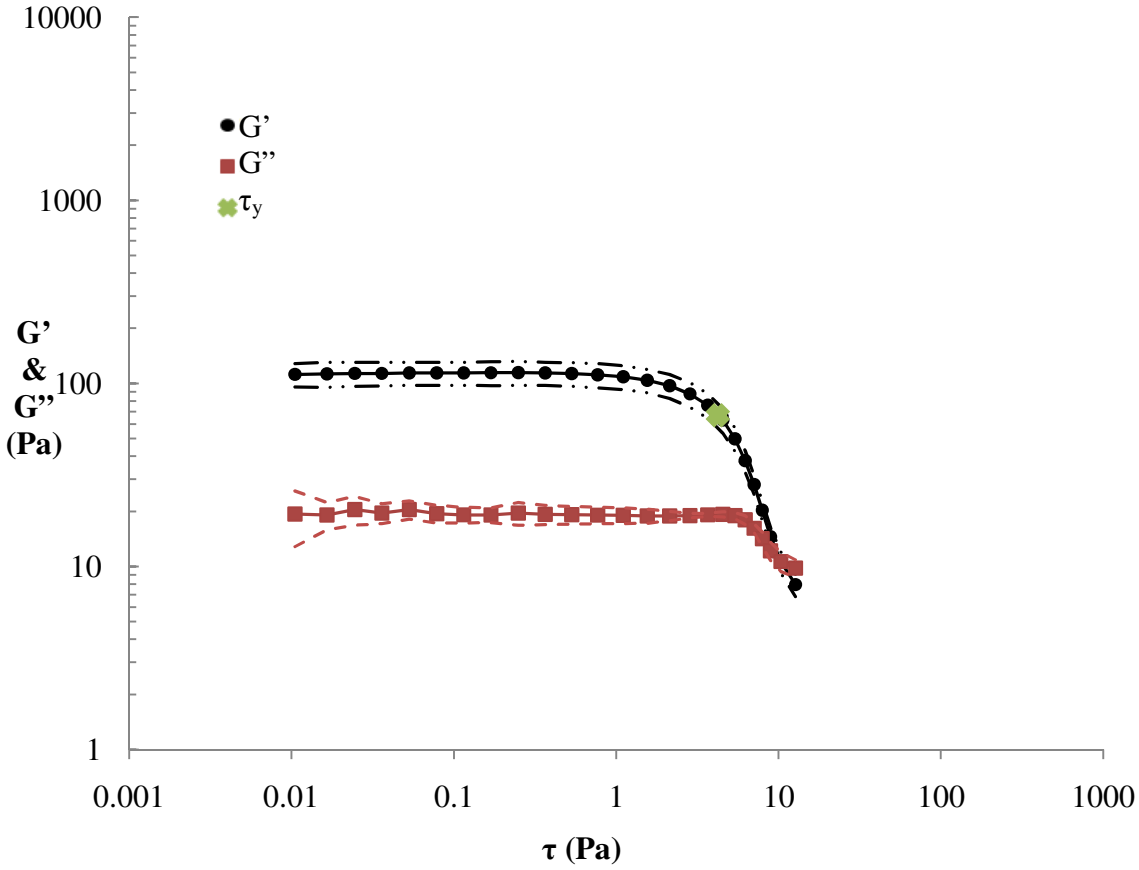

Figure B-5. Amplitude Sweep (CSS) Diagram with 95% Confidence Intervals for 30% Paraffin Wax Emulsion with 4% TEA Stearate

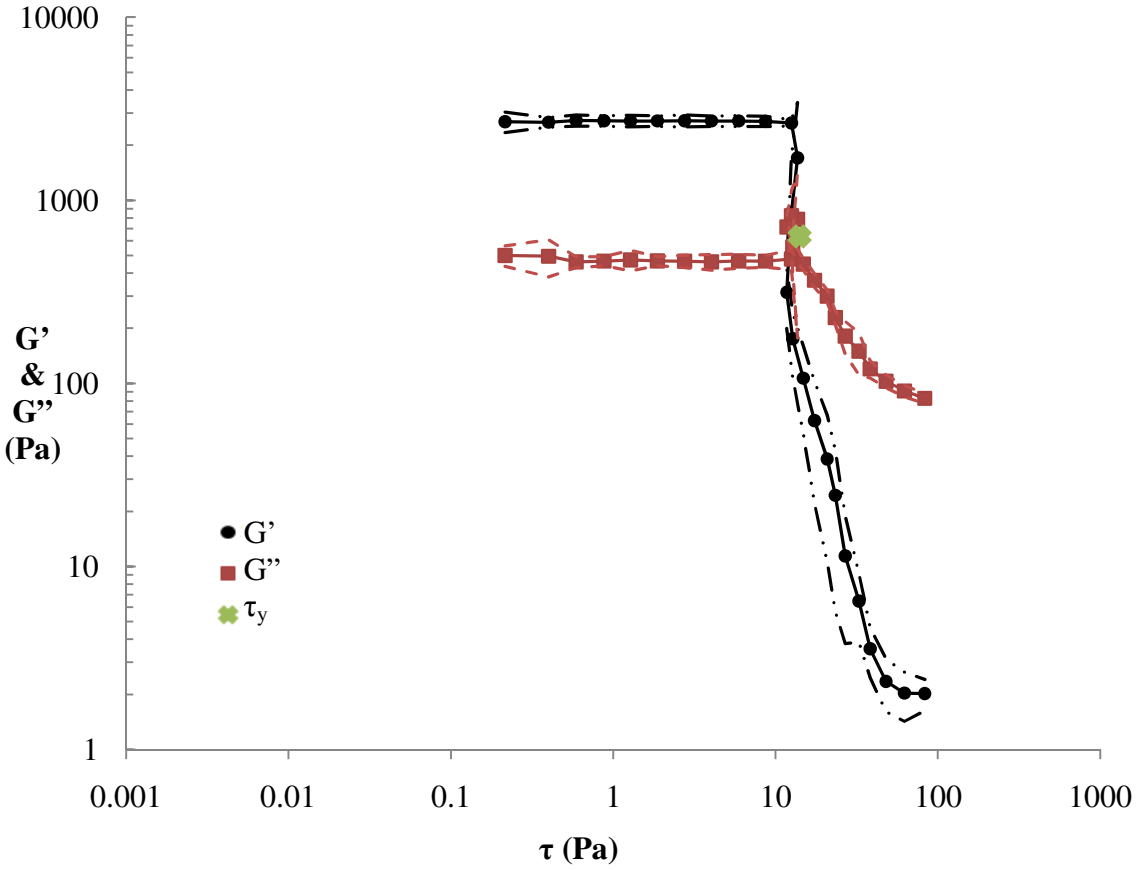

Figure B-6. Amplitude Sweep (CSS) Diagram with 95% Confidence Intervals for 30% Soy Wax Emulsion with 4% TEA Stearat

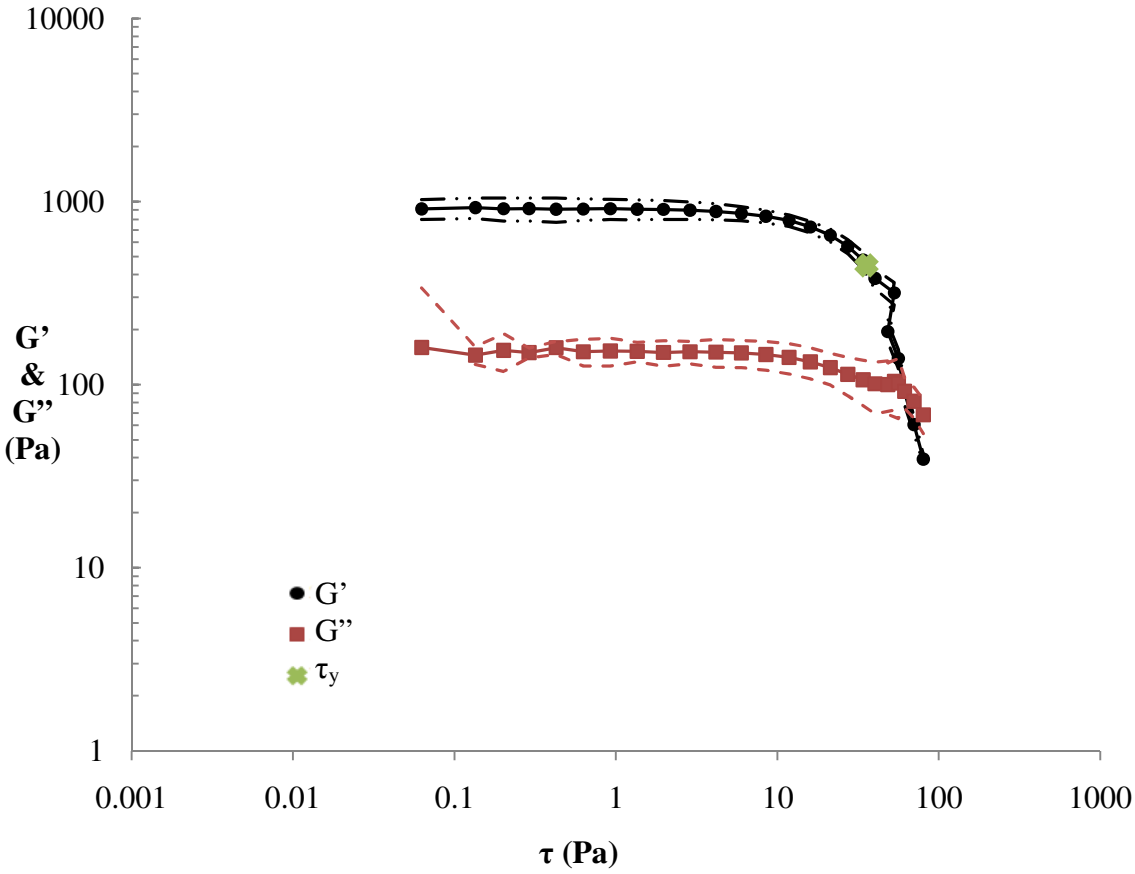

Figure B-7. Amplitude Sweep (CSS) Diagram with 95% Confidence Intervals for 30% Paraffin Wax Emulsion with 2% Span 60® and 2% TEA Stearate.

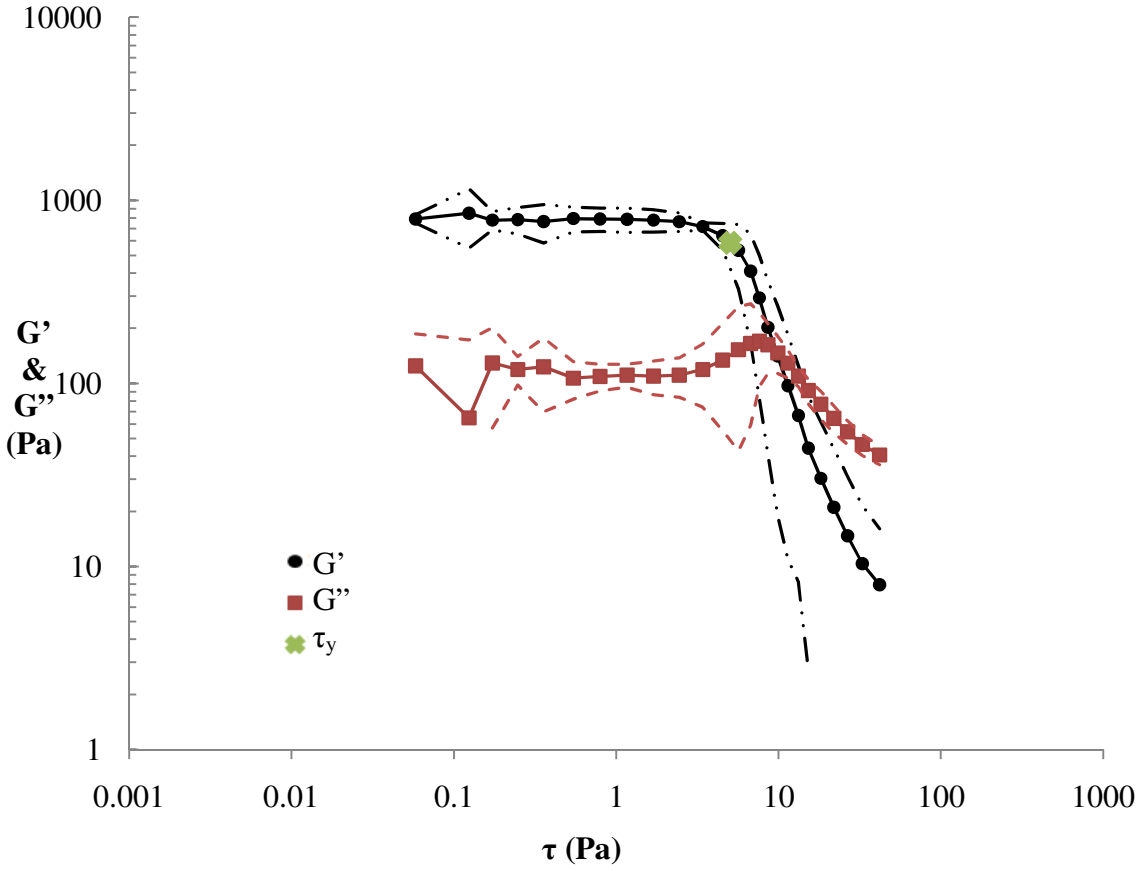

Figure B-8. Amplitude Sweep (CSS) Diagram with 95% Confidence Intervals for 30% Soy Wax Emulsion with 2% Span 60® and 2% TEA Stearate.